UNIVERZITA PALACKÉHO V OLOMOUCI

Přírodovědecká fakulta

Katedra biotechnologií

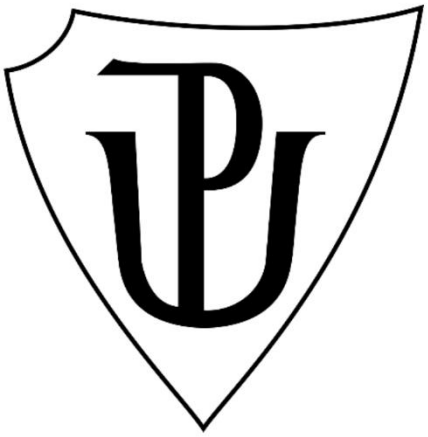

Molekulární a fenotypová analýza annexinových knock-out mutantů *Arabidopsis thaliana*

BAKALÁŘSKÁ PRÁCE

Autor:	**Emma Gentric**
Studijní program:	B0512A130007 Biotechnologie a genové inženýrství
Specializace:	Biotechnologie a genové inženýrství
Forma studia:	Prezenční
Vedoucí práce:	**Mgr. Olga Šamajová, Dr.**
Konzultant:	**Mgr. Michaela Tichá, Ph.D.**
Rok:	2024

PALACKÝ UNIVERSITY OLOMOUC

Faculty of Science

Department of Biotechnology

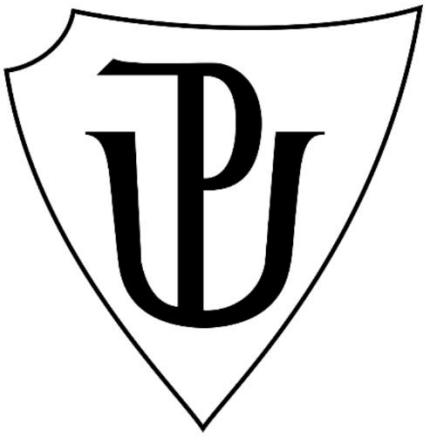

Molecular and phenotypic analysis of annexin knock-out mutants of *Arabidopsis thaliana*

BACHELOR THESIS

Author:	**Emma Gentric**
Study programme:	B0512A130007 Biotechnology and Genetic Engineering
Field of study:	Biotechnology and Genetic Engineering
Form of study:	Full
Supervisor:	**Mgr. Olga Šamajová, Dr.**
Consultant:	**Mgr. Michaela Tichá, Ph.D.**
Year:	2024

Prohlašuji, že jsem bakalářskou práci vypracovala samostatně s vyznačením všech použitých pramenů a spoluautorství. Souhlasím se zveřejněním bakalářské práce podle zákona č. 111/1998 Sb., o vysokých školách, ve znění pozdějších předpisů. Byla jsem seznámen s tím, že se na moji práci vztahují práva a povinnosti vyplývající ze zákona č. 121/2000 Sb., autorský zákon, ve znění pozdějších předpisů.

V Olomouci dne ....

I hereby declare that I developed this bachelor thesis on my own with showing all the sources and authorship. I agree with the publication of my thesis by Act. No. 111/1998 Coll., on Higher Education Institutions, as amended. I have been informed that the rights and obligations implied by Act No. 121/2000 Coll., on Copyright and Rights Related to Copyright, as amended, apply to my work.

In Olomouc on ....

Poděkování

Ráda bych vyjádřila své nejhlubší poděkování své vedoucí Mgr. Olze Šamajové, Dr., za její neocenitelné vedení, podporu a nekonečnou trpělivost. Její obětavost a laskavost byly zásadní při vypracování této práce. Vděčím rovněž Mgr. Michaele Tiché, PhD., jejíž mentorství a rady obohatily mé chápání a dovednosti. Ráda bych také poděkovala své kolegyni Kateřině Hegerové, za příjemnou spolupráci. Dále děkuji vedoucímu katedry biotechnologií prof. RNDr. Josefu Šamajovi, DrSc. za umožnění vypracování práce a celému týmu katedry za vytvoření vstřícného a příjemného prostředí. Mé poděkování poté patří především Mgr. Miroslavě Medelské, PhD., za velkou pomoc při experimentální části práce, ochotu a obětavost. V neposlední řadě děkuji své rodině za neochvějnou podporu a pochopení.

Acknowledgement

I would like to express my deepest gratitude to my supervisor, Mgr. Olga Šamajová, Dr., for her invaluable guidance, support, and endless patience. Her dedication and kindness have been instrumental in shaping this work. I am also indebted to Mgr. Michaela Tichá, PhD., whose mentorship and teachings have enriched my understanding and skills. I'd like to thank my colleague, Kateřina Hegerová, who has been my partner in crime. I'd also like to thank the head of the department of biotechnology, prof. RNDr. Josef Šamaj, DrSc. for making the work possible and to the entire team of the department for creating a welcoming and pleasant environment. My thanks go especially to Mgr. Miroslava Medelská, PhD., for her great help in the experimental part of this thesis, willingness and dedication. Finally, I extend my heartfelt thanks to my family for their unwavering support and understanding.

Bibliografická identifikace

Jméno a příjmení autora	Emma Gentric
Název práce	Molekulární a fenotypová analýza annexinových knock-out mutantů *Arabidopsis thaliana*
Typ práce	Bakalářská
Pracoviště	Katedra biotechnologií
Vedoucí práce	Mgr. Olga Šamajová, Dr.
Konzultant	Mgr. Michaela Tichá, Ph.D
Rok obhajoby práce	2024

Abstrakt

Tato bakalářská práce je zaměřena na annexiny, proteinovou rodinu přítomnou v širokém spektru eukaryotických organismů, od lidí až po rostliny. Molekuly annexinu se mohou vázat na různé molekuly, včetně fosfolipidů, aktinu a hlavně iontů vápníku. Vazebné vlastnosti annexinů významně ovlivňují jejich intracelulární role. Účastní se nesčetných buněčných procesů, jako je vesikulární transport nebo transport iontů. Kromě toho také hrají roli ve vápníkové signalizaci, která reguluje stresové reakce rostlin. U *Arabidopsis thaliana* je annexinová rodina složená z 8 genů a proteinů. Cílem této práce bylo konkrétně prozkoumat molekulární a fenotypové důsledky vyřazení genu annexinu 3, *ANNAT3*, u *Arabidopsis thaliana*. Studie využívala genotypování jako nástroj pro výběr homozygotních mutantů. Poté následovala fenotypová analýza mutantních ověřených rostlin se zvláštním zaměřením na kořeny. Získané výsledky naznačují, že ANNAT3 se ukazuje jako pozitivní regulátor délky kořenových vlásků, přičemž vykazuje negativní vliv na velikost listů.

Klíčová slova	*Arabidopsis thaliana*, annexiny, genotypování, kořenové vlásky, listové růžice, křížení
Počet stran	81
Počet příloh	6
Jazyk	Anglický (Český)

Bibliographical identification

Author's first name and surname	Emma Gentric
Title of thesis	Molecular and phenotypic analysis of annexin knock-out mutants of *Arabidopsis thaliana*
Type of thesis	Bachelor
Department	Department of Biotechnology
Supervisor	Mgr. Olga Šamajová, Dr.
Consultant	Mgr. Michaela Tichá, Ph.D
Year of defence	2024

Abstract

This bachelor thesis focuses on annexins, a protein family present in a wide range of eukaryotic organisms, spanning from humans to plants. Annexin molecules can bind to various molecules, including phospholipids, actin and most importantly, calcium ions. The binding properties of annexins have significant implications for their intracellular roles. They are involved in a myriad of cellular processes, such as membrane trafficking or ion transport. Furthermore, they also play a role in calcium signalling, which regulates plant stress responses. In *Arabidopsis thaliana*, the annexin gene and protein family consist of 8 members. This study aimed to specifically investigate the molecular and phenotypic consequences of knocking out annexin 3, *ANNAT3*, gene in *Arabidopsis thaliana*. The study employed genotyping as a tool to select homozygous mutants. This was followed by a phenotypic analysis of the mutant plants, with a particular focus on roots. The results obtained suggest that ANNAT3 emerges as a positive regulator of root hair length while exhibiting a negative influence on leaf size.

Keywords	*Arabidopsis thaliana*, annexins, genotyping, leaf rosette, root hairs, crossing
Number of pages	81
Number of appendices	6
Language	English (Czech)

CONTENT

AIMS OF THE THESIS

THEORETICAL PART

Identification and summarization of all the relevant research conducted on topics:

1. Characterization and the structure of plant annexins.
2. Sensor and channel activity of annexins.
3. Roles of annexins in membrane trafficking.
4. Involvement of annexins in plant growth and development.
5. Reactions of annexins to surrounding environment.

EXPERIMENTAL PART

1. Preparation and annotation of *A. thaliana* ANN1, ANN3 and ANN4 gene maps.
2. In silico identification of the position of T-DNA insertions of selected SALK mutant.
3. Molecular characterization and verification of selected single knock-out annexin mutants of *A. thaliana*.
4. Phenotypic analyses of verified annexin single mutants.

1 INTRODUCTION

Arabidopsis thaliana, commonly known as thale cress, belongs to the mustard family (*Brassicaceae*). It is the model plant used in many biological sciences. Its advantages include easy manipulation due to its small size and a fully annotated, relatively small genome. One of the most practical advantages is also the easy transformation by *Agrobacterium tumefaciens*, allowing the creation of knock-out mutant libraries (Meinke *et al.*, 1998; O'Malley *et al.*, 2015).

Annexins constitute a family of calcium-binding proteins found across various organisms. They diverge from typical calcium-binding proteins with EF-hand motifs, showcasing the unique endonexin fold. Besides their ability to bind calcium, many annexins interact with molecules such as actin and phospholipids. Their affinity for actin and phospholipids suggests their involvement in vesicular trafficking. The latter is very important in endocytosis, especially in rapidly growing plant tissues, such as pollen tubes or root hairs (Konopka-Postupolska, 2007; Konopka-Postupolska *et al.*, 2011; Moss & Morgan, 2004). Furthermore, annexins play roles beyond vesicular trafficking, regulating calcium transport across the plasma membrane, thus contributing to calcium signalling and stress responses. Some annexins also exhibit peroxidase activity, adding complexity to their involvement in stress responses (Laohavisit *et al.*, 2010).

This bachelor thesis focuses on characterizing annexin 3 in *A. thaliana*, ANNAT3, including both molecular and phenotypic analysis of a selected knock-out *ann3* mutant (SALK_082344C). The molecular analysis involves genotyping to identify homozygotes, facilitating the identification of distinctive phenotypic traits, particularly in the root system. Subsequently, the *ann3* mutants were crossed with *A. thaliana* mutant lines carrying fluorescent endosomal markers VTI1-mCherry, RabF2b-mCherry, a calcium sensor YC3.6 and ANNAT1 fused with GFP, ANN1-GFP. Observation of the roots of these plants enables the localisation of these markers.

2 CURRENT STATE OF THE TOPIC

2.1 *Arabidopsis thaliana* (thale cress)

Arabidopsis thaliana is a plant belonging to the mustard family (*Brassicaceae*), which puts this species within the angiosperm group among plants. The species is naturally found in a large geographical region spreading from Asia and Europe to Northern America. The plant itself is relatively small, with mature plants typically reaching heights of about 15 to 20 cm. Its flowers, measuring approximately 2 mm in length, consist of four green sepals and an inner whorl composed of four white petals. Within the inner whorl, four stamens surround a gynoecium. Upon pollination, the plant produces fruits known as siliques.

Arabidopsis thaliana serves as the primary model organism in plant science. There are several factors for this choice:

1. Its entire life cycle lasts only about six weeks.
2. The plant's small growth allows its growth in laboratories and greenhouses.
3. It is a self-pollinating plant.
4. Many produced siliques with a large number of seeds.
5. It has a relatively small genome that has been completely sequenced.
6. The existence of detailed genetic maps.
7. A relatively easy transformation by *Agrobacterium tumefaciens* (Meinke *et al.*, 1998).

The Arabidopsis genome is comprised of five chromosomes and approximately 25 500 genes (The Arabidopsis Genome Initiative, 2000). Several specialized databases are dedicated to *Arabidopsis thaliana*, which are a useful tool for organizing and providing access to information about the plant itself and research development. An example is The Arabidopsis Information Resource (TAIR), where an annotated genome, as well as phenotypic data, can be found (https://www.arabidopsis.org/index.jsp). Several research centres also provide seed stocks of mutant lines (e.g., NASC https://arabidopsis.info/).

Friedrich Laibach has been credited for initiating in the early 20th century the upswing in interest in *Arabidopsis thaliana* as well as identifying the number of the plant's chromosomes. However, a significant rise in interest and importance of the plant came only in the late 1970s and 1980s. The entire genome was successfully sequenced in the

year 2000 thanks to the Arabidopsis Genome Initiative. Nowadays, the research focuses on the characterization of each gene in the genome (Koornneef & Meinke, 2010).

2.2 Annexins

Annexins are a very large and diverse multigene protein family found across a large spectrum of organisms with the ability to bind to membrane phospholipids in a calcium-dependent manner. Generally, they are involved in various biochemical and cellular processes, including calcium ion (Ca^{2+}) and F-actin binding, peroxidase activity or their involvement in the functioning of ion channels, among many others.

With their presence across a broad spectrum of organisms, annexins have been categorized into various groups (A-E) corresponding to their provenance. The annexin A family belongs to vertebrates (including humans), while the annexin B family is found among invertebrates. The annexin C family is prominent in fungi and certain unicellular organisms, while the annexin E family is typical for protists. Plant annexins are comprised within the annexin D family (Moss & Morgan, 2004).

The origin of the name annexin is in Greek, derived from the word *annex*, which means "bring/hold together". It was selected mainly due to the key characteristic of this protein family, which is to bind to cellular structure, primarily to membranes. Historically annexins have been studied since the late 1970s and early 1980s, however under diverse names, e.g. synexin or lipocortins (Gerke & Moss, 2002). They were discovered in the process of calmodulin purification, another calcium-binding protein (Konopka-Postupolska & Clark, 2017). To this day, most of the research has been done on animal annexins, where they were also discovered rather than plant annexins (Clark & Roux, 1995).

2.2.1 Structure of plant annexins

2.2.1.1 Structural characteristics

The first members of the plant annexin family were discovered in 1989 as a pair of proteins binding to phospholipids in a calcium-dependent manner from a suspension of tomato cells (Boustead *et al.*, 1989). As annexins are present in various types of organisms, their structures can vary significantly between each annexin family. The annexin D family, the plant annexins, has a molecular weight between 32 and 42 kDa (Mortimer *et al.*, 2008). Even though there are many differences between individual annexins, the structure of a typical plant annexin contains a highly conserved fold typical

for each annexin. The fold, sometimes called the endonexin fold, consists of four repeats (I – IV), which contain approximately 70 amino acid residues (Konopka-Postupolska *et al.*, 2011). Each repeat is then constituted of five α helixes (A – E). The helixes A, B, D and E are arranged in a helix-loop-helix bundle to which the C helix is oriented perpendicularly (Dabitz *et al.*, 2005). The repeats I – IV form together the C-terminal core. The N-terminal region is usually shorter in the case of plant annexins, which is a notable difference from animal annexins where the N-terminal region is longer and thus is a more important site of post-translational modifications (Talukdar *et al.*, 2009). The annexin fold is of a slightly curved disc shape. The convex side binds calcium ions and can also attach to the membranes. The concave side, in turn, is oriented towards the cytoplasm and is available for other interactions. The N-terminal core is located on the concave side and in some documented cases is exposed only when Ca^{2+} has bound to the repeats of the C-terminal core. The N-terminal core can also participate in interactions with other proteins (Gerke *et al.*, 2005). The amino acid sequence of the core of the helix-loop-helix bundle primarily contains hydrophobic residues. In contrast, the protein surface and spaces between each domain mainly comprise of hydrophilic amino acid residues (Konopka-Postupolska & Clark, 2017).

One of the main characteristics of the annexin protein family is the ability to bind Ca^{2+}. In plant annexins, the calcium-binding sites are mostly situated on the first and fourth repeat. These sites are comprised of the (K-G-X-G-T-{38}-D/E) amino acid sequence (Mortimer *et al.*, 2008). The second and third repeats have lost this binding capacity in most cases. However, it is mainly in these two repeats of the C-terminal core that post-translational modifications, such as phosphorylation, *S*-nitrosylation or *S*-glutathionylation, may occur. These modifications can alter the calcium ion binding capability (Clark *et al.*, 2012).

Annexins exhibit the ability to bind not only to calcium but also to F-actin. The annexin-actin interaction plays a role in exocytosis and signalling pathways. The interaction occurs thanks to the isoleucine-arginine-isoleucine (IRI) motif present within the third domain. However, it is noteworthy that this interaction is rather species-specific. For example, tomato and zucchini have annexins binding to F-actin. On the other hand, cotton or maize annexins, though possessing the IRI motif, have not shown any affinity for F-actin (Mortimer *et al.*, 2008). In *Arabidopsis thaliana*, all annexins contain the IRI motif with exceptions being ANNAT3 and ANNAT4. In the case of ANNAT5, the F-actin

binding motif overlaps with the Ca^{2+} binding site (Clark *et al.*, 2001). The annexin-actin binding can also be highly modulated through post-translational modifications of annexins. It is also worth mentioning that the tomato and zucchini annexins mentioned prior bind solely to F-actin and not to G-actin. Multiple isoforms of F-actin can be found in plant cells. These isoforms are distinguished by a tissue-specific expression and also have different functions. It has been shown that annexins can bind specifically to some isoforms of actin; resulting in the specificity of cellular responses as actin plays a crucial role in them (Konopka-Postupolska, 2007).

Other structural features influencing the functions of annexins are the ATP/GTP binding sites, giving the proteins an ATP/GTPase activity. The Walker A motif (GXXXXGKT/S) is responsible for the ATPase activity, which contrasts with animal annexins whose ATPase activity does not depend on the Walker A or B motif. The DXXG motif is responsible for the protein's GTPase activity. The DXXG is a typical binding motif for GTPases (Mortimer *et al.*, 2008). The ATP/GTPase activity, similar to the F-actin binding, is species-specific. Even in one species, not all annexins possess this activity. In *Arabidopsis thaliana*, ANNAT2 and ANNAT7 have such abilities as they contain a DXXG and a Walker A sequence in the fourth domain (Clark *et al.*, 2001). In contrast, the annexin MTANN1 in *Medicago truncatula* does not contain any of these motifs in its structure (Talukdar *et al.*, 2009). These enzymatic activities are, in some cases, regulated by Ca^{2+}. Such is the case of cotton annexin GHANN1, where the GTPase activity is inhibited by Ca^{2+}, but not in maize annexins ZMANN33 and ZMANN35. As mentioned prior, the motifs, if present, are found on the fourth repeat. However, on the fourth repeat, the calcium-binding site is also present, which suggests that some competition for binding can be exhibited (Mortimer *et al.*, 2008).

Annexins also showcase peroxidase activity thanks to the S3 cluster in their structure, which consists of two cysteine residues and a methionine residue (Hofmann *et al.*, 2003). However, this characteristic will be discussed in greater detail in a later chapter.

2.2.1.2 Annexin genes

When annexins in the animal and plant kingdoms are compared, it is apparent that annexins in plants are a smaller and simpler group. The expression of annexin genes in plants is very specific to the conditions of the plant and distinct cell types. Though apparent differences between the proteins, their gene sequences have shown significant

degrees of similarity. Annexins represent a very old protein family, possibly tracing its origins back one billion years, only in photosynthetic organisms (Jami *et al.*, 2012). In evolution, the structures of genes and therefore also proteins have become more diverse. Nevertheless, plant annexins have overall stayed a highly conserved group in the process of evolution. The amino acid sequences of animal and plant annexins do not show more than 45% homology. Regardless of their limited similarity plant annexins still retain the characteristic annexin structure (Clark *et al.*, 2012).

Annexins can be found in almost every strand of the plant lineage. The number of genes encoding these proteins differs from species to species (Xu *et al.*, 2016). Nevertheless, the number of genes does not reflect the exact reality of the number of proteins in organisms due to alternative splicing, which has been suggested to affect predominantly annexins in monocotyledonous plants, creating additional transcripts (Jami *et al.*, 2012; Morgan & Fernández, 1997)**.** The presence of an alternative splicing mechanism has been documented largely in the annexin A family in vertebrates, creating different isoforms of the proteins (González-Noriega *et al.*, 2016). The chromosomal distribution of annexin genes is rather varied. In multiple plants, multiple annexin genes can be found on the same chromosome. For instance, there are four out of eight annexin genes present solely on the fifth chromosome in *Arabidopsis thaliana* (Cantero *et al.*, 2006). In the case of radish (*Raphanus sativus*), the third, fourth, fifth and seventh chromosomes all contain two annexin genes. The sixth and eighth chromosome both contain one annexin gene while no annexin gene sequences are present on the first, second and ninth chromosome (Shen *et al.*, 2021). Some annexin genes showed a tandem organisation on the chromosomes of their location. Some of the protein products of these tandem genes showed a significant similarity in their amino acid sequence, also suggesting functional similarities. When the exon-intron structure of annexin genes in different green plant lineages was put to analysis, it was discovered that the number of introns varied considerably from 0 – 8. The different number of introns, specifically the loss of introns, is an important evolutionary mechanism in annexin genes. It also shows that annexin genes in the green plant family have a common ancestry (Jami *et al.*, 2012).

2.2.1.3 Post-translational modifications

As previously mentioned, the structure of plant annexin can be altered by post-translational modifications. For this process, the proteins have several sites, such as phosphate sites or glycosylation sites. These sites are present on both the concave and

convex sides, with the calcium-binding site being present on the latter one. The modification can also affect the protein's C-terminal and the N-terminal core (Konopka-Postupolska *et al.*, 2011).

As briefly noted before, annexin exhibits peroxidase activity. This activity was found to be dependent on the post-translational modifications, namely phosphorylation, present on the protein. The peroxidase activity decreased when such a protein was dephosphorylated (Gorecka *et al.*, 2005). Rice annexins have been reported to interact with multiple kinases such as receptor-like kinases (RLK) Os01g02580, SPK-3 kinase Os01g64970, casein kinase Os01g64970 and Ste20-related protein kinase (SLK) Os10g37480. The last mentioned is a kinase functioning in the MAPK pathways (Rohila *et al.*, 2006). The association with the Ste20-like kinase is in agreement with the function of annexins in the plant's responses to stress and growth (Konopka-Postupolska *et al.*, 2011). *Arabidopsis thaliana* annexin 1 (ANNAT1) has been shown to be phosphorylated by cold-induced protein kinase open stomata 1 (OST1). This interaction changes Ca^{2+} transport and consequently impacts the plant's response to cold temperatures (Liu *et al.*, 2021). Annexins are also phosphorylated during the plant cell's response to salt stress when the SOS pathway is activated. Annexins in *Arabidopsis thaliana* are also affected by the *S*-nitrosylation of their cysteine residues (Lindermayr *et al.*, 2005). Cysteine residues are also susceptible to *S*-glutathionylation, affecting their calcium-binding ability (Konopka-Postupolska *et al.*, 2009).

2.2.1.4 Annexins in *Arabidopsis thaliana*

In the genome of *Arabidopsis thaliana*, a total of eight annexin genes were found. Out of the eight genes, two, *ANNAT3 (At2g38760)* and *ANNAT4 (At2g38750)*, were located on chromosome 2 and were organized in a tandem manner. The genes *ANNAT6 (At5g10220)* and *ANNAT7 (At5g10230)* are also in tandem though on chromosome 5. *ANNAT2 (At5g65020)* and *ANNAT8 (At5g12380)* genes are found on the same chromosome. Chromosome 1 hosts the *ANNAT1 (At1g35720)* and *ANNAT5 (At1g68090)* genes. The last four mentioned genes are not in a tandem organization. The genes *ANNAT3, ANNAT4, ANNAT5* and *ANNAT8* have a similar structure, each consisting of six exons. The four remaining genes have all lost introns, although in different positions and numbers. Despite the differing structures of these genes, some share more similarities. *ANNAT2, ANNAT6* and *ANNAT7* share 80 – 86% of their nucleotide sequence and 76 – 83% of their amino acid sequence, showing a high level of resemblance. In the

protein product of these genes, we can find the characteristic annexin sequence, which acts as the calcium-binding site. However, it is important to note that ANNAT4 essentially lacks the calcium-binding sites (Cantero *et al.*, 2006).

2.2.2 Annexins and ion channels

The connection between the cytosol and the extracellular matrix can be ensured in multiple ways, and ion channels are one of them. Ion channels represent hydrophilic pores in the cellular plasma membrane that mediate a passive, energy-independent transport of ions through the lipid bilayer. Primarily, inorganic ions such as Ca^{2+}, Cl^-, Na^+ or K^+ travel through these channels. Ion channels have shown ion selectivity, permitting specific ions to pass but not others, thanks to the narrow structure of the channels, as only ions of the appropriate charge and size may pass through. Furthermore, ion channels are not open continuously, they open and then close again. This change is regulated by stimuli, which can be of different natures, but the most common is voltage. Ion channels modulated by changes in voltage are called voltage-gated channels. The movement of ions across membranes creates and controls the electrical potential of membranes. The general structure of these channels includes α-helix transmembrane subunits, which collectively form a central pore (Alberts *et al.*, 2002).

Ca^{2+} plays a very important role in cellular processes, especially in initiating plant responses to stress. Plants primarily absorb Ca^{2+} ions through their root system and these ions are moved into and out of cells through ion channels. Several types of channels transporting Ca^{2+} have been identified in the plasma membrane (PM) of root cells, including depolarisation-activated calcium channels, hyperpolarisation-activated calcium channels, Ca^{2+}-permeable voltage-independent cation channels and Ca^{2+}-permeable outward-rectifying K^+ channels. Annexins can be found in the hyperpolarisation-activated calcium channel group (White *et al.*, 2002).

Annexins, as ion channels, have been studied mostly in animals, nevertheless, they still need to be fully understood. The channel formation in animals could involve the phospholipid bilayer disruption by a monomer of the annexin protein. The pore in the centre of the protein's structure functions as the channel's pore. In this way, the protein becomes a part of the membrane instead of just being bound to it (Kourie & Wood, 2000). Two salt bridges are necessary for the channel formation and functioning (Liemann *et al.*, 1996).

The most analysed *Arabidopsis thaliana* annexin ANNAT1, has shown ion channel formation. The surrounding conditions play a very important role in this case. In neutral pH, the ion formation requires much time. On the other hand, when pH values decrease, the time needed for ion channel formation also decreases. It was observed that at pH 5,8 the channels formed the fastest. The decrease in pH is accompanied by changes in the protein's structure, namely the exposure of hydrophobic parts of the protein. Oligomerization, considered a key feature of ion transportation, also occurs when the pH is lower than 7 (Gorecka *et al.*, 2007; Mortimer *et al.*, 2008).

The assertion that annexins function as ion channels is somewhat controversial, as most observations have been made on artificial phospholipid bilayers using *in vitro* conditions. From the beginning, the annexin-based ion channels were considered atypical (Moss & Morgan, 2004). Konopka-Postupolska *et al.* (2011) go as far as to say that these channels do not fit the definition of ion channels and propose that the term ion channel is inappropriately used for annexins.

As much as the annexins functioning as ion channels themselves is controversial, their role in regulating ion transportation through ion channels is far less controversial. It was reported that several annexins across multiple species play a role in Ca^{2+} and K^{+} movements across the plasma membrane of plant cells (Yadav *et al.*, 2018). When plants are exposed to stress stimuli, reactive oxygen species (ROS) production becomes one of the main defence mechanisms. The production of ROS is linked to concentration changes of cytoplasmic Ca^{2+} ($[Ca^{2+}]_{cyt}$). Annexins have been found to play a role in ion homeostasis and reduction of oxidative damage (Saad *et al.*, 2020). Specifically, it is an increase of $[Ca^{2+}]_{cyt}$ that is the usual change (Yadav *et al.*, 2018). *Arabidopsis thaliana* ANNAT1 has been identified as an important factor in Ca^{2+} influx and in K^{+} efflux activated by hydroxyl radical ($HO^{\bullet}$), which is generated during stress (Laohavisit *et al.*, 2012). Maize annexins, ZMANN33 and ZMANN35, have been involved in the modulation of $[Ca^{2+}]_{cyt}$ by creating an influx of calcium ions (He *et al.*, 2019). The annexin 24 from *Capsicum annuum* has also been characterized as a player in Ca^{2+} influx (Hofmann *et al.*, 2000).

2.2.3 Membrane trafficking

Transport of various chemical components within the cell and towards the outside is ensured by a system of membrane trafficking. The complex system of membrane trafficking allows cellular compartments to exchange information through the exchange of macromolecules and particles, ensuring the proper functioning of the cell. The components of the trafficking pathways slightly differ between animal and plant cells as they do not contain the same structures. However, the main organelles involved remain the same, namely the endoplasmic reticulum (ER) and the Golgi apparatus. Other components include the trans-Golgi network (TGN), multivesicular bodies/prevacuolar compartments (MVB/PVC), or several types of vacuoles such as lytic (LV) or protein storage vacuoles (PSV). The plasma membrane (PM) plays a major role in this machinery. The TGN present in plant cells is equivalent to early endosomes (EE) in animal cells. The MVB/PVC in plant cells corresponds to late endosomes (LE) in animal cells, and the vacuoles in plant cells are the equivalent of lysosomes in animal cells (Konopka-Postupolska & Clark, 2017). Membrane trafficking includes two main pathways. Endocytosis refers to the process of internalization of extracellular material into vesicles created by the invaginations of the PM (Paez Valencia *et al.*, 2016). The second one is the secretory pathway, which delivers cargo to the PM for exocytosis, vesicle fusion with the PM and the release of the cargo into the extracellular matrix. Moreover, it transports the cargo within the cell from the sites of biosynthesis (Foresti & Denecke, 2008).

Several pathways fall under the category of endocytosis, one of them being clathrin-mediated endocytosis (CME). Clathrin is a protein that forms triskelion units made of three heavy and three light chains. The cargo internalised into clathrin-coated vesicles (CCV) is sorted by adaptor proteins. Once the CCVs are released, thanks to GTPases, the vesicles lose their clathrin coat and become endosomes (Paez Valencia *et al.*, 2016). Endocytosis can also take place in a clathrin-independent manner, such as fluid-phase endocytosis, phagocytosis-like uptake or membrane microdomain-associated endocytosis. Endocytosis plays an important role in the composition and regulation of the plasma membrane, as components of the PM can also be internalised (Fan *et al.*, 2015). Internalized cargo is then delivered to the TGN/EE system and is sorted either for degradation or recycling. Cargo meant for recycling goes back to the PM by recycling endosomes, and the one meant for degradation goes to the vacuoles through MVB/LE

(Dahhan & Bednarek, 2022). The sorting of the cargo in endosomes is facilitated by the endosomal sorting complex required for transport (ESCRT), components of which are present on the TGN/EE and MVB/LE. This is due to the maturation of TGN/EE into MVB/LE, in which the ESCRT machinery is responsible for the creation of the internal vesicles of MVB (Contento & Bassham, 2012).

The secretory pathway includes the so-called early (ESP) and late (LSP) secretion pathways. The ESP includes ER and the Golgi apparatus. The traffic between them is either anterograde or retrograde. Anterograde traffic transports newly synthesized components from the ER to the Golgi apparatus, whilst retrograde traffic mediates the transport from the Golgi apparatus to the ER (Konopka-Postupolska & Clark, 2017). The anterograde transport is associated with coat protein complex II (COPII)-coated vesicles, which are generated from the ER. On the other hand, the retrograde transport is mediated by COPI-coated vesicles, which are released from the Golgi apparatus. Two types of COPI-coated vesicles can be distinguished: COPIa vesicles for the transport from Golgi to the ER and COPIb vesicles that function between the cisternae of the Golgi apparatus (Donohoe *et al.*, 2007). From Golgi secretory cargo can go either to vacuoles or through LSP towards the PM. The direction in which the cargo is directed depends on the presence of specific sorting signals and the receptors on the receiving membrane. The cargo without sorting signals is directed towards the PM, while cargo with sorting signals is transported towards specific compartments (Konopka-Postupolska & Clark, 2017).

2.2.3.1 Regulation of membrane trafficking by Ca^{2+}

Calcium is one of the many regulators of membrane trafficking. The increase of $[Ca^{2+}]_{cyt}$ serves as a trigger for membrane fusion. However, not all membrane fusions are Ca^{2+}-dependent. The secretory pathway consists of Ca^{2+}-dependent and Ca^{2+}-independent steps. The fusion of COPII vesicles is Ca^{2+}-independent, whereas the following step, the fusion between the ER and Golgi intermediate compartment (ERGIC) and the Golgi apparatus, is Ca^{2+}-dependent. It is worth mentioning that the COPII vesicles aren't completely Ca^{2+}-independent. Ca^{2+} stabilizes the vesicles and protects them from fusing back into the original membrane (Hay, 2007).

SNARE (soluble N-ethylmaleimide-sensitive-factor attachment protein (SNAP) receptor) proteins are a fundamental part of membrane fusions as they bring the fusing membranes closer. They are present on both fusing membranes, and we can distinguish

between v- (vesicle) SNAREs and t- (target) SNAREs, (Ungar & Hughson, 2003). The SNARE proteins themselves are not sensitive to Ca^{2+}, but proteins with which they interact are. The interacting proteins are mainly synaptotagmins and calmodulin, both calcium-binding proteins. Synaptotagnims are incorporated into the vesicle membrane which contains v-SNAREs. When bound to Ca^{2+}, it binds directly to the SNARE complex, triggering membrane fusion and the release of the cargo. In other words, exocytosis, specifically Ca^{2+}-dependent exocytosis. Calmodulin binds to vesicle-associated membrane protein 2 (VAMP2), also called synaptobrevin, which is a part of the SNARE complex and plays a role in SNARE membrane fusion. However, when calmodulin binds to Ca^{2+}, its effects are rather inhibitory on the assembly of the SNARE complex and, consequently, on membrane fusion (Di Giovanni *et al.*, 2010). The inhibitory effects do not stop there, though. When the SNARE complex is unassembled, its units inhibit the influx of Ca^{2+} ions but when the complex is assembled, the inhibitory effect disappears (Hay, 2007). The regulatory role of Ca^{2+} can be through the regulation of proteins involved in membrane fusion, such as calmodulin, small GTPases or actin which regulates the movements of vesicles and endosomes, or by modifying the properties of lipid bilayers. (Konopka-Postupolska & Clark, 2017).

2.2.3.2 Annexins and membrane trafficking

Annexins, though not essential, play a role in a large variety of processes within the machinery of membrane trafficking. For example, human annexin A7, also known as synexin, modulates membrane aggregation and fusion by its GTPase activity in a Ca^{2+}-dependent manner (Caohuy *et al.*, 1996). Various annexins were found in different compartments of animal cells, including the PM, nucleus, cytosol and various endomembranes, suggesting a significant functional diversity. Annexin A2, for instance, was shown to be associated with EE in a Ca^{2+}-independent manner, thereby regulating the formation of MVB (Mayran, 2003). Animal annexins have been found to be important for stabilizing COPII vesicles in a Ca^{2+}-dependent manner (Shibata *et al.*, 2015). Another important function of animal annexins involves membrane repair, induced by an influx of Ca^{2+} into the cytoplasm through diverse mechanisms. Annexin A1 and A2, for example, aggregate vesicles at the site of injury and mediate their fusion, while annexin A6 forms a “patch” that helps rupture’s sealing (Blazek *et al.*, 2015; Williams *et al.*, 2023).

In plants, annexins D, are found in various organelles, ranging from the nuclei to the PM, passing through the Golgi apparatus and TGN. Their expression levels also show

variations among different cell types (Clark *et al.*, 1998). Animal annexins can bind to membranes in a Ca^{2+}-dependent or Ca^{2+}-independent manner (Mayran, 2003). Similar to animal annexins, the binding of plant annexins to membranes can occur in a Ca^{2+}-dependent or Ca^{2+}-independent manner, with both mechanisms likely interconnected (Dabitz *et al.*, 2005). Due to annexin's ability to bind to F-actin filaments and membranes, they can engage the cytoskeleton in membrane trafficking pathways (Konopka-Postupolska, 2007). In *Arabidopsis thaliana* ANNAT1 is localized at the PM and in the cytosol (Lee *et al.*, 2004). ANNAT1 was found in association with ANNAT3 in the vacuolar proteome (Carter *et al.*, 2004). ANNAT1 is located at the periphery of epidermal root cells, while ANNAT2 is found at the periphery of epidermal cells in cotyledons and hypocotyls. This suggests their potential involvement in Golgi-mediated transport of polysaccharide precursors to the PM (Konopka-Postupolska & Clark, 2017). ANNAT3 is implicated in the maturation of MVBs and their release into vacuoles (Scheuring *et al.*, 2011). Additionally, ANNAT4 interacts with SNARE proteins at the PM, tonoplast and PCV (Figure 1) (Fujiwara *et al.*, 2014). Although annexins D lack the signalling sequences for secretion from the cell, ANNAT1 has been found in exosomes (Konopka-Postupolska & Clark, 2017; Rutter & Innes, 2017).

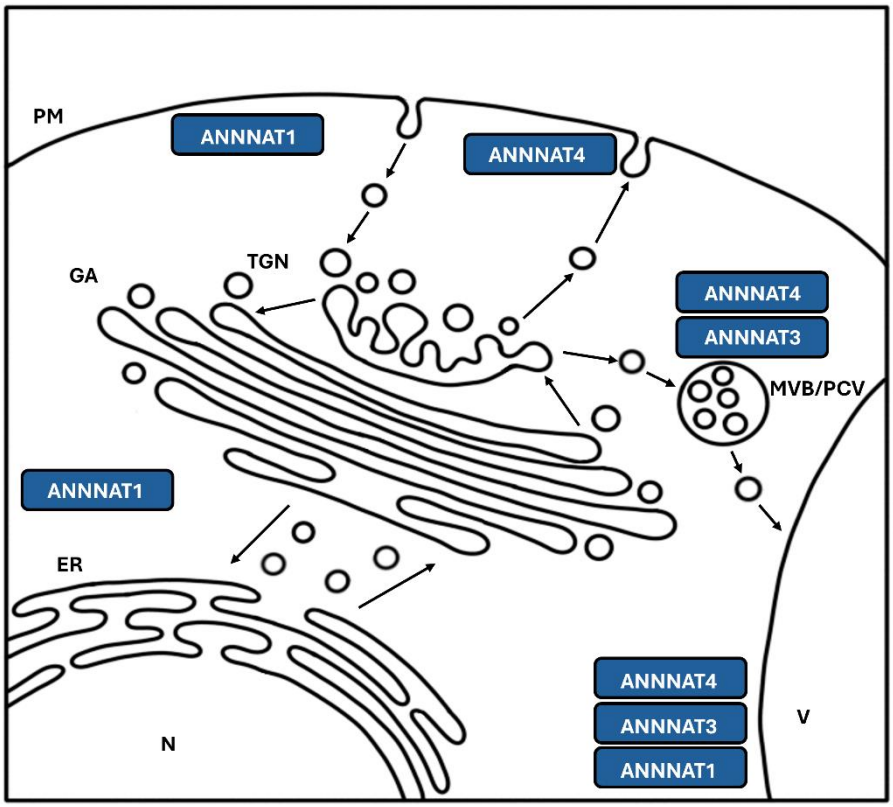

Figure 1: Overview of plant membrane trafficking and the role of *Arabidopsis thaliana* annexins (ANNAT1-4); GA – Golgi apparatus, N – nucleus, V – vacuole, PM – plasma membrane. Based on Carter et al., 2004; Lee et al., 2004; Scheuring et al., 2011; Fujiwara et al., 2014

2.2.4 Plant growth and development

2.2.4.1 Cell polarity

In the formation of some plant organs, the phenomenon of polarity, characterized by the asymmetric distribution of cellular components, plays an important role. A mature plant is formed by cell division, which can be asymmetrical, driven by the polarity of intracellular components, resulting in the formation of two distinct cells (Glanc, 2022). Polarity plays a pivotal role in nearly all tissue and organ formations, notably roots, root hairs and pollen tubes, which exhibit extreme polarization. The mechanisms by which polarity is established in plant cells are diverse, with a major mechanism involving the asymmetrical distribution of proteins and lipids at or within the PM. These molecules are synthesised intracellularly and transported to the PM via membrane trafficking pathways (Yang *et al.*, 2020).

Ca^{2+} has been identified as a regulator of cell polarity. A gradient of Ca^{2+} is observed at the tips of growing pollen tubes and root hairs predominantly facilitated by Ca^{2+} channels, including those formed by annexins. The cellular response to this gradient involves Ca^{2+} binding proteins such as calmodulin (CaM) or Ca^{2+}-dependent protein kinases (CDPK). As noted in a prior chapter, Ca^{2+} also influences membrane trafficking processes, which significantly contribute to tip growth and cell polarity establishment, thereby highlighting the importance of Ca^{2+} in these processes (Himschoot *et al.*, 2015).

2.2.4.2 Root hair growth

Root epidermal cells can be divided into two groups: the cells which form root hair, trichoblasts, and those which do not form root hairs, atrichoblasts. Root hairs are rapidly growing outgrowths of epidermal cells, vastly increasing the surface of roots (Grierson *et al.*, 2014). The differentiation of epidermal cells into trichoblasts and atrichoblasts is a result of different gene expressions issued by signalling pathways (Balcerowicz *et al.*, 2015). Once the epidermal cells have been differentiated, root hair formation can be initiated through cell expansion, which is then focused into a smaller patch. ROP GTPases accumulate at this patch, which begins to bulge out and elongate. The newly formed tip of the root hair becomes loaded with vesicles transporting new cell wall material (Grierson & Schiefelbein, 2002). These vesicles reach the tip through continuous exocytosis, which is heavily affected by the cytoskeleton. The cytoskeleton plays a crucial role in root hair growth, influencing the arrangement of cell wall components and guiding vesicles toward the growth direction, all of which is controlled by Ca^{2+} (Ketelaar *et al.*,

2008; Miller *et al.*, 1999). Ca^{2+} gradients are found in root hairs with concentrations highest at the tip and lower at the base and sides. As Ca^{2+} accumulates at the tip of the root hairs, these ions influence the cytoskeleton and vesicle transport and fusion, indicating a potential role of calcium-binding proteins, namely annexins. This, though not the only parameter, modulates the orientation of the root hair growth (Bibikova *et al.*, 1997; Monshausen *et al.*, 2008).

2.2.4.3 Annexins in plant growth and development

ANNAT1 is expressed in all parts of the plant, most abundantly in the epidermal cells of hypocotyls, roots, and root hairs. Within the root, *ANNAT1* has shown strong expression in the root cap and epidermis, with higher expression in trichoblasts than atrichoblasts. Upon initiation of root hair formation, ANNAT1 accumulates in the formed bulge, suggesting its potential role in this process. During root hair growth, the expression of *ANNAT1* relocates to the root hair itself, while decreasing in the trichoblast cell. In the root cap, the lower cells of the columella and lateral root cap cells exhibit a high ANNAT1 expression. During cell division, ANNAT1 was associated with the mitotic spindle, indicating its role in this process (Tichá *et al.*, 2020). ANNAT1 and ANNAT2 have been shown to play a role in post-phloem transport of sugars into individual cells. *annat1* and *annat2* exhibited impaired primary root growth and root cap development. The transport of sugars, which control root formation and elongation, is restricted by callose deposition in plasmodesmata, through which the sugars diffuse in post-phloem transport. ANNAT1 was shown to have antioxidant activity. The accumulation of ROS in mutant plants leads to callose deposition (Wang *et al.*, 2018). During *Arabidopsis* seed germination, all eight annexins are present. However, shortly after germination initiation, transcriptional levels of all annexins, except *ANNAT4*, exhibit a decrease, despite showing an overall increase over time. Expression patterns vary from gene to gene and tissue to tissue (Cantero *et al.*, 2006). *ANNAT5* expression was found in pollen grains and pollen tubes. Overexpression of *ANNAT5* made pollen grains more resistant to brefeldin A (BFA). On the other hand, when *ANNAT5* expression was downregulated by RNAi, the pollen grains were sterile, indicating a role of annexins in pollen development (Zhu *et al.*, 2014).

During one of the initial phases of seed germination, imbibition, when the seed's water intake is the highest, the PM is susceptible to injuries and disruptions especially when exposed to low temperatures. When maize seeds were exposed to lower temperatures, the expressions of *ZMANN33* and *ZMANN35* were reduced. The protein products of these

genes have been proposed to play a role in the repair of the damaged PM during germination (He *et al.*, 2019). In the primary developmental phase characterized by rapid growth of cotton fibres, a high expression of annexins was found, suggesting their role in cell elongation (Shin & Brown, 1999). The expression of annexins in *Mimosa pudica* was found to be higher at night than during daytime, indicating a potential role of annexins in circadian rhythms in plants (Hoshino *et al.*, 2004). Annexins have also been found in fruits such as strawberries, during whose ripening the expressions of some annexins increased. The expressions were even higher when the fruits were treated with abscisic acid (ABA), an important phytohormone during fruit ripening (Chen *et al.*, 2016).

2.2.5 Annexins and surrounding environment

As sessile organisms, plants are compelled to cope with environmental changes through stress avoidance, stress tolerance, acclimation and adaptation mechanisms. These responses produced by plants often involve alterations in cellular metabolism and physiological activities. Stressors, which are factors potentially disturbing the normal living conditions of the plant, can be divided into two groups, abiotic, involving non-living factors, and biotic, involving living organisms (Nawaz *et al.*, 2023; Tuteja & Singh Gill, 2013). In the absence of stressors, plants can grow unhindered, as their structure remains undamaged and their resources for growth are not limited. However, in the presence of stressors, plants may slow down or inhibit their growth through signalling pathways, leading to negative effects on yield (Zhang *et al.*, 2020).

There are numerous potential stressors, that can affect plants simultaneously, leading to combinations of abiotic and biotic stress. Plants have many possible response pathways that are interconnected and interact to produce complex responses (Peck & Mittler, 2020). Stress can be detected by various organelles, including proteins located in the plasma membrane. One such example is the detection of osmotic stress by calcium channel 1 (OSCA1). When cellular turgor decreases due to osmolarity changes, these channels open, allowing calcium ions, functioning as second messengers, to enter the cell. Ca^{2+} ion transporters also play a role in sensing salt stress, where changes in the Na^{+} ion concentrations result in depolarization of the PM. Annexins, among other Ca^{2+} transporters, are involved in stress responses (Zhang *et al.*, 2022). Once stress is perceived, stress-sensing sensors activate intracellular molecules that have the ability to translate this external stimulus into intracellular signals. These molecules, known as second messengers, represent key regulators of signalling pathways within the cell.

Besides Ca^{2+}, other second messengers are reactive oxygen species (ROS), cyclic nucleotides, nitric oxide (NO) and phospholipids. The signals subsequently undergo a series of kinase cascades, enabling them to reach the nuclei and regulate gene expression (Jain *et al.*, 2018).

2.2.5.1 Calcium signalling

Calcium serves as a second messenger in all eukaryotic cells (Kudla *et al.*, 2018). It also plays pivotal roles in the structure of the cell wall and membranes as well as in growth and development. Ca^{2+} ions are stored in vesicular compartments within the cell, from which they can be released. The intracellular release is dependent on the activation of phospholipase C (PLC), which hydrolyses phosphatidylinositol-4,5-bisphosphate (PIP2) into inositol trisphosphate (IP3), triggering the release, along with diacylglycerol (DAG). Ca^{2+} can also enter the cell from the extracellular space (Jain *et al.*, 2018). Normal $[Ca^{2+}]_{cyt}$ concentration typically ranges from 50 to 200 nM. However, under stress conditions, cytosolic concentrations can increase to the millimolar range. The concentration changes vary depending on the stimulus, tissue type, kinetics, amplitude, duration, and frequency, referred to as the "Ca^{2+} signature" (Xu *et al.*, 2022). These signatures must be decoded by calcium-binding proteins (CBP), which translate them into specific responses, such as protein interactions or transcriptional responses (Jain *et al.*, 2018). CBPs can be grouped into two main categories based on their mode of action: sensor relay proteins, lacking enzymatic activity but binding to targets in a Ca^{2+}-dependent manner, and sensor responder proteins, possessing enzymatic activity that may be Ca^{2+}-dependent (Pirayesh *et al.*, 2021).

Structurally CBPs are divided upon their mechanism of binding to Ca^{2+} ions into proteins presenting EF-hand domains and those lacking this domain. The EF-hand motif is a helix-loop-helix structure, where two helices are oriented perpendicularly to each other, resembling the index finger and thumb. The loop between them serves as the ion binding site. This motif is present in numerous protein families (Yáñez *et al.*, 2012). Calmodulin (CaM, Calcium modulated protein) contains four of these motifs. It is present in all eukaryotes and mediates a wide range of functions due to its interactions with a plethora of CaM-binding proteins (CaMBP). These interactions translate the calcium signal by modifying CaMBPs, either activating or inhibiting them, as some of them possess enzymatic activity. CaMBPs are grouped into CaM-regulated protein kinases (CaMK) (Jain *et al.*, 2018; Perochon *et al.*, 2011). Plants also possess a group of

calmodulin-like proteins (CML), which constitute a diverse group with many potential functions and interactions, initiating further signalling events (Perochon *et al.*, 2011). Another type of CBPs with EF-hand motifs are calcineurin B-like proteins (CBL). After the binding of Ca^{2+}, they undergo conformational changes allowing their interactions with CBL-interacting protein kinases (CIPK) (Plasencia *et al.*, 2021). Additionally, calcium-dependent protein kinases (CDPK), CDPK-related protein kinases (CRK) and calcium- and calmodulin-dependent protein kinases (CCaMK) also contain the EF-hand motif in their structure (Yip Delormel & Boudsocq, 2019).

The group of proteins lacking EF-hand motifs is functionally and structurally diverse. One such protein is phospholipase D (PLD), a phospholipid hydrolysing enzyme. It primarily hydrolyses phosphatidylcholine (PC), generating phosphatidic acid (PA), which is not only a structural element but also serves as a second messenger. PLD contains the C2 domain in its structure which binds Ca^{2+} ions, leading to conformational and functional changes (Kolesnikov *et al.*, 2012). Calnexin (CNX) and calreticulin (CRT) are chaperones found in the ER that bind Ca^{2+} ions (Del Bem, 2011). Pistil expressed Ca^{2+}-Binding Protein (PCP) is a protein expressed in pistils and anthers. It binds Ca^{2+} ions with low affinity and plays a role in pollen development and its interaction with pistils. Annexins are also part of this group of proteins lacking ER-hand motifs as they contain a structurally specific Ca^{2+} binding site. The amplified signal, which initiates a cascade of events, may ultimately target a specific transcription factor that regulates stress-responsive genes (Figure 2) (Tuteja & Mahajan, 2007).

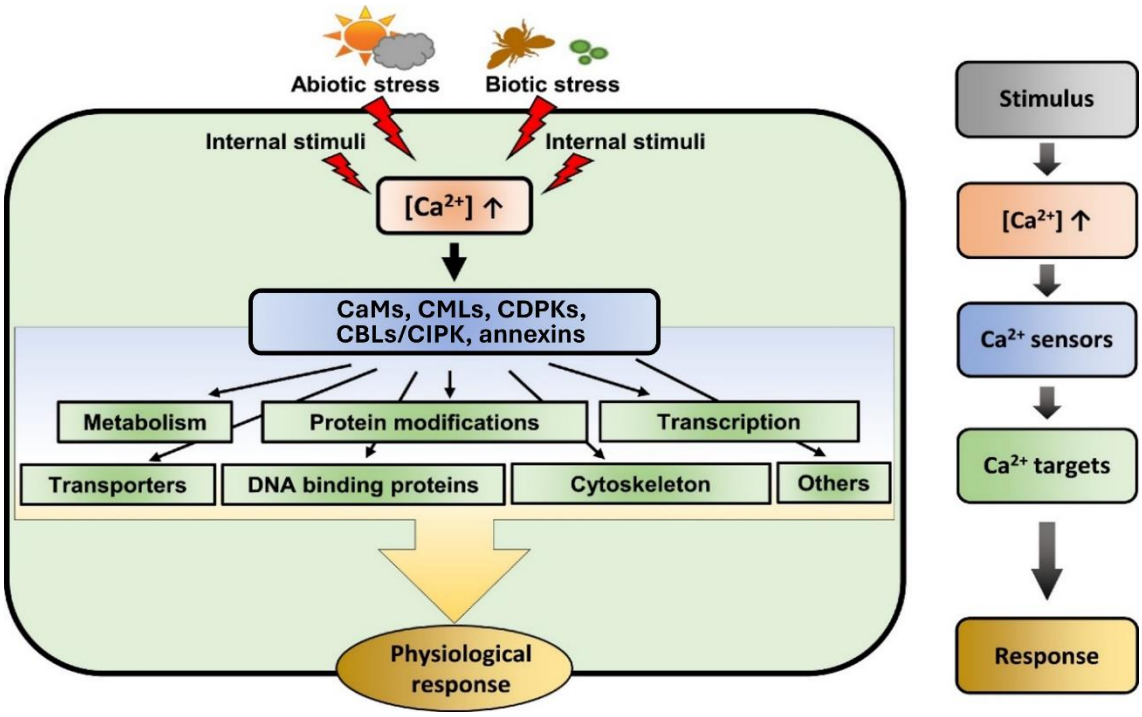

Figure 2: Overview of calcium signalling in plant cells. Adapted from Pirayesh et al., 2021, with modifications

2.2.5.2 Annexins and biotic stress

Plants recognize pathogens through specific pattern recognition receptors (PRR). They have developed effector-triggered immunity (ETI) against pathogens initiated by the protein products of R genes (R proteins). ETI stimulates programmed cell death in the infected area, triggering a hypersensitive response (HR). Pathogenesis-related (PR) genes play a significant role in these responses, as their protein products actively contribute to the plant's defence. These defences are intricately linked to phytohormones, namely jasmonic acid (JA), salicylic acid (SA) and ethylene (ET). These hormones regulate the expression of numerous genes involved in plant defence mechanisms (Iqbal *et al.*, 2021).

Annexins have been shown to participate in defence reactions, with their expressions regulated by various hormones. The responses in which annexins participate are non-specific, likely forming part of the general defence response (Yadav *et al.*, 2018). For example, tobacco annexin *NTANN12* was found to be expressed in tobacco BY-2 cell suspensions infected by *Rhodococcus fascians*, with expression levels increasing over time. However, no expression was observed in cultures infected by *Agrobacterium tumefaciens* and *Escherichia coli*. Nevertheless, as NTANN12 was involved in multiple cellular responses, it indicates the non-specificity of annexins (Vandeputte *et al.*, 2007).

Furthermore, tobacco plants overexpressing *ANNBJ1*, an *ANNAT1* homolog from *Brassica juncea*, when infected by *Phytophthora parasitica var. Nicotianae*, showed higher degrees of resistance, likely due to elevated expression of PR genes (Jami *et al.*, 2008). Additionally, *Arabidopsis thaliana* annexins ANNAT1 and ANNAT4 have been shown to interact with MiMIF-2, a macrophage migration inhibitory factor. Plants overexpressing *ANNAT1* and *ANNAT4* displayed lower susceptibility to *Meloidogyne incognita* (Zhao *et al.*, 2019).

2.2.5.3 Annexins during drought and salt stress

Salt and drought stress, along with cold temperature stress, induce osmotic stress in plants. Salt stress leads to the accumulation of Na^+, the deficiency of K^+ and changes of the cell's turgor. One of the pathways how to deal with the excess of Na^+, which is toxic for plants, is the salt overly sensitive (SOS) pathway (Lee *et al.*, 2004). This pathway comprises three main protein components: SOS3, a Ca^{2+} binding protein; SOS2, a serine/threonine protein kinase; and SOS1, an Na^+/ H^+ antiporter localized in the PM. The presence of salt stress results in an increase in cytosolic Ca^{2+} levels. Ca^{2+} binds to SOS3 which then binds to and activates SOS2, creating a SOS2-SOS3 complex. This complex subsequently interacts with and activates SOS1, prompting an efflux of Na^+ and preventing its toxicity. In addition to these central components, a wide range of other proteins are involved in the correct functioning of this pathway. One such protein is annexin 4 (ANNAT4), which functions as a calcium transporter, inducing an increase in cytosolic Ca^{2+} levels, thereby facilitating its interaction with SOS3. ANNAT4 interacts with SCaBP8, a SOS3-like Calcium Binding Protein8, which promotes its interaction with SOS2. SOS2 then phosphorylates ANNAT4 (Ali *et al.*, 2023).

Levels of ANNAT1 are elevated when treated with NaCl as well as ABA. Salt induces the translocation of ANNAT1 from the cytosol to the PM. Knockout mutants of *ANNAT1* and *ANNAT4* are sensitive to salt treatment, suggesting their involvement in salt responses in plants. Furthermore, these mutants also exhibit inhibition of germination when treated with ABA (Lee *et al.*, 2004). The expression of *ANNAT1* is upregulated under multiple stress conditions, with the most significant increase observed under ABA stress. Plants overexpressing *ANNAT1* are more tolerant to drought stress because ANNAT1 prevents the loss of turgor and subsequent wilting (Konopka-Postupolska *et al.*, 2009). Additionally, responses to stress are influenced by light. Plant cells contain cryptochromes, photoreceptors that sense light signals, regulate ion channels and induce

downstream responses. ATCRY2, a cryptochrome from *Arabidopsis thaliana*, negatively regulates drought tolerance. ATCRY2 interacts with ANNAT2 and ANNAT3, inhibiting their function in drought tolerance by negatively influencing ion flow across the PM mediated by ANNAT 2 and ANNAT3 (Liu *et al.*, 2021).

Annexins exhibit peroxidase activity. Peroxidases belong to an enzyme family that catalyses reactions in which H_2O_2 is broken down into water and oxygen. They play a crucial role in protecting cells from the harmful and toxic effects of ROS accumulation during stress (Mortimer *et al.*, 2009). Several annexins contain an S3 cluster (Cys-Met-Cys) in their structures. This S3 cluster has been suggested to act as a redox reactive centre where the peroxidase reaction takes place. However, for the peroxidase activity of annexins to be physiologically relevant, the proteins may need to undergo post-translational modifications. This activity provides annexins a significant influence on the plant's responses to stress, as ROS are generated in response to various types of abiotic stress (Gorecka *et al.*, 2005; Konopka-Postupolska *et al.*, 2009).

2.2.5.4 Annexins during temperature stress

Heat stress (HS) is sensed by cells through an increase in cytosolic Ca^{2+} levels. *ANNAT1* levels increase following HS, while knockout mutants of *ANNAT1* and *ANNAT2* are sensitive to HS, indicating a role for annexins in HS. In these mutants, expression levels of heat shock factors (HSF), which regulate heat shock proteins (HSP) levels, decrease, suggesting that the two annexins are required for the gene expression of HSFs and HSPs. The increase in Ca^{2+} levels is not as pronounced as in wild type plants, highlighting the role of annexins in calcium transport (Wang *et al.*, 2015). MYB30 is a transcription factor involved in multiple stress responses including HS. It binds to the promoters of *ANNAT1, ANNAT2, ANNAT3* and *ANNAT4*, repressing their expressions. *myb30* mutants demonstrate increased resistance to HS, with a more significant increase in Ca^{2+} levels (Liao *et al.*, 2017). Rice *ANNOS1* knockdown mutants are more sensitive to HS and drought stress. HS induces the overproduction of ROS, resulting in higher levels of *ANNOS1,* which upregulate superoxide dismutases (SOD) and catalases (CAT), enzymes involved in detoxifying these molecules (Qiao *et al.*, 2015). Annexins also play a role in low temperature stress (LT). Two annexins in wheat, p34 and p36, exhibit higher expression levels under LT. These annexins may be involved in early LT signal transduction, leading to cold acclimation (Breton *et al.*, 2000).

3 MATERIAL AND METHODS

3.1 Material

3.1.1 Plant material

Arabidopsis thaliana (L.) was selected as the plant material for the mutant lines and as the control material, for which the Columbia ecotype (Col-0) was used.

The following T-DNA insertion mutant lines were used during the experimental part:

- *ann1,* SALK_095886C
- *ann3,* SALK_082344C
- *ann4,* SALK_019725C

For crossing with *ann3* mutant *A. thaliana* lines carrying fluorescent endosomal markers, ANN1-GFP, VTI1-mCherry, RabF2b-mCherry, YC3.6, were used.

3.1.2 Chemicals and laboratory material

Duchefa Biochemie: Murashige and Skoog Medium Basal Salt Mixture

Nippon Genetics: Midori Green Advance

Sigma Aldrich: 2-(N-morpholino)ethanesulfonic acid (MES), agarose, acetic acid (CH_3COOH), glycerol, hydrochloric acid (HCl), potassium hydroxide (KOH), tris-hydrochloride (Tris-HCl)

Thermo Fisher Scientific: 5x Phire Reaction Buffer, 6x DNA Loading Dye, 10X FastDigest Green Buffer, DNA Dilution Buffer, dNTP Mix**,** Gellan gum, GeneRuler 1 kb Plus DNA Ladder, Phire Hot Start II DNA Polymerase

PENTA: Ethanol (70%, 96%), sucrose

3.1.3 Solutions

Half-strength Murashige and Skoog medium (½ MS)

1 $g \cdot l^{-1}$	2-(N-morpholino)ethanesulfonic acid (MES)
10 $g \cdot l^{-1}$	sucrose
2,15 $g \cdot l^{-1}$	Murashige and Skoog Medium Basal Salt Mixture
8 $g \cdot l^{-1}$	Gellan gun
	MilliQ water

pH 5,8, sterilized by autoclave

1x TAE buffer:

40 mM	Tris-HCl
20 mM	acetic acid
1 mM	EDTA
	MilliQ water
	pH 8,6

1% agarose gel:

1 g	agarose
1 µl	Midori Green Advance
100 ml	1x TAE buffer

Clearing solutions:

1.	60 ml	96% ethanol
	20 ml	100% glycerol
	20 ml	CH_3COOH
2.	30 ml	96% ethanol
	10 ml	100% glycerol

3.1.4 Software

ApE – A plasmid Editor (https://jorgensen.biology.utah.edu/wayned/ape/)

Epson Scan (Seiko Epson)

Image J (NIH, https://imagej.net/ij/)

ImageLab 6.1 (Bio-Rad Laboratories)

Office 365 (Microsoft)

SnapGene (Dotmatics)

ZEN Blue edition (Carl Zeiss)

ZEN Black edition (Carl Zeiss)

3.1.5 Devices

Analytical scale XA 110/2X (Radwag)

Autoclave (Stervap, MMM Group)

Automatic pipettes (Eppendorf)

Confocal laser scanning microscope (CLSM, LSM 710, Axio Imager Z2, Carl Zeiss)

Convention oven MOV-212F (Sanyo)

Epifluorescent microscope (Axio Imager.M2, Carl Zeiss)

Fluorescence stereo zoom microscope (Axio Zoom.V16, Carl Zeiss)

Fume hood (Merci)

Growth chambers (Weiss Gallenkamp)

Gel Doc EZ Imager (Bio-Rad Laboratories)

Laminar box (Merci)

Microcentrifuge tubes (Eppendorf)

pH metre EDGE (Hanna Instruments)

PowerPac™ Basic Power Supply (Bio-Rad Laboratories)

Precision balance ES1501 (BEL-Engineering)

ImageScanner III/Expression 10000XL (Seiko Epson)

Solaris Loop Sterilizer (Schuett-biotech)

Stereo microscope MSZ5000-TL-LED (A.KRÜSS Optronic GmbH)

T100 Thermal Cycler (Bio-Rad Laboratories)

Wide Mini-Sub Cell GT Cell (Bio-Rad Laboratories)

3.2 Methods

3.2.1 In silico analysis

To generate gene maps and primer design for *ANNAT1* (locus tag AT1G35720), *ANNAT3* (locus tag AT2G38760) and *ANNAT4* (locus tag AT2G38750) coupled with their modifications for the selected SALK mutant lines (SALK_095886C for *ANNAT1*, SALK_082344C for *ANNAT3* and SALK_019725 for *ANNAT4*), TAIR (The Arabidopsis Information Resource, https://www.arabidopsis.org/index.jsp) and SIGnAL (Salk Institute Genomic Analysis Laboratory, http://signal.salk.edu/) databases were used. The DNA sequences were acquired using the Sequence Viewer tool of TAIR, which allows visualisation of annotated *A. thaliana* genome. Additionally, chromosome positions and orientations of the genes were also obtained in the same way. The positions and orientation of the T-DNA insertions present in the SALK mutants, which were used during experiments, were also identified using TAIR's Sequence Viewer and polymorphisms list. As genotyping of the SALK mutant lines required forward and reverse primers, the SIGnAL T-DNA Primer Design tool was used for primer design. The information acquired from these databases was then integrated using software such as ApE (A Plasmid Editor) and SnapGene to create the gene maps. The calculations of the annealing temperatures of the primers for genotyping were determined by ThermoFisher Scientific T_m Calculator (https://www.thermofisher.com/cz/en/home/brands/thermo-scientific/molecular-biology/molecular-biology-learning-center/molecular-biology-resource-library/thermo-scientific-web-tools/tm-calculator.html).

3.2.2 Growth medium preparation

As the growth medium, ½ MS medium, prepared according to Murashige & Skoog (1962) was used. After the components were weighed out (section 3.1.5 Solutions), MES, sucrose and the basal salt mixture were then dissolved in MilliQ water. The pH was adjusted to 5,8 using KOH or HCl solutions of varying concentrations. Subsequently, this solution was poured into glass bottles containing weighed-out Gellan Gum. The bottles with the medium underwent sterilisation by autoclaving after which the medium was always poured into Petri dishes under aseptic conditions.

3.2.3 Seed sterilisation

Prior to any seed cultivation, all seeds were surface-sterilized. The sterilisation process, comprising three steps, was done in microcentrifuge tubes. Firstly, the seeds were washed in 70% (v/v) ethanol for 5 minutes, followed by a subsequent wash in 96% (v/v) ethanol

for 1 minute. Lastly, they were washed three times with water. All washes were performed by constant shaking. After the final wash, the seeds suspended in water were transferred to a sterile filtration paper using a pipette and left to dry. Upon drying the Petri dishes with the filtration paper and seeds were sterilely closed and moved to a fridge and kept at 4 °C.

3.2.4 Molecular analysis of *ANNAT3* SALK_082344C

In order to validate the presence of the T-DNA insertion in both alleles and ascertain the mutant phenotype in the *ANNAT3* SALK_082344C line seeds, a molecular analysis via genotyping was done. Seeds, obtained from NASC (https://arabidopsis.info/) were surface sterilised as described in section 3.3.2 Seed sterilisation. and they were subsequently sown on ½ MS medium and left to germinate. Subsequently, they were sown on ½ MS medium, stratified overnight, and left to germinate. Following two weeks of growth young true leaves were cut from the plants and their DNA was extracted using a dilution buffer. The leaf tissues were disrupted using a pipette tip in the buffer and incubated on the ice for at least 15 minutes to ensure efficient extraction.

Following the DNA extraction, a polymerase chain reaction (PCR) was performed using two different PCR reaction mixes, with their components listed in Table 1. These mixes contained a different combination of forward and reverse primers (Table 2). One combination was comprised of two primers specific to the wild-type allele, whereas the second mix consisted of one primer specific to the SALK line T-DNA insertion sequence and one primer specific to the wild-type allele. The wild-type allele specific primer combination encompassed a forward primer (left primer, LP) and a reverse primer (right primer, RP), both complementary to analysed DNA sequence. In the second combination, the SALK line T-DNA insertion-specific primer (LBb1.3) served as the forward primer. The reverse primers were the same in both mixes. The temperature programme is detailed in Table 3.

The PCR products were separated using gel electrophoresis on a 1% agarose gel. The gel was prepared by dissolving 1 g of agarose in 100 ml of 1x TAE buffer by boiling until complete dissolution. Following the mixture cooling by submerging it in water, 1 µl of Midory Green Advance was added for DNA visualisation before being poured into a casting tray equipped with a comb. The solidified gel was transferred into an electrophoretic chamber filled with 1x TAE buffer. Additionally, 2 µl of 6x DNA Loading

Dye were added to each sample and the negative control, which contained PCR water instead of DNA. 6 µl of each sample along with the negative control and GeneRuler ™ 1 kb Plus DNA Ladder, were loaded into the wells in the gel and left to separate at a constant electrical voltage of 100V for 30 minutes. The gel was visualised using Gel Doc^{TM} EZ Imager and analysed in the ImageLab programme. Subsequently, the confirmed homozygous plants were transferred from the ½ MS medium where they germinated into soil. Upon maturity and seed production, seeds were harvested for use in subsequent phases of the experiment.

Table 1: Components of the PCR reaction mix using Phire Hot Start II DNA Polymerase.

Mixture component	**Amount (µl)**
PCR water	6,7
5x Phire Reaction Buffer	2
Phire Hot Start II DNA Polymerase	0,2
dNTPs	0,2
Forward primer	0,2
Reverse primer	0,2
Template DNA	0,5
Total amount	10

Table 2: Sequences of the gene specific primers used for the genotyping of *ann3* SALK_082344C, ANN3-LP, ANN3-RP and the T-DNA insertion-specific primer LBb1.3.

Primer	**Sequence**
ANN3-LP	TCCTCAAAACGAAAAATCTCG
ANN3-RP	CATAGCCGCCTCAATAGTAGC
LBb1.3	ATTTTGCCGATTTCGGAAC

Table 3: Temperature programme for genotyping using Phire Hot Start II DNA Polymerase used for the genotyping of *ann3* SALK_082344C.

Step	**Temperature**	**Time**	**Cycle number**
Initial denaturation	98 °C	5 min.	1x
Denaturation	98 °C	5 s	
Annealing	59,9 °C	5 s	40x
Extension	72 °C	20 s	
Final extension	72 °C	1 s	1x
Cooling	4 °C	∞	-

3.2.5 Phenotypic analysis of *ANNAT3* SALK_082344C

The phenotype of *ann3* SALK_082344C plants was analysed using seeds originating from different plants whose homozygosity was verified through genotyping. Due to this, *ann3* plants were categorized into two groups *ann3(L1)* and *ann3(L4)*, with the number in the brackets representing the number of the parent plant used in genotyping. This designation is used throughout the entire phenotypic analysis. After being verified, these plants were planted into soil and their seeds were harvested, surface sterilised and sown onto ½ MS medium. The seeds were sown in triplicate on each Petri dish from each parent plant together with three Col-0 seeds serving as control against which the phenotypes of *ann3* seeds were compared. The dishes containing the seeds were placed in the fridge at 4 °C for their stratification for two days. Subsequently, Petri dishes were partially covered with black opaque plastic foil to mimic natural conditions and placed vertically in a growth chamber (21 °C, 70% humidity, with a photoperiod of 16h light and 8h dark). The seeds remained under sterile conditions in the growth chamber until the 21st day of the analysis.

3.2.5.1 Root phenotypic analysis

The germination rates of the seeds were analysed 24 (1 day after germination, DAG1), 48 (DAG2) and 72 (DAG3) hours after they were placed into the growth chamber. The analysis was conducted by observing the seeds using a zoom microscope (Axio Zoom.V16, Carl Zeiss). The percentage of germinated seeds in each group on each Petri dish was counted. These percentages served for the calculation of the final average germination rates.

Primary root length analysis began on DAG4 when all Petri dishes were scanned. The scanning was repeated on DAG7, DAG10 and on DAG14. On the 14th day due to excessive root length, plants were transferred onto fresh ½ MS medium to facilitate measurement. To measure their primary roots, they were carefully transferred from their original medium to a new one, orienting them for accurate length measurement. The plants subjected to this procedure were excluded from further analysis. The root lengths were then measured using the Image J programme and averages for each day and each group of plants were calculated.

On DAG4, roots were additionally examined using a zoom microscope to visualise the first root hair bulge. The distance from the root tip to the first root hair bulge was

measured using the Image J programme and averages were calculated for each set of plants.

Subsequently, on DAG7, the roots were once more examined by zoom microscope, though this time not in their entire length, for the length of the root hairs present in the bottom half of the roots. The lengths were then measured by using Image J programme. The measured root hair lengths were categorized into intervals, and the percentages of root hairs within each interval were calculated. These percentages served for the calculation of averages for each group of plants.

On DAG14 the number of lateral roots was analysed on the plants which were taken out from their original Petri dishes into new ones. These dishes were scanned, and besides the root length the number of lateral roots was counted using the Image J programme. Average values were determined for each set of plants.

3.2.5.2 Leaf phenotypic analysis

Leaf analysis was conducted on the 21st day after germination as the final step of the phenotypic analysis. Following the analysis, the plants were discarded, and the leaf analysis was conducted under non-sterile conditions.

To analyse leaf morphology, leaf rosettes were detached from their roots. They were then carefully dissembled using tweezers and a stereomicroscope (MSZ5000-TL-LED, A.KRÜSS Optronic GmbH). Disassembly commenced from the cotyledons and proceeded sequentially to the smallest leaves present. The leaves, along with their petioles, were laid down in sequential order on a ½ MS medium to ensure the absence of air bubbles.

Furthermore, leaf rosettes were also evaluated for both fresh and dry weights. Rosettes were firstly separated from their roots and promptly weighed in pre-weighed paper bags to minimize water loss. Subsequently, the bags containing the rosettes were placed in an oven at 70 °C for 24 hours. Afterwards, the dry weight of the rosettes was determined.

The leaf phenotype also involved stomatal analysis. For this, the third true leaves from Col-0, *ann3(L1)* and *ann3(L4)* plants were removed from the leaf rosettes. These leaves were then placed into a first decolorizing solution consisting of glycerol, 96% (v/v) ethanol and acetic acid in a 1:3:1 ratio. The solution was replaced every 20 minutes until most chlorophyll content was removed. For the clearing of remaining chlorophyll, the

leaves were transferred into a second decolorizing solution containing 96% (v/v) ethanol and glycerol (3:1 v/v) overnight. After decolourization, the leaves were mounted in a drop of 100% glycerol on microscope slides, ensuring no bubbles under or on the leaves were present and secured with cover glasses. Leaves prepared this way, were subsequently observed using an epifluorescent microscope (Axio Imager.M2, Carl Zeiss) under bright field conditions for the phenotype of their stomata. Afterwards, the images underwent post-processing according to Melicher *et al.* (2024) in ZEN Blue software for stomatal size measurement, calculated as the area of individual stomata, with averages determined for each set of plants.

3.2.6 Crossing

In order to generate mutant lines for visualizing vesicular trafficking, crossing was performed. For this, *ann3* SALK_082344C plants were crossed with transgenic *A. thaliana* lines carrying fluorescently labelled endosomal markers. Specifically, endosomal markers VTI1, a v-SNARE protein, and RabF2b, a small GTPase, were selected. Both markers were fused with mCherry red fluorescent protein. Additionally, *ann3* plants were crossed with a transgenic line carrying the fluorescent calcium sensor YC3.6 (yellow chameleon 3.6). YC3.6 consists of two fluorescent protein domains, cyan fluorescent protein (CFP) and yellow fluorescent protein (YFP), separated by a calcium-binding protein domain known as calmodulin (CaM) and a calmodulin-binding peptide (M13). In the absence of calcium ions, CaM doesn't bind to M13, resulting in CFP fluorescence emission. When calcium ions bind to CaM, it induces a conformational change, causing CaM to bind to M13. This leads to a decrease in the distance between CFP and YFP domains, thereby facilitating Förster resonance energy transfer (FRET) interaction between them. Consequently, the emission intensity of YFP fluorescence increases while that of CFP fluorescence decreases. By measuring the ratio of YFP fluorescence to CFP fluorescence (YFP/CFP ratio), changes in intracellular calcium levels can be quantified (Whitaker, 2010). Furthermore, a separate cross was conducted between *ann3* plants and those carrying ANNAT1 fused with green fluorescent protein (GFP), termed ANN1-GFP. In this cross *ann3* plants were used as the maternal parent.

The crossing process was done using a stereomicroscope by selecting immature closed flower buds on the *ann3* plants. These buds were carefully opened to expose the pistils and immature anthers, which were subsequently removed with tweezers, to minimize damage to the pistils. Subsequently, open flowers from the paternal plants,

where self-pollination had already occurred and the anthers were rich in bright yellow pollen, were gently detached and the pollen was gently applied onto the exposed stigma. Afterward, the opened flower buds were closed by gently pressing together the separated sepals and petals using tweezers. To prevent confusion or errors, surrounding buds, flowers and siliques on the same branch were removed. The flowers were then allowed to mature, leading to the development of siliques containing seeds. Once the siliques started to change colour from green to yellow and the brown seeds become visible, they were carefully harvested and placed into small microcentrifuge tubes. These tubes had holes in their lids to prevent mould formation. Subsequently, the siliques were left to dry, facilitating the release of mutant seeds.

The plants grown from the collected seeds of the first generation were analysed using a confocal laser scanning microscope (CLSM, LSM 710, Axio Imager Z2, Carl Zeiss). Firstly, the seeds were manually extracted from the siliques, surface sterilised and left in a fridge (4 °C) for two days. Subsequently, the seeds were sown onto ½ MS medium and placed in a growth chamber (21 °C, 70% humidity, with a photoperiod of 16h light and 8h dark). On DAG11 and DAG12, the seedlings were observed under a microscope. Double-sided clear tape was placed on the sides of a microscopic slide and between the bands of tape a droplet of water was placed. The tips of primary and lateral roots were separated and placed into the droplet of water on the microscopic slide. A cover glass was placed over the roots on the tape. The samples were prepared this way under sterile conditions. The samples were subsequently observed using a CLSM microscope.

Additionally, from the same plants of the first generation that were observed underwent microscopic observation, true leaves were isolated for genotyping to confirm their homozygous character for the presence of the T-DNA insertion in both alleles of the *ANNAT3* gene. The genotyping procedure followed the same methodology as previously described, under identical conditions (section 3.2.4)

3.2.7 Statistical analysis

Germination rates, analysis of lateral roots, and stomatal area were analysed in two technical replicates. Leaf rosette weights were analysed in a technical triplicate. All other experiments were conducted as single technical replicates. To evaluate the quantitative results obtained, a one-way ANOVA (analysis of variance) was applied, utilizing a marginal significance level of P>0,05.

4 RESULTS

4.1 *In silico* analysis

Gene maps for *ANNAT1*, *ANNAT3*, and *ANNAT4* alongside their corresponding SALK mutant lines, were created through *in silico* analysis utilizing the TAIR database.

The analysis of the genes unveiled that *ANNAT1* is located on chromosome 1 within the coordinates 13225168-13227239 bp. In contrast, both *ANNAT3* and *ANNAT4* are situated on chromosome 2, with *ANNAT3* present on coordinates 16200944-16202669 bp and *ANNAT4* on 16196265-16198577 bp (Table 4). Using the sequences retrieved from TAIR database sequence gene maps were created (Figure 3, Supplementary data 1 – 3). The analysis of the sequences allowed comparison of the numbers of exons and introns as well as to identification of UTR sequences and start/stop codons. The *ANNAT1* sequence comprises three exons and two introns, while the *ANNAT3* and *ANNAT4* sequences contain six exons and five introns each. *ANNAT1* and *ANNAT3* exhibit a forward orientation, whereas *ANNAT4* displays a reversed orientation.

The gene maps were then subsequently adapted for their selected SALK mutants (Figure 4. Supplementary data 4 – 6), with T-DNA insertion site coordinates retrieved from the TAIR database (Table 5). In *ANNAT1* SALK_095886C line, the T-DNA is inserted into the third exon in a reversed orientation. Similarly, the T-DNA insertion in the *ANNAT3* SALK_082344C line is located in the third exon and is also reversed. In *ANNAT4* SALK_019725C line the insertion is also reversed, however, it is present in the first exon. Additionally, the maps include primers obtained through the SIGnAL T-DNA Primer Design tool. For each mutant, a pair of primers specific to the gene sequence, LP (left/forward primer) and RP (right/reverse primer), are indicated in the maps, along with a primer specific to the T-DNA insertion (LBb1.3). However, only the primers for the *ANNAT3* SALK_082344C mutant were utilized in subsequent parts of the experiment.

Table 4: Brief characterization of genes utilised in the *in silico* analysis

Gene	Chromosome	Coordinates
AT1G35720 (*ANNAT1*)	1	13225168-13227239 bp
AT2G38760 (*ANNAT3*)	2	16200944-16202669 bp
AT2G38750 (*ANNAT4*)	2	16196265-16198577 bp

Table 5: Summary of selected SALK mutant lines for *ANNAT1*, *ANNAT3*, and *ANNAT4*

Gene	SALK line	Insertion position	Insertion site
AT1G35720 (*ANNAT1*)	SALK_095886C	13226616 bp	3rd exon
AT2G38760 (*ANNAT3*)	SALK_082344C	16201532 bp	3rd exon
AT2G38750 (*ANNAT4*)	SALK_019725C	16196673 bp	1st exon

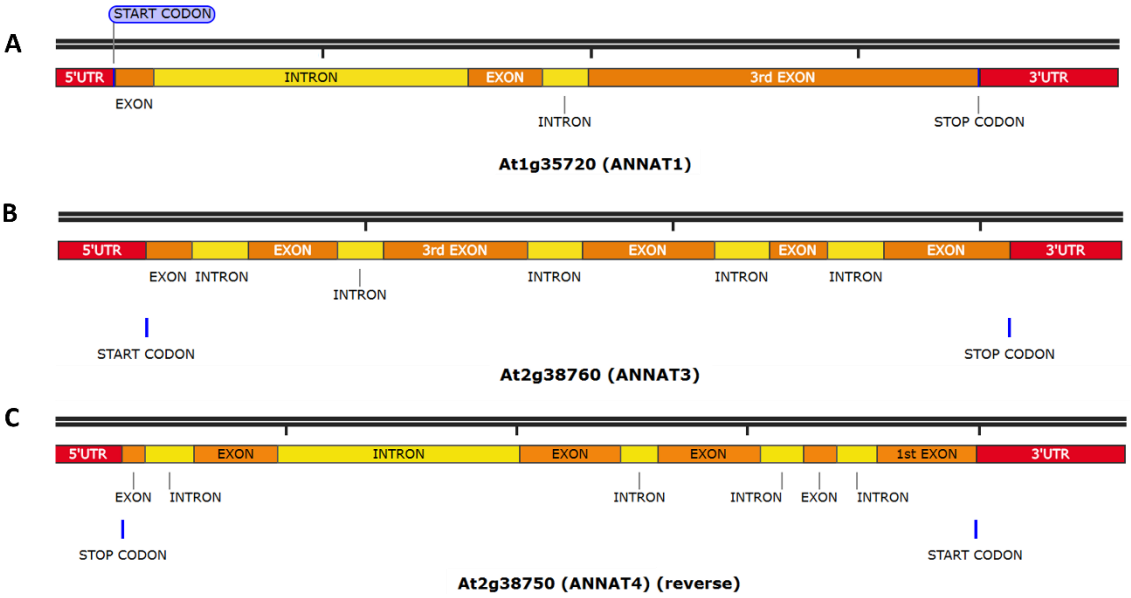

Figure 3: Gene maps of *ANNAT1* (A), *ANNAT3* (B) and *ANNAT4 (C)*. *ANNAT1* and *ANNAT3* are in forward orientation, *ANNAT4* is in reverse orientation, UTRs in red, exons in orange, introns in yellow, stop/start codons in blue. Visualisation prepared in SnapGene software.

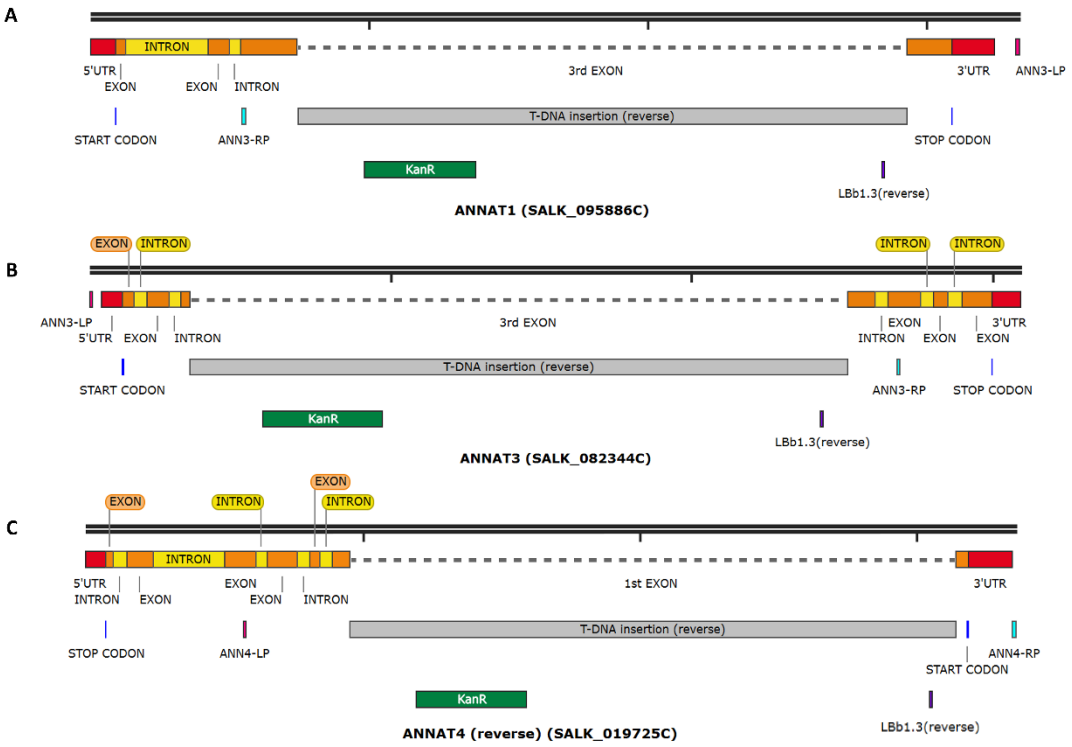

Figure 4: Gene maps of *ANNAT1* SALK_095886C (A), *ANNAT3* SALK_082344C (B), *ANNAT4* SALK_019725C (C). *ANNAT1* and *ANNAT3* are in forward orientation, *ANNAT4* is in reverse orientation, UTRs in red, exons in orange, introns in yellow, stop/start codons in blue, T-DNA insertion in grey, kanamycin resistance (KanR) in green, LP primers in pink, RP primers in cyan, LBB1.3 primer in purple. Visualisation prepared in SnapGene software.

4.2 Molecular analysis of *ANNAT3* SALK_082344C mutants

To verify the presence of T-DNA insertion in the gene of interest in both alleles, indicating homozygosity, genotyping was performed on purchased SALK seeds of the T3 generation. The genotyping included DNA extraction, PCR amplification and subsequent separation of DNA through gel electrophoresis on a 1% agarose gel. Two sets of primers were used: one containing two gene-specific primers and the second one containing one gene-specific primer and one primer specific for the T-DNA insertion. This analysis was carried out for *ANNAT3* SALK_082344C seeds (Figure 4B). The genotyping was performed multiple times as to obtain multiple homozygotes serving as multiple biological replicates during later parts of the experiment.

On the agarose gel (Figure 5), no bands were observed in the gene-specific primer combination alone (Figure 5A), except for those of Col-0 plants used as controls, which did not contain the insertion in either allele. Homozygotes were identified by the presence of a single band in the case of the one gene-specific primer and one insertion-specific primer combination, indicating the presence of the T-DNA insertion in both alleles of the *ANNAT3* gene (Figure 5B). It is worth noting that caution was exercised to avoid misinterpretation, as bands could potentially appear in both primer combinations for heterozygotes, where one allele possessed the T-DNA insertion and the other did not. However, such plants were not identified.

Subsequently, plants confirmed as homozygous were transferred from the ½ MS medium to soil for propagation. Here, they were allowed to develop flowers and later siliques with seeds. The harvested seeds were then used in subsequent analyses.

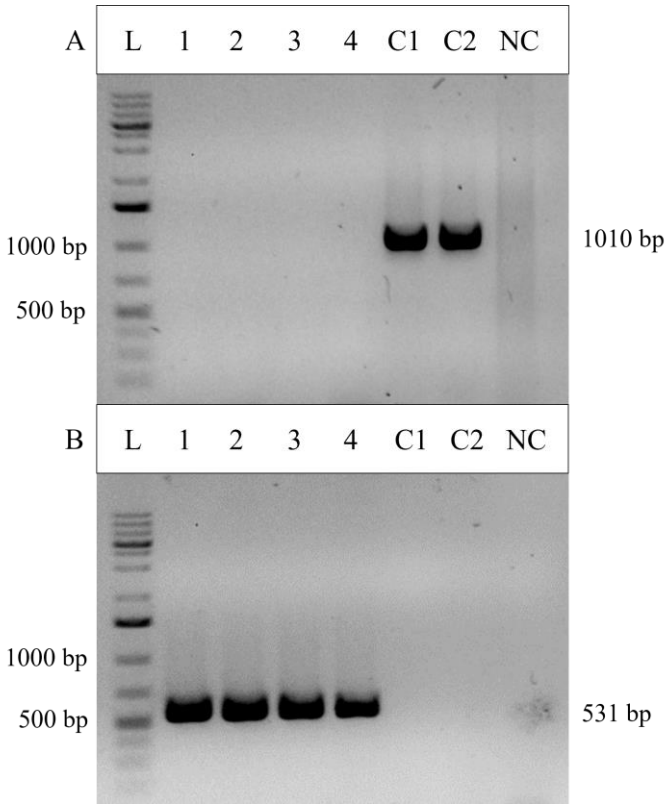

Figure 5: Representative genotyping results of agarose gel electrophoresis of PCR products of *ANNAT3* SALK_082344C mutants. (A) Gene-specific primers, (B) gene-specific primer with a T-DNA insertion-specific primer. L – GeneRuler™ 1 kb Plus DNA Ladder, 1-4 – samples from individual SALK_082344C plants, C – control (Col-0), NC – negative control (PCR water). Predicted size of PCR product for *ANNAT3* wild-type allele is 1010 bp and for mutant allele 531 bp.

4.3 Phenotypic analysis of *ANNAT3* SALK_082344C mutants

Seeds were harvested from the confirmed homozygotes and these seeds were utilized for the phenotypic analysis. The analysis involved comparing control plants (Col-0), which lacked the T-DNA insertion, and *ANNAT3* SALK_082344C plants. The *ANNAT3* line was represented by seeds obtained from two randomly chosen parent plants, *ann3(L1)* and *ann3(L4)*, with the number in the bracket indicating the parent plants from which the seeds were obtained.

4.3.1 Germination rates

The initial phase of the analysis focused on the germination rates of the seeds, which were evaluated over the first 72 hours with screenings conducted using a ZOOM microscope every 24 hours (Figure 6). Figure 7 presents the averages of the germination rates obtained by combining the averages of individual Petri dishes. The germination rates for Col-0 seeds were 74% at 24 hours, 95% at 48 hours, and 96.67% at 72 hours. Similarly, *ann3(L1)* seeds showed a germination rate of 77% rate at 24 hours, 93% at 48 hours, and

94,42% at 72 hours. In contrast, *ann3(L4)* seeds displayed the highest germination rate, reaching 94% already at 24 hours, and maintaining 97% at both 48 and 72 hours. Over the first three days of germination, the only noticeable differences were observed on DAG1, where Col-0 and *ann3(L1)* showed lower rates compared to *ann3(L4)*. However, these differences were insignificant on DAG2 and DAG3. The variation observed between *ann3* seeds was determined to be statistically insignificant, whereas the difference between Col-0 and *ann3(L4)* was significant.

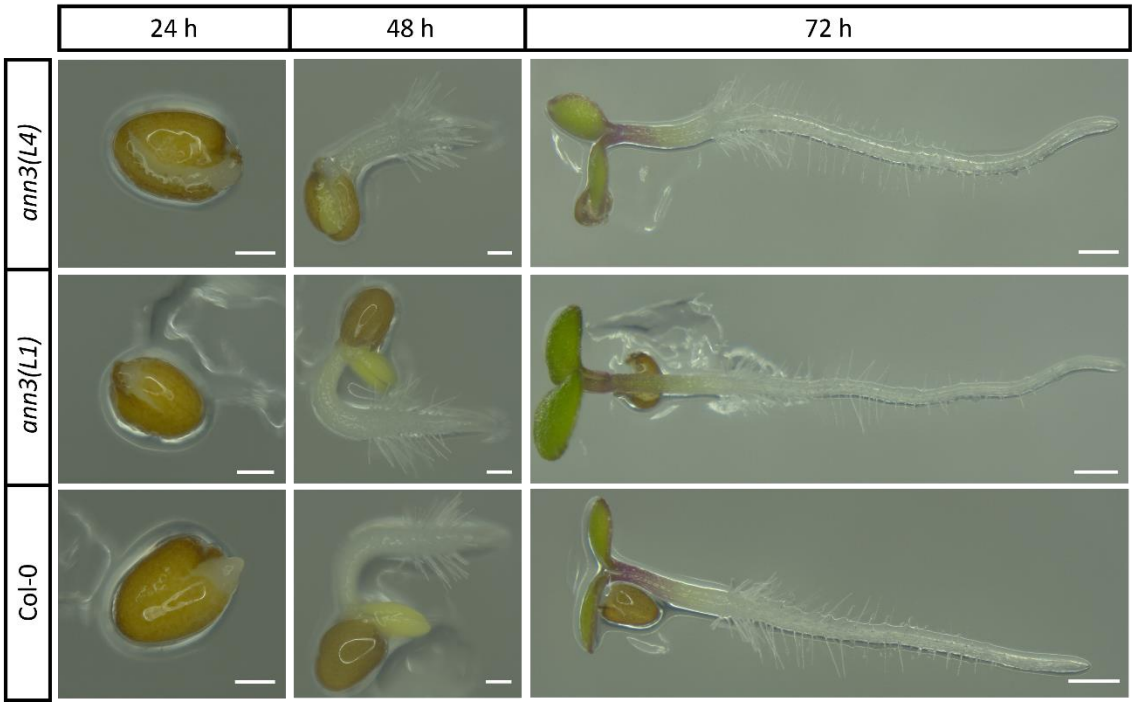

Figure 6: Germination of *A. thaliana* Col-0, *ann3(L1)* and *ann3(L4)* seeds during the first 72 h. Scale bar 200 µm for 24 h and 48 h, 500 µm for 72 h.

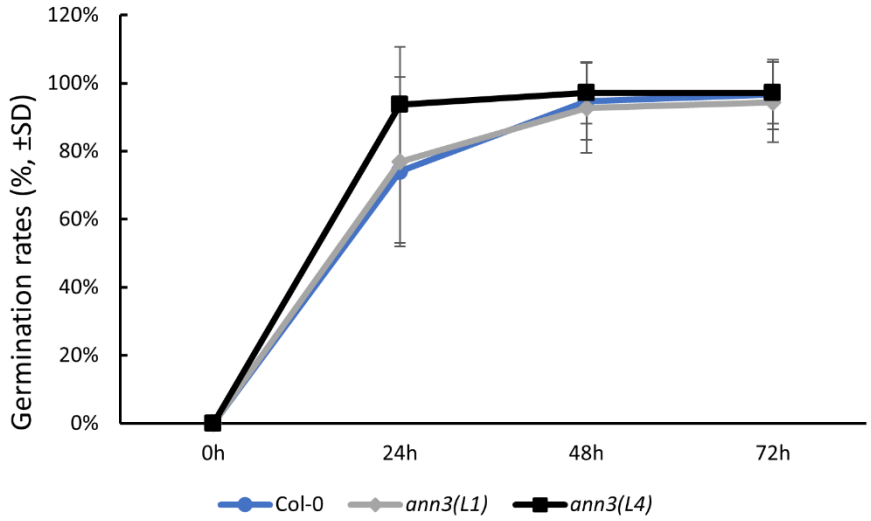

Figure 7: Germination rates of *A. thaliana* Col-0 (N = 70), *ann3(L1)* (N = 65) and *ann3(L4)* (N = 61) seeds over the first 72 hours of germination. Statistical significance at P < 0,05 for 24h.

4.3.2 Root phenotypic analysis

The phenotypic analysis of roots included the measurement of primary root length, the distance between the first root hair bulge and the root tip, the length of root hairs and the determination of lateral root numbers.

The length of primary roots was evaluated on DAG4, DAG7, DAG10 and DAG14 by scanning the Petri dishes containing growing plantlets (Figure 8). Overall, roots of *ann3* plants were longer though the only significant difference in the root lengths was observed on DAG4 between *ann3(L4)* and Col-0 plants. On DAG4, the average length of Col-0 roots was 1,00 cm, compared to 1,10 cm for *ann3(L1)* plants and 1,13 cm for *ann3(L4)* plants. By DAG7, root lengths increased to 3,53 cm for Col-0 plants and to 3,58 cm and 3,63 cm for *ann3(L1)* and *ann3(L4)* roots, respectively. No significant differences were observed on DAG10, with average root lengths of 6,95 cm for Col-0 roots, 7,01 cm for *ann3(L1)* roots and 7,06 cm for *ann3(L4)* roots. For the analysis on DAG14, the roots had to be manually oriented on a new medium to measure the length of the entire roots. The average length of Col-0 roots was 11,56 cm, compared to 12,29 cm for *ann3(L1)* roots and 11,71 cm for *ann3(L4)* roots.

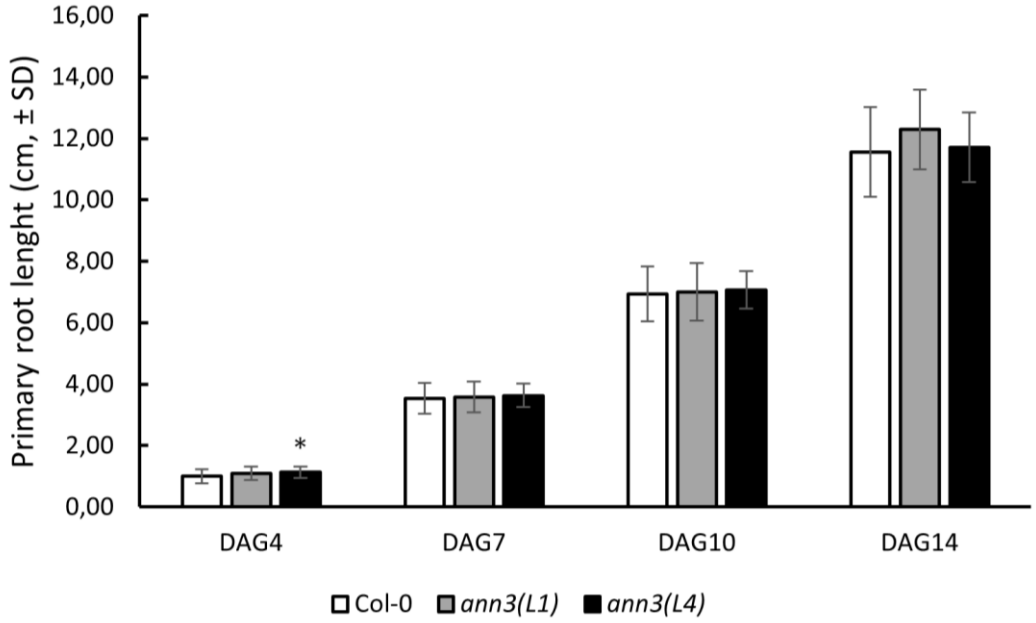

Figure 8: Average lengths of primary roots of *A. thaliana* Col-0, *ann3(L4)* and *ann3(L1)* plantlets on DAG4, 7, 10 and 14. DAG4: Col-0 N = 31, *ann3(L1)* N = 32, *ann3(L4)* N = 29; DAG7 and 10: Col-0 N = 28, *ann3(L1)* N = 28, *ann3(L4)* N = 27; DAG14: Col-0 N = 28, *ann3(L1)* N = 26, *ann3(L4)* N = 26. Statistical significance at $P < 0,05$ for DAG4 (∗).

On DAG4, the roots were observed using a ZOOM microscope (Figure 9) and the distance between the first emerging root hair bulge and the primary root tip was measured (Figure 10). No significant difference was found. The average distance for Col-0 plants was 962,21 µm, 984,03µm for *ann3(L1)* and 906,70 µm for *ann3(L4)* plants.

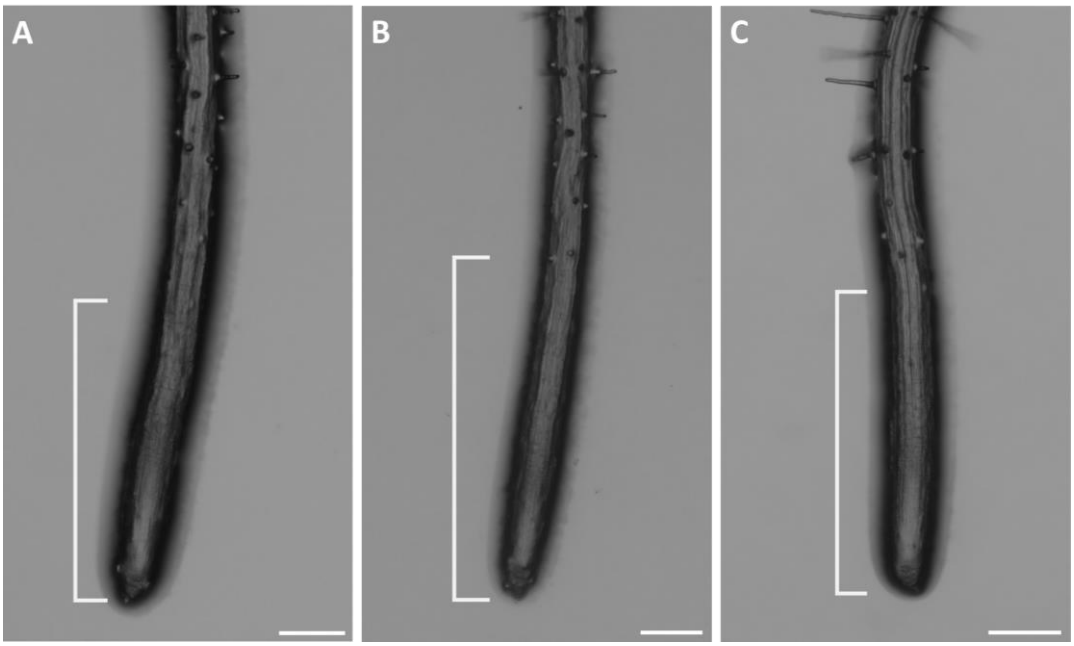

Figure 9: Distances between *A. thaliana* root tips and first root hair bulges on Col-0 (A), *ann3(L1)* (B) and *ann3(L4)* (C) roots on DAG4. Scale bar 200 µm.

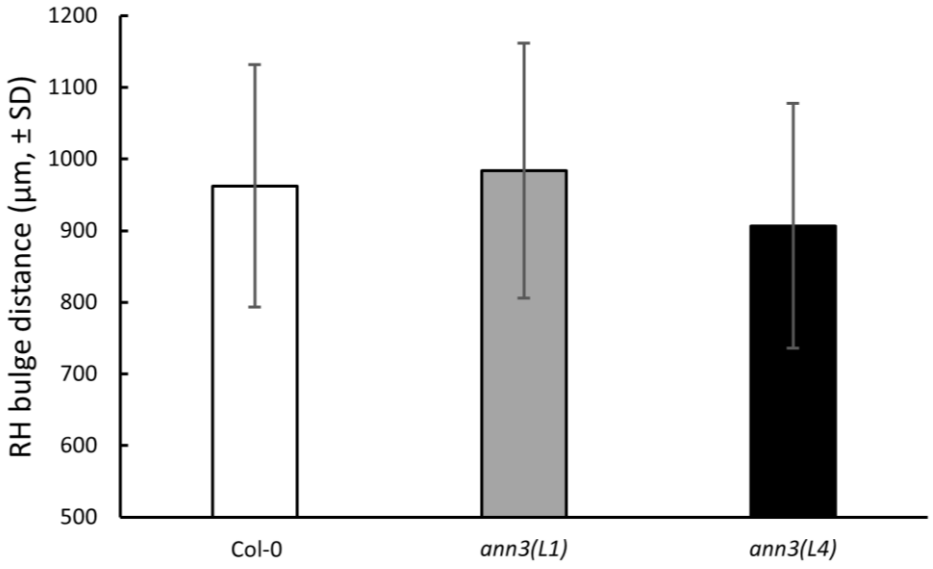

Figure 10: Average distances between root tips and first root hair (RH) bulges of *A. thaliana* Col-0*, ann3(L1)* and *ann3(L4)* plantlets measured on DAG4. N = 10. No statistical significance between samples.

On DAG7, the roots were observed using a ZOOM microscope (Figure 11) and the lengths of root hair starting from the root tip to about the middle of the primary root were measured (Figure 12). The measured root hair lengths were grouped into intervals, and the percentages of root hairs within these intervals were calculated. These percentages served for the calculation of averages for each group of plants. Overall, root hairs of Col-0 plants exhibited greater length compared to those of *ann3* plants. However, across all three groups, the largest proportion of root hairs fell into the 100-199 µm interval. Specifically, 29,74 % of Col-0 root hairs fell into this interval, while it was 31,13 % for *ann3(L1)* and 36,77 % for *ann3(L4)*. The difference between Col-0 and *ann3(L4)* was statistically significant. In the intervals of 200-299 µm and 400-499 µm, the differences between Col-0 and *ann3* root hairs were also significant, with differences observed between Col-0 and *ann3(L1)* in the 200-299 µm and Col-0 and *ann3(L4)* in the case of the 400-499 µm interval.

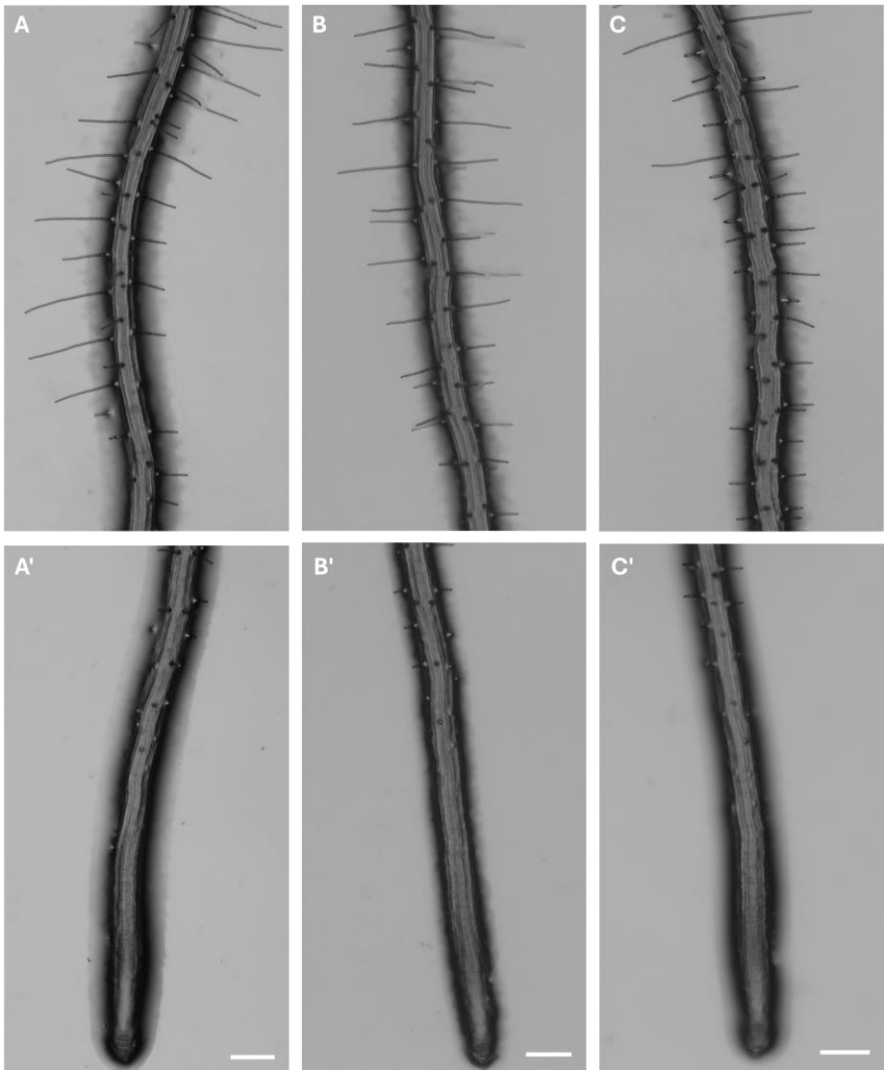

Figure 11: Root hair phenotype of *A. thaliana* Col-0 (A,A'), *ann3(L1)* (B,B') and *ann3(L4)* (C,C') plants analysed on DAG7. Scale bar 200 µm.

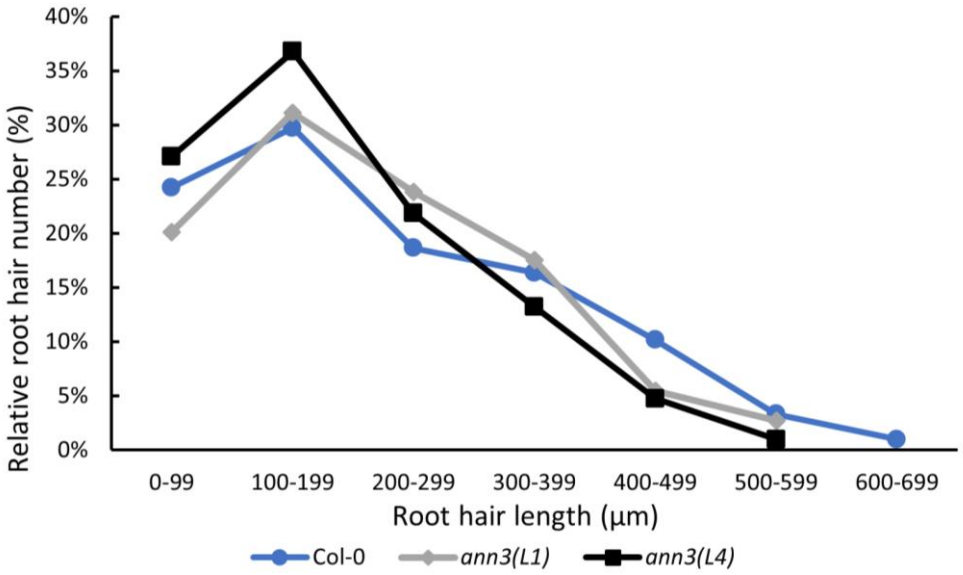

Figure 12: Relative distribution of root hair lengths in *A. thaliana* Col-0, *ann3(L1)* and *ann3(L4)* plants. Images of root hairs for measurement were captured on DAG7. Statistical significance at $P < 0,05$ for intervals of 100-199, 200-299, 400-499.

The number of lateral roots was counted on DAG14 on plants whose roots were manipulated for the analysis of their entire length. The average number of lateral roots for Col-0 plants was 32, whilst it was 38 for *ann3(L1)* and 31 for *ann3(L4)* (Figure 13). The only significant difference was discovered between *ann3* groups themselves.

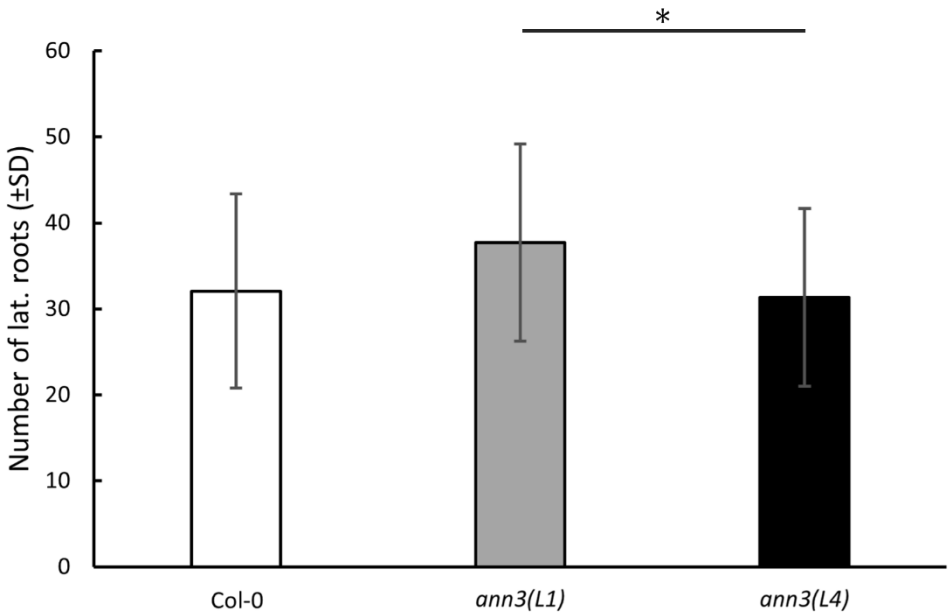

Figure 13: Average number of lateral roots present on *A. thaliana* Col-0, *ann3(L1)* and *ann3(L4)* plants on DAG14. Col-0 N=28, *ann3(L1)* N=28, *ann3(L4)* N=27. Statistical significance at $P < 0,05$ (∗)

4.3.3 Leaf phenotypic analysis

Leaf rosettes were harvested on DAG21 and subjected to analysis of both their fresh weight and dry weight (Figure 14). Immediately after harvesting, rosettes from individual groups of plants were placed in separate paper bags for the measurement of their fresh weight. Subsequently, the bags containing the rosettes were placed in an oven for the determination of dry weights. Comparing the relative weights of *ann3* rosettes, calculated per gram of Col-0 rosettes, revealed higher values in both fresh and dry weights. For 1 g of fresh weight of Col-0 leaf rosettes, the weight of *ann3(L1)* and *ann3(L4)* was 1,150 g and 1,018 g, respectively. Similarly, for 1 g of dry weight of Col-0 leaf rosettes, the weight of *ann3(L1)* and *ann3(L4)* was 2,099 g and 1,390 g, respectively.

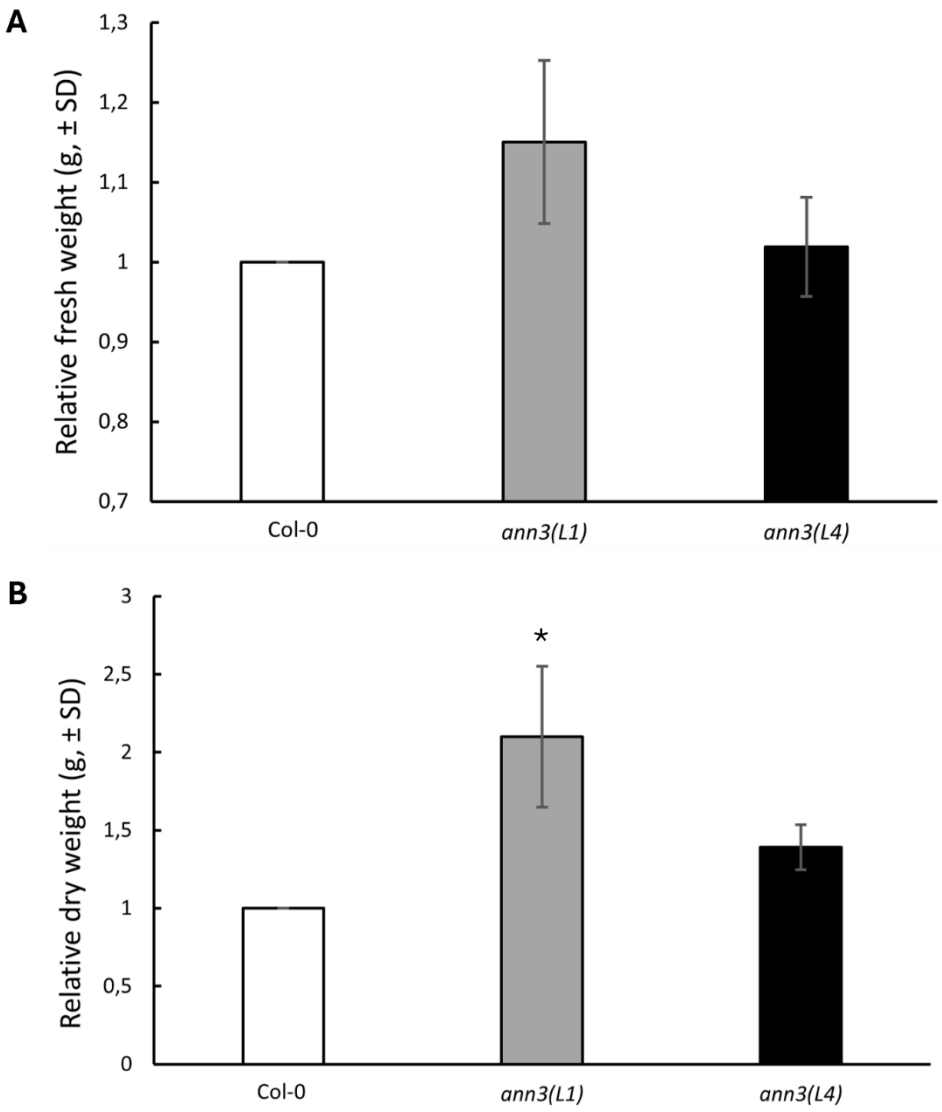

Figure 14: Relative fresh (A) and dry (B) weight of leaf rosettes of *A. thaliana* Col-0, *ann3(L1)* and *ann3(L4)* harvested on DAG21. Statistical significance at $P < 0,05$ (∗).

On DAG21, the leaf rosettes were disassembled, and the individual leaves were spread out flat starting from the cotyledons to the smallest of true leaves on ½ MS medium (Figure 15). It was observed that the cotyledons and true leaves of both *ann3* plant groups exhibited larger sizes and greater number of leaves compared to Col-0 plants. Additionally, *ann3(L4)* rosettes contained more leaves than *ann3(L1)*, yet both still contained more leaves than Col-0. The petioles of *ann3* leaves were also visibly longer than those of Col-0 leaves.

Figure 15: Dissembled leaf rosettes of *A. thaliana* Col-0, *ann3(L1)* and *ann3(L4)* plants on DAG21. Scale bar 2 cm.

Furthermore, on DAG21, third true leaves were removed from leaf rosettes and placed in a clearing solution. After chlorophyll removal, the leaves were mounted onto microscopic slides using glycerol. Leaves prepared this way were then observed by an epifluorescent microscope (Figure 16) for the purpose of analysing their stomatal area (Figure 17). The average area of Col-0 stomata was 563,45 μm^2. The area of *ann3* stomata was 597,39 μm^2 for *ann3(L1)* and 504,73 μm^2 for *ann3(L4)* respectively. Significant differences were evident between all three groups, even within *ann3* stomata where the *ann3(L4)* average was smaller than Col-0, yet the *ann3(L1)* average was higher than Col-0.

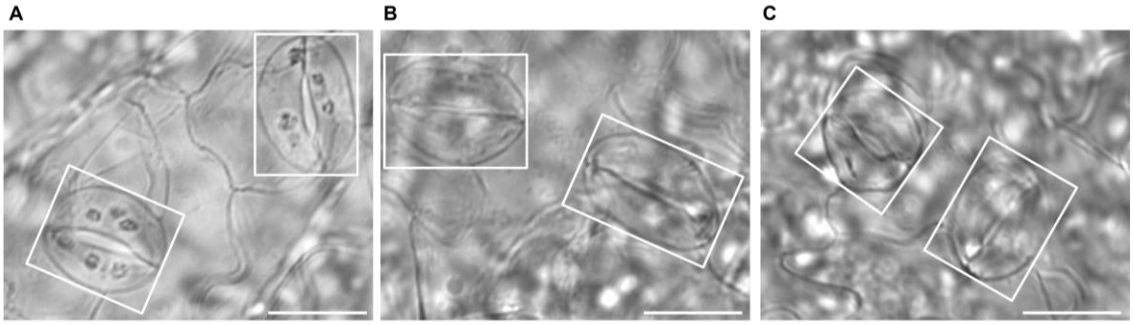

Figure 17: Stomata on decolorized third true leaves of *A. thaliana* Col-0 (A), *ann3(L1)* (B) and *ann3(L4)* harvested on DAG21. Scale bar 20 µm.

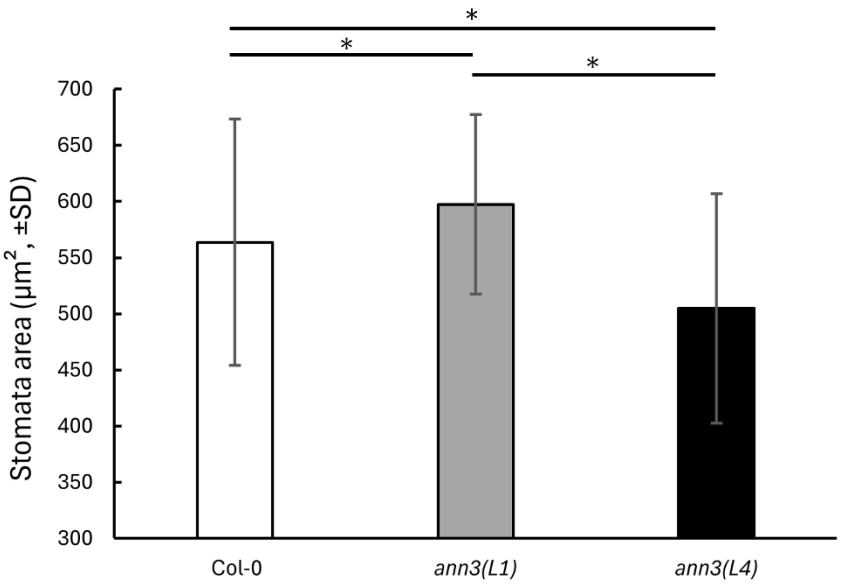

Figure 16: Average area of stomata on third true leaves of *A. thaliana* Col-0, *ann3(L1)* and *ann3(L4)* harvested on DAG21. Statistical significance at $P < 0,05$ (∗).

4.3.4 Crossing

For all crosses, siliques developed, and seeds were subsequently extracted. Afterwards, the seeds were germinated for 11 and 12 days and were observed on those specific days. Unfortunately, the seeds collected from the *ann3*xYC3.6 crossing did not germinate, rendering any further analysis impossible. The seeds from the crosses involving lines carrying VTI1 and RabF2b fused with mCherry did germinate. However, despite successful germination, none of the analysed roots exhibited any fluorescent signal, thereby precluding the analysis of vesicular trafficking in *ann3* mutants. Interestingly, the only fluorescent signal observed was in the roots of *ann3* plants bearing ANN1-GFP. The ANN1-GFP signal was consistently present in several plants from seeds originating from the same silique, appearing in both primary and lateral roots. Even though its presence in all cases, the signal was relatively weak.

At the tips of primary roots (Figure 18), the ANN1-GFP signal was detected in every cell, including border cells, albeit in varying abundance. The signal was most prominent in the cells of the root cap, both in the columella cap cells and also in the lateral cap cells. Within the meristematic root zone, the signal was predominantly present in epidermal cells, with a lower intensity observed in inner tissues. In the elongation zone of primary roots (Figure 19), the signal was observed in epidermal cells, including both trichoblasts and atrichoblasts. The signal was most abundant at the plasma membrane, with weaker intensity observed towards the cell centre. Additionally, the signal was visible in emerging root hair bulges and elongating root hairs. In some epidermal cells distinct spots resembling vesicles, with higher signal intensities, were present at the cell periphery.

At the lateral root tips (Figure 20), the signal was comparatively weaker than the one in primary roots, yet it followed a similar distribution pattern. The highest signal intensity was observed in cells of the columella cap, while the lowest intensity was observed in inner tissues. Signal distribution in epidermal cells and lateral root cap cells mirrored that of the surrounding tissues, albeit with notably lower intensity compared to primary roots. Within the elongation zone of lateral roots, the signal was localized at the root hair bulges as well as at the tips of growing root hair (Figure 21), with minimal signal detected in other cells. Conversely, in differentiated root hairs (Figure 22), the signal was distributed throughout the entire root hair, with higher intensities predominantly observed at the cell periphery. Additionally, the signal was present in epidermal cells, once again delineating

plasma membranes. The homozygous nature of the examined plants was confirmed through genotyping (Figure 23).

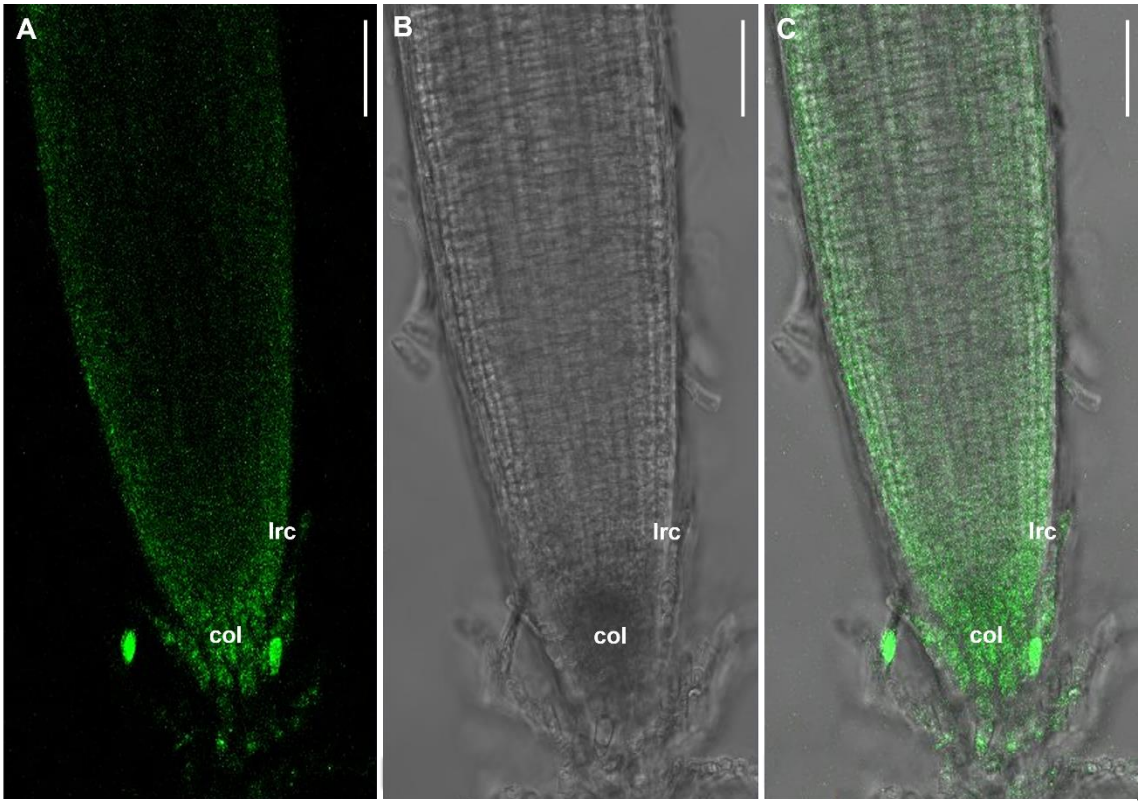

Figure 18: Primary root tip of *ann3* bearing ANN1-GFP. GFP fluorescence (A), brightfield (B), merged channels (C). Columella (col), lateral root cap (lrc). Scale bar 50 µm.

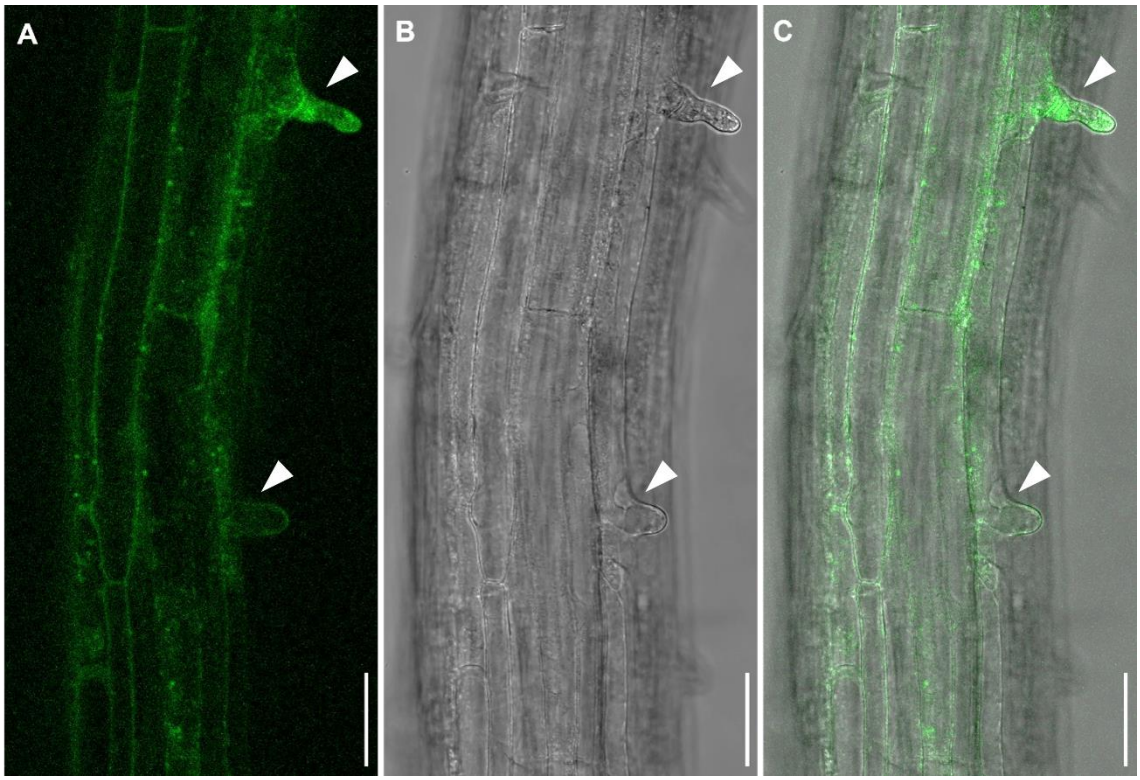

Figure 20: Differentiation zone of *ann3* primary root bearing ANN1-GFP. GFP fluorescence (A), brightfield (B), merged channels (C). Arrowheads point to root hair bulges. Scale bar 50 µm.

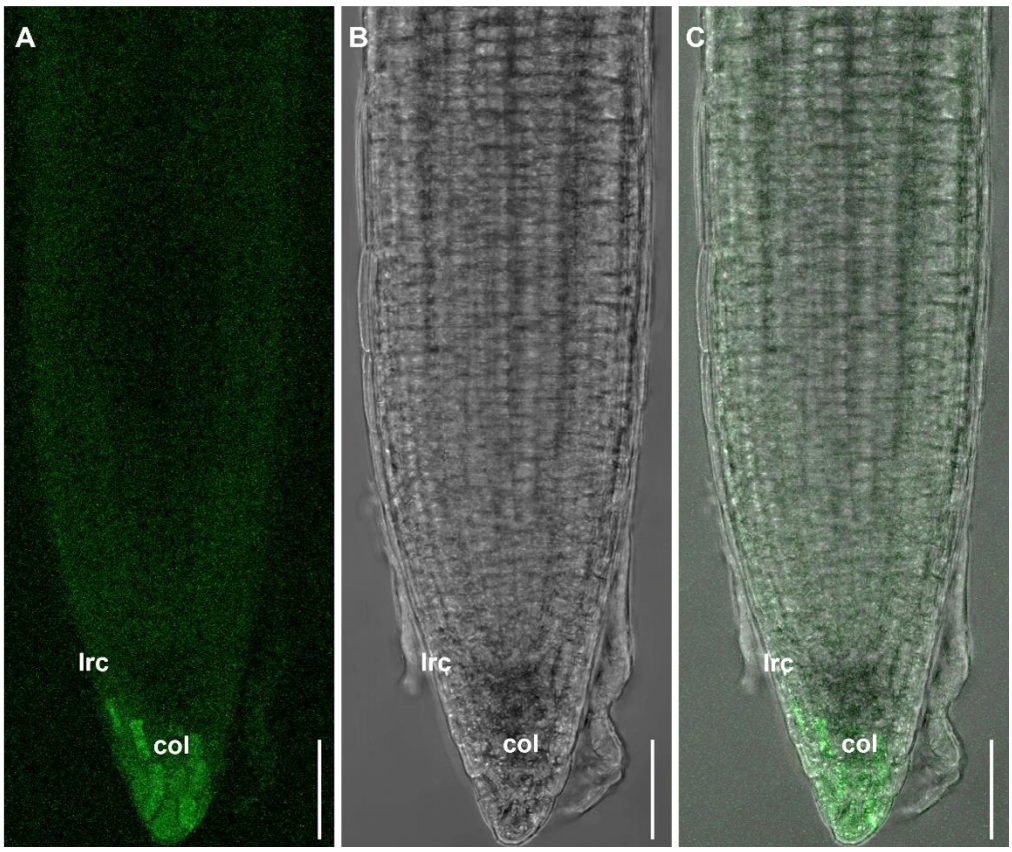

Figure 19: Tip of *ann3* lateral roots bearing ANN1-GFP. GFP fluorescence (A), brightfield (B), merged channels (C). Columella (col), lateral root cap (lrc). Scale bar 50 µm.

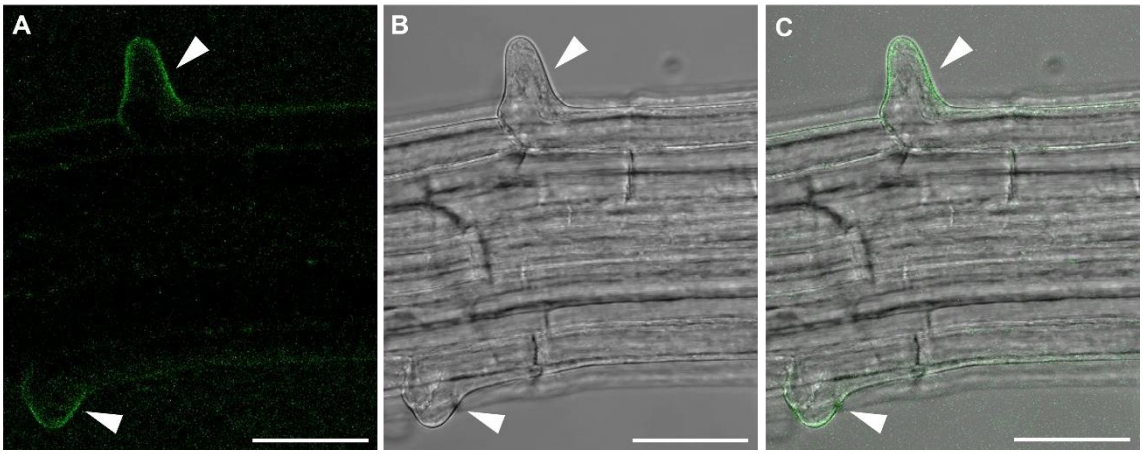

Figure 22: Differentiation zone of lateral root with growing root hairs of *ann3* bearing ANN1-GFP. GFP fluorescence (A), brightfield (B), merged channels (C). Arrowheads point to root hair bulges. Scale bar 50 µm.

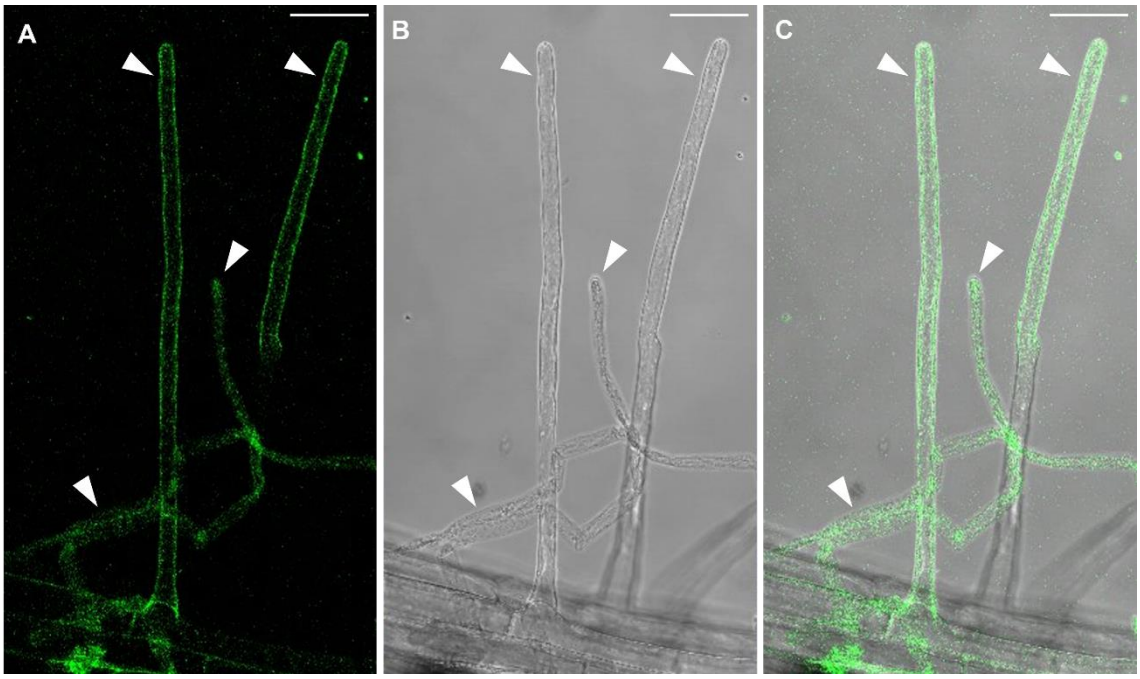

Figure 21: Differentiated root hairs on the lateral root of *ann3* bearing ANN1-GFP. GFP fluorescence (A), brightfield (B), merged channels (C). Arrowheads point to root hairs. Scale bar 50 µm.

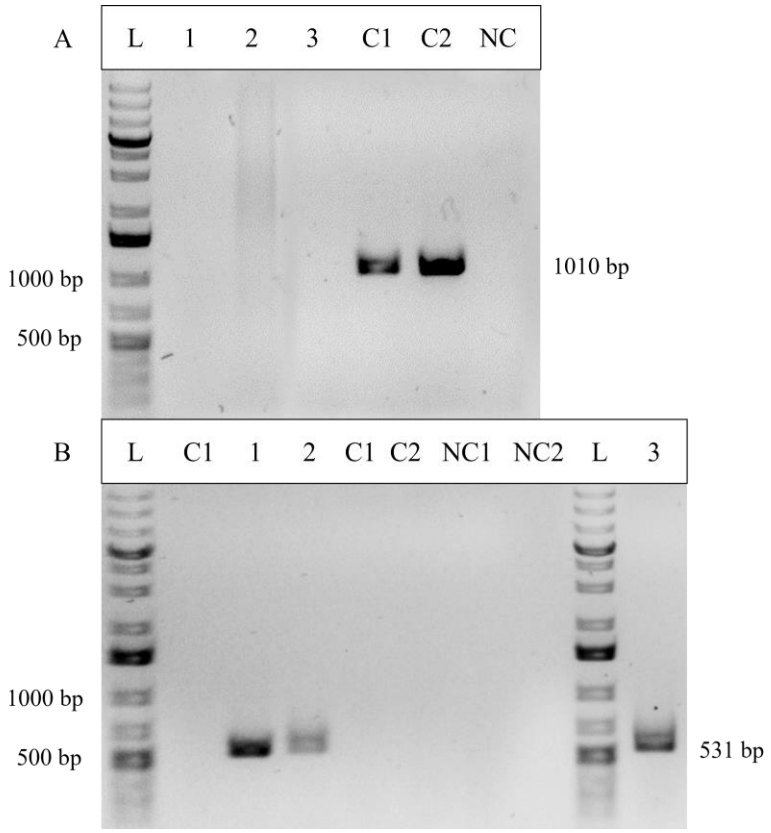

Figure 23: Representative genotyping results of agarose gel electrophoresis of PCR products of *ann3* bearing ANN1-GFP. (A) Gene-specific primers, (B) gene-specific primer with a T-DNA insertion-specific primer. L – GeneRuler™ 1 kb Plus DNA Ladder, 1-3 – samples from individual SALK_082344C plants, C1-3 – control (Col-0), NC1-2 – negative control (PCR water). The PCR product for wild-type allele is 1010 bp and for mutant allele is 531 bp.

5 DISCUSSION

Annexins constitute a significant multigene gene family prevalent across eukaryotes. While most research has traditionally focused on vertebrate annexins, particularly those in humans, there has been a shift in attention towards plant annexins. Plant annexins have been shown to play essential roles in rapidly growing tissues, such as pollen tubes and root systems (Laohavisit *et al.*, 2012; Zhu *et al.*, 2014). However, not all members of the annexin D family have undergone thorough investigation to date. The majority of research has been done on annexin 1 in *A. thaliana*, overshadowing other annexins in the same species. Nevertheless, more light is being shed on other plant annexins, including annexin 3 in *A. thaliana*, as presented in this thesis.

The *in silico* analysis, leading to the generation of gene maps, served as a base for subsequent molecular analysis. Genotyping of the *ANNAT3* SALK_082344C T-DNA insertion mutant identified homozygous plants with T-DNA insertions present in both alleles of the gene. Obtaining a homozygous mutant line with a stably knocked-out gene is crucial for functional studies. However, identifying homozygotes from a mixture of heterozygous and wild type of SALK seeds can be challenging. However, in the case of *ann3* SALK_082344C, all genotyped plants were found to be homozygous.

The analysis of germination rates revealed differences in favour of *ann3* seeds with both studied groups having higher germination rates though only one being statistically significant, pointing to a negative regulatory role of ANNAT3 in germination. *ANNAT3* expression has been reported in dry seeds as well as on DAG1. Among eight *A. thaliana* annexins, *ANNAT3* exhibits the lowest expression on DAG1 (Cantero *et al.*, 2006). This could indicate a minor role compared to other annexins during the earliest stages of germination. While the results suggest a potential negative regulatory role of ANNAT3 in germination, the reported low expression levels complicate drawing a definitive conclusion and point to the need for further research.

ANNAT3 expression is present in every plant tissue, although at different levels, with the highest abundance observed in roots and flowers and lower levels in leaves (Clark *et al.*, 2001). However, the results of the root phenotype analysis surprisingly showed only slight differences. Based on studies of other annexins and the high expression of *ANNAT3* in roots, significant changes in root phenotype were assumed. Although the lengths of primary roots of *ann3* plants were generally longer, they were not significantly longer

except on DAG4. These results are consistent with those reported by Xu *et al.* (2023), which also demonstrated no significant difference in the primary root length of *ann3* SALK_082344C.

The analysis of the number of lateral roots showed no differences, as one *ann3* line had more lateral roots, while the second line had fewer. These results raise questions about the specific role of ANNAT3 in lateral root development and its possible relationship with auxin signalling. ANNAT3 has been previously associated with regulating the transport of PIN proteins, which are transporters responsible for auxin movement across the plasma membrane (Xu *et al.*, 2023). Given that lateral root growth, especially their formation, is tightly linked to auxin, these results raise a question about the exact function of ANNAT3 in auxin distribution (Jing & Strader, 2019). Auxin not only regulates the formation of lateral roots but also influences their number (Kawai *et al.*, 2022). As previously mentioned, it would be appropriate to assume that *ann3* plants would differ in the number of lateral roots. Even though ANNAT1 has also been linked to auxin transport, expression level of ANN1-GFP decreased upon lateral root formation and emergence, as revealed in transgenic *A. thaliana* expressing *proANN1::ANN1:GFP* construct (Tichá *et al*., 2020). However, in *ann1* mutants, the number of lateral roots increased, questioning the role of annexins in lateral root formation and highlighting the need for further research (Wang *et al.*, 2022).

As a calcium-binding protein, ANNAT3 holds the potential for involvement in polar growth, in which Ca^{2+} ions play a pivotal role. ANNAT1 has been found to be abundantly present in trichoblast cells, followed by localisation in root hair bulges and root hairs themselves (Clark *et al.*, 2005; Tichá *et al.*, 2020). Notably, *ann1* mutants exhibited longer distances between the root tip and the first root hair bulges, indicating its role in root hair formation (Tichá, 2020). Considering the structural and functional similarities of annexins and the results of research on ANNAT1 mentioned above, it was thought that *ann3* plants would display a significant root hair phenotype. However, analysis of *ann3* SALK_082344C revealed no difference in the distances between the root tip and the first root hair bulges, with one *ann3* line having a greater average distance while the second line having a shorter distance. Consequently, it is challenging to conclude a specific role of ANNAT3 in the formation process of root hairs.

However, significant differences were observed in the length of root hairs with *ann3* mutants generally displaying shorter root hairs. Root hairs of *ann3* failed to reach the longest lengths observed in wild-type plants and the longest root hairs were observed in smaller numbers in the case of *ann3*. These observations suggest a possible positive regulatory role of ANNAT3 in root hair growth. The length of root hairs has been shown to be dose-dependent on Ca^{2+} ions (Monshausen *et al.*, 2008). Since annexins are calcium-binding proteins they are thought to play a role in root hair formation and elongation (Clark *et al.*, 2001). Other calcium-binding proteins have also been identified to play a role in root hair growth by facilitating signal transduction between Ca^{2+} and the PM (Kato *et al.*, 2013). Despite the association of annexins with calcium binding, their exact role in root hair growth remains to be fully understood. However, the obtained results suggest a potential role of ANNAT3 in elongation rather than formation of root hairs.

The results of the leaf analysis revealed significant differences. Particularly in the size of leaf rosettes upon disablement, with the *ann3* rosettes being visibly bigger. This was further confirmed by examining the fresh and dry weight of the rosettes, which showed an increase in both cases for both *ann3* plant groups. Given that *ANNAT3* is expressed in leaves, albeit not as abundantly as in roots where the expression is the highest, these findings could indicate a potentially negative role of ANNAT3 in leaf development (Clark *et al.*, 2001). Calcium is a very important factor affecting the size of above-ground plant tissues. Studies have shown that when plants were exposed to higher amounts of exogenous Ca^{2+} ions, biomass levels increased (Weng *et al.*, 2022; White, 2003). Consequently, it would be possible to assume that the knockout of a calcium-binding protein gene, such as *ANNAT3*, would have negative effects on biomass production. Yet the slightly unexpected results here indicate a different trend in the case of *ANNAT3*.

On the other hand, further leaf analysis of stomata did not reveal any consistent differences as once again one *ann3* line exhibited larger stomata while the second line had smaller ones. These differences were observed when compared to Col-0 as well as between the lines themselves. These differences point to the conclusion that even though ANNAT3 may regulate leaf size, it may not affect stomatal size. Although *ANNAT3* expression has been analysed and identified in leaves, it has not been analysed in stomatal cells. Thus, its role in stomatal cells remains unexplored, complicating phenotype prediction and functional understanding. ANNAT1 has been shown to be present in guard

cells, but not their precursor cells, potentially suggesting the possible presence of ANNAT3 (Tichá *et al.*, 2020). Further research needs to be done on the role of annexins in stomatal development and function. Additionally, studies have also shown the presence of ANNAT1 in trichomes and the role of annexins in the promotion of trichome formation and elongation (Li *et al.*, 2013; Tichá *et al.*, 2020). However, similar investigations regarding ANNAT3 are lacking, leaving numerous questions unanswered. As most research on plant annexins has overall been focused on their role in the root system, more detailed studies of their roles in above-ground parts of plants are necessary.

As previously discussed, annexins are primarily thought to have roles in roots. However, the obtained results do not exhibit the significant differences that were anticipated. Although some variances in the root phenotype of *ann3* plants were noted, they were not as pronounced as those observed in the leaf phenotype. Unexpectedly, the leaf phenotype displayed notable distinctions, despite the lower abundance of ANNAT3 in leaves. All these unexpected results could originate from various factors.

One potential factor is the utilisation of a SALK T-DNA insertion mutant, which often carries more than one insertion (O'Malley *et al.*, 2015). While one insertion might target the gene of interest, here *ANNAT3*, another insertion may be present elsewhere in the genome, potentially affecting other genes. Consequently, the observed phenotype could result from the disruption of several genes.

Additionally, another factor that may have influenced the phenotype of the observed plants is environmental conditions. Annexins are known to be sensitive to growth conditions, including light conditions or the growth medium (Wang *et al.*, 2018; Wang *et al.*, 2022). A previous study on T-DNA insertion mutants of ANNAT1 and ANNAT2 showed a significant impact of growth medium components on root phenotype. The study compared the root phenotype on a no-sucrose versus sucrose medium. The phenotypes on the no-sucrose medium showed shorter primary roots and growth defects in the columella cells, while when grown on a sucrose medium there were no differences, suggesting the choice of growth medium to be vital (Wang *et al.*, 2018). During the experiments with *ann3*, the plants were consistently grown on a 1% sucrose ½ MS medium, indicating that the observed phenotype may have been mitigated or rescued by the presence of exogenous sucrose.

The attempt to visualize vesicular transport and calcium dynamics by crossing *ann3* mutant plants with transgenic lines bearing VTI1-mCherry, RabF2b-mCherry, and YC3.6 was unsuccessful, hindering the examination of ANNAT3's role in vesicular trafficking. However, the cross did yield *ann3* plants bearing GFP-labelled ANNAT1, enabling subsequent localization of ANNAT1-GFP in *ann3*. Similarly to ANNAT3, ANNAT1 is also mostly expressed in roots, for this reason, roots were subjected to microscopic observation (Clark *et al.*, 2001).

The localization of ANN1-GFP in *ann3* in both primary and lateral roots of *ann3* was predominantly observed in the root cap, both in the columella cap cells and also in the lateral cap cells. Contrastingly, the signal intensity was noticeably lower in the meristematic zone. These results are in accordance with those observed by Tichá *et al.*, (2020), where the same *proANN1::ANN1:GFP* construct was used.

Fluorescent signal of ANN1-GFP in the elongation zones of primary and lateral roots was mainly observed in epidermal cells. As these cells are vacuolated most of the cytoplasm is displaced towards the cell periphery. The signal was concentrated within the cytosol pushed to the cellular membranes, which corresponds with previous studies (Lee *et al.*, 2004). Interestingly, conspicuous spots displaying heightened signal intensity were also observed at the cellular periphery, potentially indicating endosomal localization, although this pattern has not been previously documented, raising many questions.

Within emerging root hair bulges and developing root hairs, the signal was predominantly localized at the peripheries. However, the signal was also present in the cytoplasm. As root hairs are also largely vacuolated one might presume that the GFP signal would be less predominant in the central parts of root hairs, nevertheless, here the results do not follow this pattern (Grierson *et al.*, 2014). Yet, this once again mirrors prior observations, albeit with variations in signal intensity at the tips of root hairs, as in the presented results no particular difference between the tip regions the and remaining root hair surface was visible (Tichá *et al.*, 2020).

The subtle differences between the observed and previously reported localisation of ANNAT1, may arise from minor morphological variations attributed to the use of *ann3* plants. While the phenotype was analysed, it was not examined in such depth. The absence of specific intracellular localization and functional studies of ANNAT3 complicates conclusive interpretations based solely on these findings, underscoring the

need for further investigation in this area. Furthermore, the relationship between ANNAT1 and ANNAT3 which remains unexplored, requires attention. Notably, ANNAT4 has been reported to interact with ANNAT1 (Huh *et al.*, 2010). Another factor influencing the observed ANNAT1 localisation is the relatively weak signal intensity in the root tissues, which could be linked to the utilization of the ANNAT1 native promoter (*proANN1*).

6 CONCLUSION

The theoretical part of this bachelor thesis outlined a characterisation of the protein family of annexins. This characterisation delved into their protein and gene structure in plants, followed by a functional analysis and their various roles in cells, emphasizing their role as calcium-binding proteins, particularly their liaison to ion channels. Given their presumed involvement in membrane trafficking, a large chapter was dedicated to membrane trafficking and the influence of calcium and annexins on vesicular transport. Additionally, the impact of annexins on plant growth and development was examined in a following chapter. Lastly, considering their multifaceted roles outlined in previous chapters, attention was given to their involvement in the interactions between plants and their surrounding environment.

In the experimental part, a thorough characterisation of the *ANNAT3* T-DNA insertion SALK_082344C mutant was conducted. The process involved employing genotyping, which facilitated the successful identification of homozygotes, harboring the T-DNA insertion present in both alleles of the gene. Subsequently, the phenotype of these homozygotes was analysed. Thanks to the observed results possible roles of ANNAT3 were suggested. It was found that ANNAT3 might have a negative influence on germination. Additionally, another negative role was recorded in leaf development. Contrastingly, further analysis pointed to a positive regulatory role in root hair growth. Collectively, the observed results hint at a comprehensive role of ANNAT3 in the development of *A. thaliana* plants. However, it is noteworthy that these results do not necessarily fully support the idea that annexins have mostly roles within the root system.

The further part of the phenotypic analysis aimed to elucidate the role of annexin 3 in vesicular trafficking and its effect on intracellular calcium through the creation of mutants VTI1-mCherry, RabF2b-mCherry, and YC3.6, which was unfortunately unsuccessful, leaving space for more studies. Nevertheless, throughout the process of crossing *ann3*xANN1-GFP mutants were obtained. Their analysis helped to confirm a previous localisation study (Tichá *et al.*, 2020). The localisation pattern revealed that ANNAT1 is primarily localised in the root cap of primary and lateral roots. The localisation was also linked to root hairs, root hair bulges, as well as growing root hairs.

7 REFERENCES

Alberts, B., Johnson, A., Lewis, J., Raff, M., Roberts, K., & Walter, P. (2002). *Molecular biology of the cell* (4th ed). Garland Science New York.

Ali, A., Petrov, V., Yun, D.-J., & Gechev, T. (2023). Revisiting plant salt tolerance: Novel components of the SOS pathway. *Trends in Plant Science*, *28*(9), 1060–1069. https://doi.org/10.1016/j.tplants.2023.04.003

Balcerowicz, D., Schoenaers, S., & Vissenberg, K. (2015). Cell Fate Determination and the Switch from Diffuse Growth to Planar Polarity in Arabidopsis Root Epidermal Cells. *Frontiers in Plant Science*, *6*. https://doi.org/10.3389/fpls.2015.01163

Bibikova, T. N., Zhigilei, A., & Gilroy, S. (1997). Root hair growth in Arabidopsis thaliana is directed by calcium and an endogenous polarity. *Planta*, *203*(4), 495–505. https://doi.org/10.1007/s004250050219

Blazek, A. D., Paleo, B. J., & Weisleder, N. (2015). Plasma membrane repair: A central process for maintaining cellular homeostasis. *Physiology*, *30*(6), 438–448.

Boustead, C. M., Smallwood, M., Small, H., Bowles, D. J., & Walker, J. H. (1989). Identification of calcium-dependent phospholipid-binding proteins in higher plant cells. *FEBS Letters*, *244*(2), 456–460. https://doi.org/10.1016/0014-5793(89)80582-4

Breton, G., Vazquez-Tello, A., Danyluk, J., & Sarhan, F. (2000). Two Novel Intrinsic Annexins Accumulate in Wheat Membranes in Response to Low Temperature. *Plant and Cell Physiology*, *41*(2), 177–184. https://doi.org/10.1093/pcp/41.2.177

Cantero, A., Barthakur, S., Bushart, T. J., Chou, S., Morgan, R. O., Fernandez, M. P., Clark, G. B., & Roux, S. J. (2006). Expression profiling of the Arabidopsis annexin gene family during germination, de-etiolation and abiotic stress. *Plant Physiology and Biochemistry*, *44*(1), 13–24. https://doi.org/10.1016/j.plaphy.2006.02.002

Caohuy, H., Srivastava, M., & Pollard, H. B. (1996). Membrane fusion protein synexin (annexin VII) as a Ca2+/GTP sensor in exocytotic secretion. *Proceedings of the National Academy of Sciences*, *93*(20), 10797–10802. https://doi.org/10.1073/pnas.93.20.10797

Carter, C., Pan, S., Zouhar, J., Avila, E. L., Girke, T., & Raikhel, N. V. (2004). The Vegetative Vacuole Proteome of *Arabidopsis thaliana* Reveals Predicted and Unexpected Proteins[W]. *The Plant Cell*, *16*(12), 3285–3303. https://doi.org/10.1105/tpc.104.027078

Chen, J., Mao, L., Mi, H., Lu, W., Ying, T., & Luo, Z. (2016). Involvement of three annexin genes in the ripening of strawberry fruit regulated by phytohormone and calcium signal transduction. *Plant Cell Reports*, *35*(4), 733–743. https://doi.org/10.1007/s00299-015-1915-5

Clark, G. B., Dauwalder, M., & Roux, S. J. (1998). Immunological and biochemical evidence for nuclear localization of annexin in peas. *Plant Physiology and Biochemistry*, *36*(9), 621–627. https://doi.org/10.1016/S0981-9428(98)80010-7

Clark, G. B., Lee, D., Dauwalder, M., & Roux, S. J. (2005). Immunolocalization and histochemical evidence for the association of two different Arabidopsis annexins with secretion during early seedling growth and development. *Planta*, *220*(4), 621–631. https://doi.org/10.1007/s00425-004-1374-7

Clark, G. B., Morgan, R. O., Fernandez, M., & Roux, S. J. (2012). Evolutionary adaptation of plant annexins has diversified their molecular structures, interactions and functional roles. *New Phytologist*, *196*(3), 695–712. https://doi.org/10.1111/j.1469-8137.2012.04308.x

Clark, G. B., & Roux, S. J. (1995). Annexins of Plant Cells. *Plant Physiology*, *109*(4), 1133–1139. https://doi.org/10.1104/pp.109.4.1133

Clark, G. B., Sessions, A., Eastburn, D. J., & Roux, S. J. (2001). Differential Expression of Members of the Annexin Multigene Family in Arabidopsis. *Plant Physiology*, *126*(3), 1072–1084. https://doi.org/10.1104/pp.126.3.1072

Contento, A. L., & Bassham, D. C. (2012). Structure and function of endosomes in plant cells. *Journal of Cell Science*, *125*(15), 3511–3518. https://doi.org/10.1242/jcs.093559

Dabitz, N., Hu, N.-J., Yusof, A. M., Tranter, N., Winter, A., Daley, M., Zschörnig, O., Brisson, A., & Hofmann, A. (2005). Structural Determinants for Plant Annexin−Membrane Interactions. *Biochemistry*, *44*(49), 16292–16300. https://doi.org/10.1021/bi0516226

Dahhan, D. A., & Bednarek, S. Y. (2022). Advances in structural, spatial, and temporal mechanics of plant endocytosis. *FEBS Letters*, *596*(17), 2269–2287. https://doi.org/10.1002/1873-3468.14420

Del Bem, L. E. V. (2011). The evolutionary history of calreticulin and calnexin genes in green plants. *Genetica*, *139*(2), 255–259. https://doi.org/10.1007/s10709-010-9544-y

Di Giovanni, J., Iborra, C., Maulet, Y., Lévêque, C., El Far, O., & Seagar, M. (2010). Calcium-dependent Regulation of SNARE-mediated Membrane Fusion by Calmodulin. *Journal of Biological Chemistry*, *285*(31), 23665–23675. https://doi.org/10.1074/jbc.M109.096073

Donohoe, B. S., Kang, B.-H., & Staehelin, L. A. (2007). Identification and characterization of COPIa- and COPIb-type vesicle classes associated with plant and algal Golgi. *Proceedings of the National Academy of Sciences*, *104*(1), 163–168. https://doi.org/10.1073/pnas.0609818104

Fan, L., Li, R., Pan, J., Ding, Z., & Lin, J. (2015). Endocytosis and its regulation in plants. *Trends in Plant Science*, *20*(6), 388–397. https://doi.org/10.1016/j.tplants.2015.03.014

Foresti, O., & Denecke, J. (2008). Intermediate Organelles of the Plant Secretory Pathway: Identity and Function. *Traffic*, *9*(10), 1599–1612. https://doi.org/10.1111/j.1600-0854.2008.00791.x

Fujiwara, M., Uemura, T., Ebine, K., Nishimori, Y., Ueda, T., Nakano, A., Sato, M. H., & Fukao, Y. (2014). Interactomics of Qa-SNARE in Arabidopsis thaliana. *Plant and Cell Physiology*, *55*(4), 781–789. https://doi.org/10.1093/pcp/pcu038

Gerke, V., Creutz, C. E., & Moss, S. E. (2005). Annexins: Linking Ca2+ signalling to membrane dynamics. *Nature Reviews Molecular Cell Biology*, *6*(6), 449–461. https://doi.org/10.1038/nrm1661

Gerke, V., & Moss, S. E. (2002). Annexins: From Structure to Function. *Physiological Reviews*, *82*(2), 331–371. https://doi.org/10.1152/physrev.00030.2001

Glanc, M. (2022). Plant cell division from the perspective of polarity. *Journal of Experimental Botany*, *73*(16), 5361–5371. https://doi.org/10.1093/jxb/erac227

González-Noriega, A., Michalak, C., Cervantes-Roldán, R., Gómez-Romero, V., & León-Del-Río, A. (2016). Two translation initiation codons direct the expression of annexin VI 64kDa and 68kDa isoforms. *Molecular Genetics and Metabolism*, *119*(4), 338–343. https://doi.org/10.1016/j.ymgme.2016.10.002

Gorecka, K. M., Konopka-Postupolska, D., Hennig, J., Buchet, R., & Pikula, S. (2005). Peroxidase activity of annexin 1 from Arabidopsis thaliana. *Biochemical and Biophysical Research Communications*, *336*(3), 868–875. https://doi.org/10.1016/j.bbrc.2005.08.181

Gorecka, K. M., Thouverey, C., Buchet, R., & Pikula, S. (2007). Potential Role of Annexin AnnAt1 from Arabidopsis thaliana in pH-Mediated Cellular Response to Environmental Stimuli. *Plant and Cell Physiology*, *48*(6), 792–803. https://doi.org/10.1093/pcp/pcm046

Grierson, C., Nielsen, E., Ketelaarc, T., & Schiefelbein, J. (2014). Root hairs. *The Arabidopsis Book/American Society of Plant Biologists*, *12*.

Grierson, C., & Schiefelbein, J. (2002). Root Hairs. *The Arabidopsis Book/American Society of Plant Biologists*, *1*.

Hay, J. C. (2007). Calcium: A fundamental regulator of intracellular membrane fusion? *EMBO Reports*, *8*(3), 236–240. https://doi.org/10.1038/sj.embor.7400921

He, F., Gao, C., Guo, G., Liu, J., Gao, Y., Pan, R., Guan, Y., & Hu, J. (2019). Maize annexin genes *ZmANN33* and *ZmANN35* encode proteins that function in cell membrane recovery during seed germination. *Journal of Experimental Botany*, *70*(4), 1183–1195. https://doi.org/10.1093/jxb/ery452

Himschoot, E., Beeckman, T., Friml, J., & Vanneste, S. (2015). Calcium is an organizer of cell polarity in plants. *Biochimica et Biophysica Acta (BBA) - Molecular Cell Research*, *1853*(9), 2168–2172. https://doi.org/10.1016/j.bbamcr.2015.02.017

Hofmann, A., Delmer, D. P., & Wlodawer, A. (2003). The crystal structure of annexin Gh1 from Gossypium hirsutum reveals an unusual S3 cluster. Implications for cellulose synthase complex formation and oxidative stress response. *European Journal of Biochemistry*, *270*(12), 2557–2564. https://doi.org/10.1046/j.1432-1033.2003.03612.x

Hofmann, A., Proust, J., Dorowski, A., Schantz, R., & Huber, R. (2000). Annexin 24 from Capsicum annuum. *Journal of Biological Chemistry*, *275*(11), 8072–8082. https://doi.org/10.1074/jbc.275.11.8072

Hoshino, D., Hayashi, A., Temmei, Y., Kanzawa, N., & Tsuchiya, T. (2004). Biochemical and immunohistochemical characterization of Mimosa annexin. *Planta*, *219*(5). https://doi.org/10.1007/s00425-004-1285-7

Huh, S. M., Noh, E. K., Kim, H. G., Jeon, B. W., Bae, K., Hu, H.-C., Kwak, J. M., & Park, O. K. (2010). Arabidopsis Annexins AnnAt1 and AnnAt4 Interact with Each Other and Regulate Drought and Salt Stress Responses. *Plant and Cell Physiology*, *51*(9), 1499–1514. https://doi.org/10.1093/pcp/pcq111

Iqbal, Z., Iqbal, M. S., Hashem, A., Abd_Allah, E. F., & Ansari, M. I. (2021). Plant Defense Responses to Biotic Stress and Its Interplay With Fluctuating Dark/Light Conditions. *Frontiers in Plant Science*, *12*, 631810. https://doi.org/10.3389/fpls.2021.631810

Jain, M., Nagar, P., Goel, P., Singh, A. K., Kumari, S., & Mustafiz, A. (2018). Second Messengers: Central Regulators in Plant Abiotic Stress Response. In S. M. Zargar & M. Y. Zargar (Eds.), *Abiotic Stress-Mediated Sensing and Signaling in Plants: An Omics Perspective* (pp. 47–94). Springer Singapore. https://doi.org/10.1007/978-981-10-7479-0_2

Jami, S. K., Clark, G. B., Ayele, B. T., Ashe, P., & Kirti, P. B. (2012). Genome-wide Comparative Analysis of Annexin Superfamily in Plants. *PLoS ONE*, *7*(11), e47801. https://doi.org/10.1371/journal.pone.0047801

Jami, S. K., Clark, G. B., Turlapati, S. A., Handley, C., Roux, S. J., & Kirti, P. B. (2008). Ectopic expression of an annexin from Brassica juncea confers tolerance to abiotic and biotic stress treatments in transgenic tobacco. *Plant Physiology and Biochemistry*, *46*(12), 1019–1030. https://doi.org/10.1016/j.plaphy.2008.07.006

Jing, H., & Strader, L. (2019). Interplay of Auxin and Cytokinin in Lateral Root Development. *International Journal of Molecular Sciences*, *20*(3), 486. https://doi.org/10.3390/ijms20030486

Kato, M., Aoyama, T., & Maeshima, M. (2013). The Ca2+-binding protein PC aP2 located on the plasma membrane is involved in root hair development as a possible signal transducer. *The Plant Journal*, *74*(4), 690–700.

Kawai, T., Akahoshi, R., Shelley, I. J., Kojima, T., Sato, M., Tsuji, H., & Inukai, Y. (2022). Auxin Distribution in Lateral Root Primordium Development Affects the Size and Lateral Root Diameter of Rice. *Frontiers in Plant Science*, *13*, 834378. https://doi.org/10.3389/fpls.2022.834378

Ketelaar, T., Galway, M. E., Mulder, B. M., & Emons, A. M. C. (2008). Rates of exocytosis and endocytosis in *Arabidopsis* root hairs and pollen tubes. *Journal of Microscopy*, *231*(2), 265–273. https://doi.org/10.1111/j.1365-2818.2008.02031.x

Kolesnikov, Y. S., Nokhrina, K. P., Kretynin, S. V., Volotovski, I. D., Martinec, J., Romanov, G. A., & Kravets, V. S. (2012). Molecular structure of phospholipase D and regulatory mechanisms of its activity in plant and animal cells. *Biochemistry (Moscow)*, *77*(1), 1–14. https://doi.org/10.1134/S0006297912010014

Konopka-Postupolska, D. (2007). Annexins: Putative linkers in dynamic membrane–cytoskeleton interactions in plant cells. *Protoplasma*, *230*(3–4), 203–215. https://doi.org/10.1007/s00709-006-0234-7

Konopka-Postupolska, D., & Clark, G. (2017). Annexins as Overlooked Regulators of Membrane Trafficking in Plant Cells. *International Journal of Molecular Sciences*, *18*(4), 863. https://doi.org/10.3390/ijms18040863

Konopka-Postupolska, D., Clark, G., Goch, G., Debski, J., Floras, K., Cantero, A., Fijolek, B., Roux, S., & Hennig, J. (2009). The Role of Annexin 1 in Drought Stress in Arabidopsis. *Plant Physiology*, *150*(3), 1394–1410. https://doi.org/10.1104/pp.109.135228

Konopka-Postupolska, D., Clark, G., & Hofmann, A. (2011). Structure, function and membrane interactions of plant annexins: An update. *Plant Science*, *181*(3), 230–241. https://doi.org/10.1016/j.plantsci.2011.05.013

Koornneef, M., & Meinke, D. (2010). The development of Arabidopsis as a model plant. *The Plant Journal*, *61*(6), 909–921. https://doi.org/10.1111/j.1365-313X.2009.04086.x

Kourie, J. I., & Wood, H. B. (2000). Biophysical and molecular properties of annexin-formed channels. *Progress in Biophysics and Molecular Biology*, *73*(2–4), 91–134. https://doi.org/10.1016/S0079-6107(00)00003-1

Kudla, J., Becker, D., Grill, E., Hedrich, R., Hippler, M., Kummer, U., Parniske, M., Romeis, T., & Schumacher, K. (2018). Advances and current challenges in calcium signaling. *New Phytologist*, *218*(2), 414–431. https://doi.org/10.1111/nph.14966

Laohavisit, A., Brown, A. T., Cicuta, P., & Davies, J. M. (2010). Annexins: Components of the Calcium and Reactive Oxygen Signaling Network. *Plant Physiology*, *152*(4), 1824–1829. https://doi.org/10.1104/pp.109.145458

Laohavisit, A., Shang, Z., Rubio, L., Cuin, T. A., Véry, A.-A., Wang, A., Mortimer, J. C., Macpherson, N., Coxon, K. M., Battey, N. H., Brownlee, C., Park, O. K., Sentenac, H., Shabala, S., Webb, A. A. R., & Davies, J. M. (2012). *Arabidopsis* Annexin1 Mediates the Radical-Activated Plasma Membrane Ca^{2+}—And K^{+}-Permeable Conductance in Root Cells. *The Plant Cell*, *24*(4), 1522–1533. https://doi.org/10.1105/tpc.112.097881

Lee, S., Lee, E. J., Yang, E. J., Lee, J. E., Park, A. R., Song, W. H., & Park, O. K. (2004). Proteomic Identification of Annexins, Calcium-Dependent Membrane Binding Proteins That Mediate Osmotic Stress and Abscisic Acid Signal Transduction in Arabidopsis. *The Plant Cell*, *16*(6), 1378–1391. https://doi.org/10.1105/tpc.021683

Li, B., Li, D., Zhang, J., Xia, H., Wang, X., Li, Y., & Li, X. (2013). Cotton AnnGh3 Encoding an Annexin Protein is Preferentially Expressed in Fibers and Promotes Initiation and Elongation of Leaf Trichomes in Transgenic Arabidopsis. *Journal of Integrative Plant Biology*, *55*(10), 902–916. https://doi.org/10.1111/jipb.12063

Liao, C., Zheng, Y., & Guo, Y. (2017). MYB30 transcription factor regulates oxidative and heat stress responses through ANNEXIN-mediated cytosolic calcium signaling in *Arabidopsis*. *New Phytologist*, *216*(1), 163–177. https://doi.org/10.1111/nph.14679

Liemann, S., Benz, J., Burger, A., Voges, D., Hofmann, A., Huber, R., & Göttig, P. (1996). Structural and Functional Characterisation of the Voltage Sensor in the Ion Channel Human Annexin V. *Journal of Molecular Biology*, *258*(4), 555–561. https://doi.org/10.1006/jmbi.1996.0268

Lindermayr, C., Saalbach, G., & Durner, J. (2005). Proteomic Identification of *S*-Nitrosylated Proteins in Arabidopsis. *Plant Physiology*, *137*(3), 921–930. https://doi.org/10.1104/pp.104.058719

Liu, Q., Ding, Y., Shi, Y., Ma, L., Wang, Y., Song, C., Wilkins, K. A., Davies, J. M., Knight, H., Knight, M. R., Gong, Z., Guo, Y., & Yang, S. (2021). The calcium transporter ANNEXIN1 mediates cold-induced calcium signaling and freezing tolerance in plants. *The EMBO Journal*, *40*(2), e104559. https://doi.org/10.15252/embj.2020104559

Liu, T., Du, L., Li, Q., Kang, J., Guo, Q., & Wang, S. (2021). AtCRY2 Negatively Regulates the Functions of AtANN2 and AtANN3 in Drought Tolerance by Affecting Their Subcellular Localization and Transmembrane Ca2+ Flow. *Frontiers in Plant Science*, *12*, 754567. https://doi.org/10.3389/fpls.2021.754567

Mayran, N. (2003). Annexin II regulates multivesicular endosome biogenesis in the degradation pathway of animal cells. *The EMBO Journal*, *22*(13), 3242–3253. https://doi.org/10.1093/emboj/cdg321

Meinke, D. W., Cherry, J. M., Dean, C., Rounsley, S. D., & Koornneef, M. (1998). Arabidopsis thaliana: A Model Plant for Genome Analysis. *Science, New Series*, *282*(5389), 662+679-682.

Melicher, P., Dvořák, P., Řehák, J., Šamajová, O., Pechan, T., Šamaj, J., & Takáč, T. (2024). Methyl viologen-induced changes in the Arabidopsis proteome implicate PATELLIN 4 in oxidative stress responses. *Journal of Experimental Botany*, *75*(1), 405–421. https://doi.org/10.1093/jxb/erad363

Miller, D. D., De Ruijter, N. C., Bisseling, T., & Emons, A. M. C. (1999). The role of actin in root hair morphogenesis: Studies with lipochito-oligosaccharide as a growth stimulator and cytochalasin as an actin perturbing drug. *The Plant Journal*, *17*(2), 141–154.

Monshausen, G. B., Messerli, M. A., & Gilroy, S. (2008). Imaging of the Yellow Cameleon 3.6 Indicator Reveals That Elevations in Cytosolic Ca2+ Follow Oscillating Increases in Growth

in Root Hairs of Arabidopsis. *Plant Physiology*, *147*(4), 1690–1698. https://doi.org/10.1104/pp.108.123638

Morgan, R. O., & Fernández, M. P. (1997). Annexin gene structures and molecular evolutionary genetics. *Cellular and Molecular Life Sciences (CMLS)*, *53*(6), 508–515. https://doi.org/10.1007/s000180050064

Mortimer, J. C., Coxon, K. M., Laohavisit, A., & Davies, J. M. (2009). Heme-independent soluble and membrane-associated peroxidase activity of a *Zea mays* annexin preparation. *Plant Signaling & Behavior*, *4*(5), 428–430. https://doi.org/10.4161/psb.4.5.8297

Mortimer, J. C., Laohavisit, A., Macpherson, N., Webb, A., Brownlee, C., Battey, N. H., & Davies, J. M. (2008). Annexins: Multifunctional components of growth and adaptation. *Journal of Experimental Botany*, *59*(3), 533–544. https://doi.org/10.1093/jxb/erm344

Moss, S. E., & Morgan, R. O. (2004). The annexins. *Genome Biology*, *5*(4), 219. https://doi.org/10.1186/gb-2004-5-4-219

Murashige, T., & Skoog, F. (1962). A Revised Medium for Rapid Growth and Bio Assays with Tobacco Tissue Cultures. *Physiologia Plantarum*, *15*(3), 473–497. https://doi.org/10.1111/j.1399-3054.1962.tb08052.x

Nawaz, M., Sun, J., Shabbir, S., Khattak, W. A., Ren, G., Nie, X., Bo, Y., Javed, Q., Du, D., & Sonne, C. (2023). A review of plants strategies to resist biotic and abiotic environmental stressors. *Science of The Total Environment*, *900*, 165832. https://doi.org/10.1016/j.scitotenv.2023.165832

O'Malley, R. C., Barragan, C. C., & Ecker, J. R. (2015). *A User's Guide to the Arabidopsis T-DNA Insertional Mutant Collections*.

Paez Valencia, J., Goodman, K., & Otegui, M. S. (2016). Endocytosis and Endosomal Trafficking in Plants. *Annual Review of Plant Biology*, *67*(1), 309–335. https://doi.org/10.1146/annurev-arplant-043015-112242

Peck, S., & Mittler, R. (2020). Plant signaling in biotic and abiotic stress. *Journal of Experimental Botany*, *71*(5), 1649–1651. https://doi.org/10.1093/jxb/eraa051

Perochon, A., Aldon, D., Galaud, J.-P., & Ranty, B. (2011). Calmodulin and calmodulin-like proteins in plant calcium signaling. *Biochimie*, *93*(12), 2048–2053. https://doi.org/10.1016/j.biochi.2011.07.012

Pirayesh, N., Giridhar, M., Ben Khedher, A., Vothknecht, U. C., & Chigri, F. (2021). Organellar calcium signaling in plants: An update. *Biochimica et Biophysica Acta (BBA) - Molecular Cell Research*, *1868*(4), 118948. https://doi.org/10.1016/j.bbamcr.2021.118948

Plasencia, F. A., Estrada, Y., Flores, F. B., Ortíz-Atienza, A., Lozano, R., & Egea, I. (2021). The Ca2+ Sensor Calcineurin B–Like Protein 10 in Plants: Emerging New Crucial Roles for Plant Abiotic Stress Tolerance. *Frontiers in Plant Science*, *11*, 599944. https://doi.org/10.3389/fpls.2020.599944

Qiao, B., Zhang, Q., Liu, D., Wang, H., Yin, J., Wang, R., He, M., Cui, M., Shang, Z., Wang, D., & Zhu, Z. (2015). A calcium-binding protein, rice annexin OsANN1, enhances heat stress tolerance by modulating the production of H_2O_2. *Journal of Experimental Botany*, *66*(19), 5853–5866. https://doi.org/10.1093/jxb/erv294

Rohila, J. S., Chen, M., Chen, S., Chen, J., Cerny, R., Dardick, C., Canlas, P., Xu, X., Gribskov, M., Kanrar, S., Zhu, J.-K., Ronald, P., & Fromm, M. E. (2006). Protein-protein interactions of tandem affinity purification-tagged protein kinases in rice. *The Plant Journal*, *46*(1), 1–13. https://doi.org/10.1111/j.1365-313X.2006.02671.x

Rutter, B. D., & Innes, R. W. (2017). Extracellular Vesicles Isolated from the Leaf Apoplast Carry Stress-Response Proteins. *Plant Physiology*, *173*(1), 728–741. https://doi.org/10.1104/pp.16.01253

Saad, R. B., Ben Romdhane, W., Ben Hsouna, A., Mihoubi, W., Harbaoui, M., & Brini, F. (2020). Insights into plant annexins function in abiotic and biotic stress tolerance. *Plant Signaling & Behavior*, *15*(1), 1699264. https://doi.org/10.1080/15592324.2019.1699264

Scheuring, D., Viotti, C., Krüger, F., Künzl, F., Sturm, S., Bubeck, J., Hillmer, S., Frigerio, L., Robinson, D. G., Pimpl, P., & Schumacher, K. (2011). Multivesicular Bodies Mature from the *Trans* -Golgi Network/Early Endosome in *Arabidopsis*. *The Plant Cell*, *23*(9), 3463–3481. https://doi.org/10.1105/tpc.111.086918

Shen, F., Ying, J., Xu, L., Sun, X., Wang, J., Wang, Y., Mei, Y., Zhu, Y., & Liu, L. (2021). Characterization of Annexin gene family and functional analysis of RsANN1a involved in heat tolerance in radish (Raphanus sativus L.). *Physiology and Molecular Biology of Plants*, *27*(9), 2027–2041. https://doi.org/10.1007/s12298-021-01056-5

Shibata, H., Kanadome, T., Sugiura, H., Yokoyama, T., Yamamuro, M., Moss, S. E., & Maki, M. (2015). A New Role for Annexin A11 in the Early Secretory Pathway via Stabilizing Sec31A Protein at the Endoplasmic Reticulum Exit Sites (ERES). *Journal of Biological Chemistry*, *290*(8), 4981–4993. https://doi.org/10.1074/jbc.M114.592089

Shin, H., & Brown, R. M. (1999). GTPase Activity and Biochemical Characterization of a Recombinant Cotton Fiber Annexin1. *Plant Physiology*, *119*(3), 925–934. https://doi.org/10.1104/pp.119.3.925

Talukdar, T., Gorecka, K. M., De Carvalho-Niebel, F., Downie, J. A., Cullimore, J., & Pikula, S. (2009). Annexins - calcium- and membrane-binding proteins in the plant kingdom: Potential role in nodulation and mycorrhization in Medicago truncatula. *Acta Biochimica Polonica*, *56*(2). https://doi.org/10.18388/abp.2009_2451

The Arabidopsis Genome Initiative. (2000). Analysis of the genome sequence of the flowering plant Arabidopsis thaliana. *Nature*, *408*(6814), 796–815. https://doi.org/10.1038/35048692

Tichá, M. (2020). *Role of annexins and cytoskeleton in plant development and stress responses* [Ph.D. thesis]. Palacký University Olomouc, Czech Republic.

Tichá, M., Richter, H., Ovečka, M., Maghelli, N., Hrbáčková, M., Dvořák, P., Šamaj, J., & Šamajová, O. (2020). Advanced Microscopy Reveals Complex Developmental and Subcellular Localization Patterns of ANNEXIN 1 in Arabidopsis. *Frontiers in Plant Science*, *11*, 1153. https://doi.org/10.3389/fpls.2020.01153

Tuteja, N., & Mahajan, S. (2007). Calcium Signaling Network in Plants: An Overview. *Plant Signaling & Behavior*, *2*(2), 79–85. https://doi.org/10.4161/psb.2.2.4176

Tuteja, N., & Singh Gill, S. (Eds.). (2013). *Plant Acclimation to Environmental Stress*. Springer New York. https://doi.org/10.1007/978-1-4614-5001-6

Ungar, D., & Hughson, F. M. (2003). SNARE Protein Structure and Function. *Annual Review of Cell and Developmental Biology*, *19*(1), 493–517. https://doi.org/10.1146/annurev.cellbio.19.110701.155609

Vandeputte, O., Lowe, Y. O., Burssens, S., Van Raemdonck, D., Hutin, D., Boniver, D., Geelen, D., El Jaziri, M., & Baucher, M. (2007). The tobacco Ntann12 gene, encoding an annexin, is induced upon Rhodoccocus fascians infection and during leafy gall development. *Molecular Plant Pathology*, *8*(2), 185–194. https://doi.org/10.1111/j.1364-3703.2007.00385.x

Wang, J., Song, J., Clark, G., & Roux, S. J. (2018). ANN1 and ANN2 Function in Post-Phloem Sugar Transport in Root Tips to Affect Primary Root Growth. *Plant Physiology*, *178*(1), 390–401. https://doi.org/10.1104/pp.18.00713

Wang, X., Han, L., Yin, H., Zhao, Z., Cao, H., Shang, Z., & Kang, E. (2022). AtANN1 and AtANN2 are involved in phototropism of etiolated hypocotyls of *Arabidopsis* by regulating auxin distribution. *AoB PLANTS*, *14*(1), plab075. https://doi.org/10.1093/aobpla/plab075

Wang, X., Ma, X., Wang, H., Li, B., Clark, G., Guo, Y., Roux, S., Sun, D., & Tang, W. (2015). Proteomic Study of Microsomal Proteins Reveals a Key Role for Arabidopsis Annexin 1 in Mediating Heat Stress-Induced Increase in Intracellular Calcium Levels. *Molecular & Cellular Proteomics*, *14*(3), 686–694. https://doi.org/10.1074/mcp.M114.042697

Weng, X., Li, H., Ren, C., Zhou, Y., Zhu, W., Zhang, S., & Liu, L. (2022). Calcium Regulates Growth and Nutrient Absorption in Poplar Seedlings. *Frontiers in Plant Science*, *13*, 887098. https://doi.org/10.3389/fpls.2022.887098

Whitaker, M. (2010). Genetically Encoded Probes for Measurement of Intracellular Calcium. In *Methods in Cell Biology* (Vol. 99, pp. 153–182). Elsevier. https://doi.org/10.1016/B978-0-12-374841-6.00006-2

White, P. J. (2003). Calcium in Plants. *Annals of Botany*, *92*(4), 487–511. https://doi.org/10.1093/aob/mcg164

White, P. J., Bowen, H. C., Demidchik, V., Nichols, C., & Davies, J. M. (2002). Genes for calcium-permeable channels in the plasma membrane of plant root cells. *Biochimica et*

Biophysica Acta (BBA) - Biomembranes, *1564*(2), 299–309. https://doi.org/10.1016/S0005-2736(02)00509-6

Williams, J. K., Ngo, J. M., Lehman, I. M., & Schekman, R. (2023). Annexin A6 mediates calcium-dependent exosome secretion during plasma membrane repair. *eLife*, *12*, e86556. https://doi.org/10.7554/eLife.86556

Xu, J., Han, L., Xia, S., Zhu, R., Kang, E., & Shang, Z. (2023). ATANN3 Is Involved in Extracellular ATP-Regulated Auxin Distribution in Arabidopsis thaliana Seedlings. *Plants*, *12*(2), 330. https://doi.org/10.3390/plants12020330

Xu, L., Tang, Y., Gao, S., Su, S., Hong, L., Wang, W., Fang, Z., Li, X., Ma, J., Quan, W., Sun, H., Li, X., Wang, Y., Liao, X., Gao, J., Zhang, F., Li, L., & Zhao, C. (2016). Comprehensive analyses of the annexin gene family in wheat. *BMC Genomics*, *17*(1), 415. https://doi.org/10.1186/s12864-016-2750-y

Xu, T., Niu, J., & Jiang, Z. (2022). Sensing Mechanisms: Calcium Signaling Mediated Abiotic Stress in Plants. *Frontiers in Plant Science*, *13*, 925863. https://doi.org/10.3389/fpls.2022.925863

Yadav, D., Boyidi, P., Ahmed, I., & Kirti, P. B. (2018). Plant annexins and their involvement in stress responses. *Environmental and Experimental Botany*, *155*, 293–306. https://doi.org/10.1016/j.envexpbot.2018.07.002

Yáñez, M., Gil-Longo, J., & Campos-Toimil, M. (2012). Calcium Binding Proteins. In Md. S. Islam (Ed.), *Calcium Signaling* (Vol. 740, pp. 461–482). Springer Netherlands. https://doi.org/10.1007/978-94-007-2888-2_19

Yang, K., Wang, L., Le, J., & Dong, J. (2020). Cell polarity: Regulators and mechanisms in plants. *Journal of Integrative Plant Biology*, *62*(1), 132–147. https://doi.org/10.1111/jipb.12904

Yip Delormel, T., & Boudsocq, M. (2019). Properties and functions of calcium-dependent protein kinases and their relatives in *Arabidopsis thaliana*. *New Phytologist*, *224*(2), 585–604. https://doi.org/10.1111/nph.16088

Zhang, H., Zhao, Y., & Zhu, J.-K. (2020). Thriving under Stress: How Plants Balance Growth and the Stress Response. *Developmental Cell*, *55*(5), 529–543. https://doi.org/10.1016/j.devcel.2020.10.012

Zhang, H., Zhu, J., Gong, Z., & Zhu, J.-K. (2022). Abiotic stress responses in plants. *Nature Reviews Genetics*, *23*(2), 104–119. https://doi.org/10.1038/s41576-021-00413-0

Zhao, J., Li, L., Liu, Q., Liu, P., Li, S., Yang, D., Chen, Y., Pagnotta, S., Favery, B., Abad, P., & Jian, H. (2019). A MIF-like effector suppresses plant immunity and facilitates nematode parasitism by interacting with plant annexins. *Journal of Experimental Botany*, *70*(20), 5943–5958. https://doi.org/10.1093/jxb/erz348

Zhu, J., Wu, X., Yuan, S., Qian, D., Nan, Q., An, L., & Xiang, Y. (2014). Annexin5 Plays a Vital Role in Arabidopsis Pollen Development via Ca2+-Dependent Membrane Trafficking. *PLoS ONE*, *9*(7), e102407. https://doi.org/10.1371/journal.pone.0102407

TAIR. https://www.arabidopsis.org/index.jsp (5.12.2022)

SIGnaL. http://signal.salk.edu/tdnaprimers.2.html (5.12.2022)

ThermoFisher T_m calculator.https://www.thermofisher.com/cz/en/home/brands/thermo-scientific/molecular-biology/molecular-biology-learning-center/molecular-biology-resource-library/thermo-scientific-web-tools/tm-calculator.html (8.2.2023)

8 LIST OF ABBREVIATIONS

½ MS	half-strength Murashige and Skoog medium
ABA	abscisic acid
ANNAT1, 2, 3, 4, 5, 6, 7, 8	*Arabidopis thaliana* annexin 1, 2, 3, 4, 5, 6, 7, 8
ANNBJ1	*Brassica juncea* annexin 1
ANOVA	analysis of variance
ATCRY2	*Arabidopsis thaliana* cryptochrome 2
ATP	adenosine triphosphate
ATPase	adenosine triphosphatase
BFA	brefeldin A
bp	base pairs
BY-2	cell line derived from *Nicotiana tabacum*
Ca^{2+}	calcium ion
CaM	calmodulin
CaMBP	calmodulin-binding protein
CaMK	calmodulin-regulated protein kinases
CAT	catalase
CBL	calcineurin B-like protein
CBP	calcium-binding protein
CCaMK	calcium/calmodulin-dependent protein kinase
CCV	clathrin-coated vesicle
CDPK	calcium-dependent protein kinase
CFP	cyan fluorescent protein
CH3COOH	acetic acid
CIPK	CBL-interacting protein kinase
CLSM	confocal laser scanning microscopy
CME	clathrin-mediated endocytosis
CML	calmodulin-like protein
CNX	calnexin
Col-0	*Arabidopsis thaliana* ecotype Columbia-0
COPI	coat protein complex i
COPII	coat protein complex ii
CRK	CDPK-related protein kinase

CRT	calreticulin
DAG	days after germination
DAG	diacylglycerol
DNA	deoxyribonucleic acid
EDTA	ethylenediaminetetraacetic acid
EE	early endosome
ER	endoplasmic reticulum
ERGIC	endoplasmic reticulum-Golgi intermediate compartment
ESCRT	endosomal sorting complex required for transport
ESP	early secretion pathway
ET	ethylene
ETI	effector-triggered immunity
FRET	Förster resonance energy transfer
GFP	green fluorescent protein
GHANN1	*Gossypium hirsutum* annexin 1
GTase	guanosine triphosphatase
GTP	guanosine triphosphate
H_2O_2	hydrogen peroxide
HCl	hydrochloric acid
HR	hypersensitive response
HS	heat stress
HSF	heat shock factor
HSP	heat shock protein
IP3	inositol-1,4,5-trisphosphate
IRI	isoleucine-arginine-isoleucine (actin-binding motif)
JA	jasmonic acid
K^+	potassium ion
KanR	kanamycin resistance
kb	kilobase pairs
kDa	kilodalton (mass unit)
KOH	potassium hydroxide
LBb1.3	left border of the T-DNA region
LP	left primer
LSP	late secretion pathway

LT	low temperature
LV	lytic vacuole
M13	CaM binding domain of rabbit skeletal muscle myosin light chain kinase
MES	2-(N-morpholino)ethanesulfonic acid
MilliQ water	high-purity water produced by a MilliQ water purification system
MiMIF-2	*Meloidogyne incognita* macrophage migration inhibitory factor 2
MTANN1	*Medicago truncatula* annexin 1
MVB/PVC	multivesicular bodies/prevacuolar compartment
MYB30	myeloblastosis 30 transcription factor
Na^+	sodium ion
NaCl	sodium chloride
NO	nitric oxide
NTANN12	*Nicotiana benthamiana* annexin 12
OSCA1	hyperosmolality-gated calcium-permeable channel 1
OST1	open stomata 1
PA	phosphatidic acid
PC	phosphatidylcholine
PCP	pistil expressed Ca^{2+} binding protein
PCR	polymerase chain reaction
PIN	PIN-FORMED proteins
PIP2	phosphatidylinositol-4,5-bisphosphate
PLC	phospholipase c
PLD	phospholipase d
PM	plasma membrane
PR	pathogenesis-related
proANN1	native promoter of *ANNAT1* gene
PRR	pattern recognition receptor
PSV	protein storage vacuole
RabF2b	Ras protein RabF2b
RLK	receptor-like kinase
RNA	ribonucleic acid

RNAi	RNA interference
ROP	Rho-related GTPase of plants
ROS	reactive oxygen species
RP	right primer
S3	cysteine-methionine-cysteine (redox reactive centre)
SA	salicylic acid
SCaBP8	SOS3-like calcium binding protein8
SD	standard deviation
SIGnAL	Salk Institute Genomic Analysis Laboratory
SLK	Ste20-related protein kinase
SNAP	soluble N-ethylmaleimide-sensitive-factor attachment protein
SNARE	soluble N-ethylmaleimide-sensitive factor attachment protein receptor
SPK-3	sphingosine kinase 3
SOD	superoxide dismutase
SOS	salt overly sensitive
TAE	tris-acetate-EDTA buffer
TAIR	The Arabidopsis Information Resource
T-DNA	transfer DNA
TGN	trans-Golgi network
T_m	annealing temperature
Tris-HCl	tris(hydroxymethyl)aminomethane hydrochloride
UTR	untranslated region
v/v	volume/volume
VAMP2	vesicle-associated membrane protein 2
VTI1	vesicle transport v-SNARE 1
YC3.6	yellow cameleon 3.6 (calcium sensor)
YFP	yellow fluorescent protein
ZMANN33, ZMANN35	*Zea mays* annexin 33, 35

9 LIST OF FIGURES

10 LIST OF TABLES

11 SUPPLEMENTARY DATA

cggacaggccacgtcgtgtcctaaacctcttagcctttccctttataagtcaatcttgtgtcggcttcgactcccaacatacacaaa
acactaaaagtagaagaaaaATGGCGACTCTTAAGGTTTCTGATTCTGTTCCTGCTCCTT
CTGATGATGCTGAGCAATTGAGAACCGCTTTTGAAGgtataatagtttcatgattcttcttgttac
gttctctgtttttgttaccttcttgtttacatgatcagtatccacttttgtaaaagtgatgtgaatctgttggttttcgtttggtgggttatt
gtatgatcatttgttttgattgtttttcatgtggatcgatctttgttttggtccgatgatatgaatgttgtgtcggtagcgttttatgatcatt
tgtacgatgatgtagatcgagattgttccttcatggatcggatcagtgacaatgatctcctttctttgtgtgatctataacaatcttttg
tgttagtgatgaagttttgattgtctgatcatgttgataatgacaatgattacattcacacgagatcttgattgagttgtgttttgattct
cactgtcacagatctgtcttcttagtctagatctataatgtagttacgtgtaatacaacactaagatcttaagatttatattttgtgaatc
tgtttgaccggttctgttattatggatctgaagtgtgtgtgacttggatctgaagtatgtgactttgatggttatgtaaagtgaatctga
ttcgtgtttCGAACGAGGACTTGATCATATCAATCTTGGCTCACAGAAGTGCTGAAC
AGAGGAAAGTCATCAGGCAAGCATACCACGAAACCTACGGCGAAGACCTTC
TCAAGACTCTTGACAAGGAGCTCTCTAACGATTTCGAGgttcggttttcggacttttaagtat
cgacttttaaacatcttgtgtgaagtcattgtattctaattggttttttggtcatggacagAGAGCTATCTTGTTGTGG
ACTCTTGAACCCGGTGAGCGTGATGCTTTATTGGCTAATGAAGCTACAAAAA
GATGGACTTCAAGCAACCAAGTTCTTATGGAAGTTGCTTGCACAAGGACATC
AACGCAGCTGCTTCACGCTAGGCAAGCTTACCATGCTCGCTACAAGAAGTCT
CTTGAAGAGGACGTTGCTCACCACACTACCGGTGACTTCAGAAAGCTTTTGG
TTTCTCTTGTTACCTCATACAGGTACGAAGGAGATGAAGTGAACATGACATTG
GCTAAGCAAGAAGCTAAGCTGGTCCATGAGAAAATCAAGGACAAGCACTAC
AATGATGAGGATGTTATTAGAATCTTGTCCACAAGAAGCAAAGCTCAGATCA
ATGCTACTTTTAACCGTTACCAAGATGATCATGGCGAGGAAATTCTCAAGAGT
CTTGAGGAAGGAGATGATGATGACAAGTTCCTTGCACTTTTGAGGTCAACCA
TTCAGTGCTTGACAAGACCAGAGCTTTACTTTGTCGATGTTCTTCGTTCAGCA
ATCAACAAAACTGGAACTGATGAAGGAGCACTCACTAGAATTGTGACCACA
AGAGCTGAGATTGACTTGAAGGTCATTGGAGAGGAGTACCAGCGCAGGAAC
AGCATTCCTTTGGAGAAAGCTATTACCAAAGACACTCGTGGAGATTACGAGA
AGATGCTCGTCGCACTTCTCGGTGAAGATGATGCTTAAtcaatcaatcctccacagagaaa
cataagctgctctacagcttctgttatctcttatctccctctctctctttgatgagtttcaaatcgtttgattttgtttctacaaaaacct
tgtttgtttctgttgtgtgttttgagttcctaaataatgcaaaagagagagacagagagaaccagtgtggtctcttaagttatatatat
atgaagagcattggcctaaaacacagactaacaagtagttctggttttgac

Supplementary Figure 1: Gene map of *ANNAT1*. UTRs in red, exons in orange, introns in yellow, stop/start codons in blue.

caaacaccatccccagctacataattacacctcctaagtaaataactccgccttgaggaaaaaaaactaaaacggctctaaattg
aaaacaaaagaagagagagagagagagagacgaagaaacagagagattctctcgaaaATGGCCACCATTAG
AGTACCAAACGAAGTTCCTTCTCCAGCTCAGGATTCTGAAACTCTCAAACAA
GCTATTCGCGgtacgttacatccatagccgcaagcatttgttgtgtgattcgatgcattaagacataaatctctgaatgaa
agttttctcattcttgtagGATGGGGAACAGATGAGAAGGCGATTATACGAGTTTTAGGGC
AAAGAGACCAGAGCCAGAGAAGGAAGATTAGAGAAAGTTTTAGAGAGATTT
ATGGCAAAGATCTTATCGATGTTCTATCCTCCGAACTGTCTGGTGATTTCATGgt
aattatttctctaacatttctcaatcacgacttgagatttttttctaaaaagatgtgatttgattgaattgcagAAAGCTGTGG
TTTCGTGGACGTATGATCCAGCAGAGAGAGACGCAAGGCTTGTGAACAAGAT
TTTGAACAAGGAGAAGAAGAAGAAAAGCTTAGAGAATTTGAAGGTTATAGT
AGAGATCTCTTGCACGACTTCCCCAAACCATTTGATTGCTGTGAGGAAAGCT
TATTGTTCACTCTTTGACTCTTCTCTTGAAGAACACATTGCTTCTTCTCTGCCT
TTTCCTCTTGCAAAGgtcagtcctttcttcaagattagataagacatttttttggttttgtttgccttatgagaagctcaa
aatgttgattgtatgaaattgcagTTACTGGTGACATTGGCAAGTACATTCAGATATGACAAA
GATAGGACTGATGCAGAAGTAGCTACTATTGAGGCGGCTATGCTACGTGAAG
CCATAGAGAAGAAACAATTAGATCATGACCATGTCCTGTACATATTAGGAACG
CGTAGTATCTATCAGCTCAGAGAAACTTTTGTTGCTTACAAGAAGAATTATGG
GGTCACAATTGATAAGgttcagattctcatggtttggtttggtgactttggtctcatgtgtttggttttcttttcttggatt
ataacatgttgtgttgtatggacagGATGTTGATGGATGTCCAGGAGATGCTGATCTGAGAA
GTCTATTGAAGGTGGCAATCTTTTGTATTGATACTCCTGAGAAACACTTTGCA
AAGgtactacactaaacatttgagcaagactagagtcaaaaagtattttgaaggtgttttgtttgttccttaagtttttgtgttttaat
ttggcagGTGGTAAGAGATTCGATTGAGGGTTTTGGAACAGATGAGGATTCGTTG
ACGAGGGCGATTGTGACGCGTGCAGAGATCGATTTGATGAAAGTAAGAGGA
GAGTATTTCAACATGTATAATACAAGCATGGACAATGCTATTACTGGTGATATT
TCTGGAGACTACAAGGACTTCATTATCACCTTACTTGGATCCAAAATCTGAtcgt
ctttcgtttctttgtcagttgttatattcttggctttgcttgtgacttgtataatcaatcaatacattgtattccaactccagtttgaattgtt
taaaaaataatcaaatttctcttgattcttgcatttttgaatcaaagcaaatctatgtttaattttgttttcaaaattcg

Supplementary Figure 2: Gene map of *ANNAT3*. UTRs in red, exons in orange, introns in yellow, stop/start codons in blue.

ctaaaacacccttctcttctcccataaaccacaacattacccttaatcatcatataaaacgtcttgtccctcttccatagatttccaca
gaaaccaaaccaagagccggaaatcaaaaacagtaataaaagatcaactgcaagaaaATGGCTCTTCCTCTCG
AGCTCGAAAGCCTCACTGAAGCCATCTCAGCTGgtaattgtaatatttaattcttgattttattatggt
tcttggaagatacaaagaatgatttggatttgagattgaaaatctaaaaaatgtatgtttgttgtttatagGGATGGGAATG
GGAGTTGATGAGAATGCATTGATAAGCACACTGGGGAAATCGCAAAAGGAA
CATAGAAAATTGTTTAGGAAAGCAAGCAAAAGTTTCTTTGTTGAAGATGAGG
AAAGAGCTTTTGAGAAATGTCATGATCACTTCGTCAGACACCTCAAGCTTGA
GTTCTCCCGCTTCAATgtcagttcttttcttccattaatcttctttccatttttaacattttctaaatgtttttaccaaataaa
aaatctttattttggggtcaaacctaataataaatggaaccattcttgtttttacctaataaaagtataaacccaaccatatgttacaat
ttaatacaaaaaactaaaacaattctaaaattgcttaatttggttaatgtaattaatacagaaactatataacaaaaataattattaca
gctggtttatttttttctttatgaattagtatttataaaggatctcaaacatttctttaaaaataaaccaataatttactgctcaaaaaatca
cagaagatgatacgatggaaatgatgaagtttttcattcataactaattggtcaatgagtagataaaattcacattctatttcaaaaa
tagttgacaatgagtgaaaaagtcacattctagtattgaaacgtatctccacttcagatatggaattttaagaacaatttggtgtgtg
atgtgtagACTGCGGTGGTGATGTGGGCAATGCATCCATGGGAGAGAGATGCAAG
GTTGGTGAAGAAAGCTTTGAAGAAAGGAGAAGAAGCTTACAACCTCATCGT
TGAGGTCTCATGCACACGCTCTGCTGAGGATCTCCTCGGTGCACGTAAAGCT
TACCACTCTCTCTTCGACCAATCAATGGAAGAAGACATTGCCTCTCACGTCCA
CGGTCCTCAGCGCAAGgtcaatatttttatatactctagtgtgttggtctctttcaaacttcttttatctcactcattgtct
ctgttttttgtgcagTTGCTTGTGGGGCTCGTGAGTGCTTATAGATACGAAGGAAATAA
GGTGAAGGATGATTCTGCCAAATCCGATGCTAAGATTCTAGCCGAAGCAGTG
GCTTCTTCAGGCGAAGAAGCCGTGGAGAAGGATGAGGTTGTTAGGATTTTGA
CCACAAGAAGCAAACTTCATCTCCAACATCTCTACAAACACTTTAACGAAAT
CAAAGGCTCTGATCTTCTTGGGgtaacataaatataacaacaactcacttcttgtatatactaatgttttgatatt
ctctaatgaaaatcttgtggtttaatttggtcattagGGTGTATCTAAGTCTTCTCTTCTCAATGAAGC
ATTGATTTGTTTGCTCAAACCGGCTCTGTATTTCAGCAAGgtatatatgaaccatattcttca
ttgcggttgttttataacgccaatttctgcgtttgtgtttatgttttgtcgtgatttggttttagATTTTGGATGCGTCTCT
GAACAAAGACGCAGACAAGACTACCAAGAAATGGTTGACAAGAGTGTTCGT
TACAAGAGCAGATCATAGTGATGAGATGAATGAGATCAAAGAAGAGTACAAT
AACCTTTATGGTGAGACTTTGGCTCAAAGAATCCAAGAGAAGATAAAAGGG
AACTACAGAGATTTCTTGCTCACACTTCTCTCCAAATCCGATTGAtttcgtgttgagaa
acctattaccaatacttttggttattgaagatttatgatttccctttttatggttttatgtttctaattcctaaatttgcgttttctctaccgttt
ggtaataaagacatgaaaatttgatgaactcggtgaatcgagagtaagagttttgcgattgtgacaatgagtgattaatacaagg
attaagctccaataaaaaaatgttgcataaatcagaaatgaaacttgtaactcttcttttctttatgtgaaacttgtaactctatttgaa
agattctatgtgaccactaaaccgaattacgg

Supplementary Figure 3: Gene map of *ANNAT4*. UTRs in red, exons in orange, introns in yellow, stop/start codons in blue.

taattcataaagtgtaagaaacacgtggcagaagaattaataattcgtttgggatattttggtatatacggacaggccacgtcgt
gtcctaaacctcttagcctttccctttataagtcaatcttgtgtcggcttcgactcccaacatacacaaaacactaaaagtagaaga
aaaATGGCGACTCTTAAGGTTTCTGATTCTGTTCCTGCTCCTTCTGATGATGCTG
AGCAATTGAGAACCGCTTTTGAAGgtataatagtttcatgattcttcttgttacgttctctgtttttgttaccttc
ttgtttacatgatcagtatccacttttgtaaaagtgatgtgaatctgttggttttcgtttggtgggttattgtatgatcatttgttttgattg
tttttcatgtggatcgatctttgttttggtccgatgatatgaatgttgtgtcggtagcgttttatgatcatttgtacgatgatgtagatcg
agattgttccttcatggatcggatcagtgacaatgatctcctttctttgtgtgatctataacaatcttttgtgttagtgatgaagttttgat
tgtctgatcatgttgataatgacaatgattacattcacacgagatcttgattgagttgtgttttgattctcactgtcacagatctgtcttc
ttagtctagatctataatgtagttacgtgtaatacaacactaagatcttaagatttatattttgtgaatctgtttgaccggttctgttatta
tggatctgaagtgtgtgtgacttggatctgaagtatgtgactttgatggttatgtaaagtgaatctgattcgtgtttttcgcagGAT
GGGGTACGAACGAGGACTTGATCATATCAATCTTGGCTCACAGAAGTGCTGA
ACAGAGGAAAGTCATCAGGCAAGCATACCACGAAACCTACGGCGAAGACCT
TCTCAAGACTCTTGACAAGGAGCTCTCTAACGATTTCGAGgttcggttttcggacttttaag
tatcgacttttaaacatcttgtgtgaagtcattgtattctaattggttttttggtcatggacagAGAGCTATCTTGTTGT
GGACTCTTGAACCCGGTGAGCGTGATGCTTTATTGGCTAATGAAGCTACAAA
AAGATGGACTTCAAGCAACCAAGTTCTTATGGAAGTTGCTTGCACAAGGACA
TCAACGCAGCTGCTTCACGCTAGGCAAGCTTACCATGCTCGCTACAAGAAGT
CTCTTGAAGAGGACGTTGCTCACCACACTACCGGTGACTTCAGAAAGCTTTT
GGTTTCTCTTGTTACCTCATACAGGTACGAAGGAGATGAAGTGAACATGACAT
TGGCTAAGCAAGAAGCTAAGCTGGTCCATGAGAAAATCAAGGACAAGCACT
ACAATGATGAGGATGTTATTAGAATCTTGTCCACAAGAAGCAAAGCTCAGAT
CAATGCTACTTTTAACCGTTACCAAGATGCCTGTGGTTGGCATGCACATACAA
ATGGACGAACGGATAAACCTTTTCACGCCCTTTTAAATATCCGATTATTCTAAT
AAACGCTCTTTTCTCTTAGGTTTACCCGCCAATATATCCTGTCAAACACTGATA
GTTTAAACTGAAGGCGGGAAACGACAATCTGATCATGAGCGGAGAATTAAG
GGAGTCACGTTATGACCCCCGCCGATGACGCGGGACAAGCCGTTTTACGTTT
GGAACTGACAGAACCGCAACGTTGAAGGAGCCACTCAGCCGCGGGTTTCTG
GAGTTTAATGAGCTAAGCACATACGTCAGAAACCATTATTGCGCGTTCAAAA
GTCGCCTAAGGTCACTATCAGCTAGCAAATATTTCTTGTCAAAAATGCTCCAC
TGACGTTCCATAAATTCCCCTCGGTATCCAATTAGAGTCTCATATTCACTCTCA
ATCCAAATAATCTGCACCGGATCTGGATCGTTTCGCATGATTGAACAAGATGG
ATTGCACGCAGGTTCTCCGGCCGCTTGGGTGGAGAGGCTATTCGGCTATGAC
TGGGCACAACAGACAATCGGCTGCTCTGATGCCGCCGTGTTCCGGCTGTCAG
CGCAGGGGCGCCCGGTTCTTTTTGTCAAGACCGACCTGTCCGGTGCCCTGAA
TGAACTGCAGGACGAGGCAGCGCGGCTATCGTGGCTGGCCACGACGGGCGT
TCCTTGCGCAGCTGTGCTCGACGTTGTCACTGAAGCGGGAAGGGACTGGCT
GCTATTGGGCGAAGTGCCGGGGCAGGATCTCCTGTCATCTCACCTTGCTCCTG
CCGAGAAAGTATCCATCATGGCTGATGCAATGCGGCGGCTGCATACGCTTGAT
CCGGCTACCTGCCCATTCGACCACCAAGCGAAACATCGCATCGAGCGAGCAC
GTACTCGGATGGAAGCCGGTCTTGTCGATCAGGATGATCTGGACGAAGAGCA
TCAGGGGCTCGCGCCAGCCGAACTGTTCGCCAGGCTCAAGGCGCGCATGCC
CGACGGCGATGATCTCGTCGTGACCCATGGCGATGCCTGCTTGCCGAATATCA
TGGTGGAAAATGGCCGCTTTTCTGGATTCATCGACTGTGGCCGGCTGGGTGT
GGCGGACCGCTATCAGGACATAGCGTTGGCTACCCGTGATATTGCTGAAGAG
CTTGGCGGCGAATGGGCTGACCGCTTCCTCGTGCTTTACGGTATCGCCGCTCC
CGATTCGCAGCGCATCGCCTTCTATCGCCTTCTTGACGAGTTCTTCTGAGCGG
GACTCTGGGGTTCGAAATGACCGACCAAGCGACGCCCAACCTGCCATCACG
AGATTTCGATTCCACCGCCGCCTTCTATGAAAGGTTGGGCTTCGGAATCGTTT
TCCGGGACGCCGGCTGGATGATCCTCCAGCGCGGGGATCTCATGCTGGAGTT
CTTCGCCCACGGGATCTCTGCGGAACAGGCGGTCGAAGGTGCCGATATCATT

ACGACAGCAACGGCCGACAAGCACAACGCCACGATCCTGAGCGACAATATG
ATCGGGCCCGGCGTCCACATCAACGGCGTCGGCGGCGACTGCCCAGGCAAG
ACCGAGATGCACCGCGATATCTTGCTGCGTTCGGATATTTTCGTGGAGTTCCC
GCCACAGACCCGGATGATCCCCGATCGTTCAAACATTTGGCAATAAAGTTTCT
TAAGATTGAATCCTGTTGCCGGTCTTGCGATGATTATCATATAATTTCTGTTGA
ATTACGTTAAGCATGTAATAATTAACATGTAATGCATGACGTTATTTATGAGAT
GGGTTTTTATGATTAGAGTCCCGCAATTATACATTTAATACGCGATAGAAAACA
AAATATAGCGCGCAAACTAGGATAAATTATCGCGCGCGGTGTCATCTATGTTA
CTAGATCGGGCCTCCTGTCAATGCTGGCGGCGGCTCTGGTGGTGGTTCTGGT
GGCGGCTCTGAGGGTGGTGGCTCTGAGGGTGGCGGTTCTGAGGGTGGCGGC
TCTGAGGGAGGCGGTTCCGGTGGTGGCTCTGGTTCCGGTGATTTTGATTATGA
AAAGATGGCAAACGCTAATAAGGGGGCTATGACCGAAAATGCCGATGAAAA
CGCGCTACAGTCTGACGCTAAAGGCAAACTTGATTCTGTCGCTACTGATTACG
GTGCTGCTATCGATGGTTTCATTGGTGACGTTTCCGGCCTTGCTAATGGTAATG
GTGCTACTGGTGATTTTGCTGGCTCTAATTCCCAAATGGCTCAAGTCGGTGAC
GGTGATAATTCACCTTTAATGAATAATTTCCGTCAATATTTACCTTCCCTCCCTC
AATCGGTTGAATGTCGCCCTTTTGTCTTTGGCCCAATACGCAAACCGCCTCTC
CCCGCGCGTTGGCCGATTCATTAATGCAGCTGGCACGACAGGTTTCCCGACT
GGAAAGCGGGCAGTGAGCGCAACGCAATTAATGTGAGTTAGCTCACTCATTA
GGCACCCCAGGCTTTACACTTTATGCTTCCGGCTCGTATGTTGTGTGGAATTG
TGAGCGGATAACAATTTCACACAGGAAACAGCTATGACCATGATTACGCCAA
GCTTGCATGCCTGCAGGTCCCCAGATTAGCCTTTTCAATTTCAGAAAGAATGC
TAACCCACAGATGGTTAGAGAGGCTTACGCAGCAGGTCTCATCAAGACGATC
TACCCGAGCAATAATCTCCAGGAAATCAAATACCTTCCCAAGAAGGTTAAAG
ATGCAGTCAAAAGATTCAGGACTAACTGCATCAAGAACACAGAGAAAGATAT
ATTTCTCAAGATCAGAAGTACTATTCCAGTATGGACGATTCAAGGCTTGCTTC
ACAAACCAAGGCAAGTAATAGAGATTGGAGTCTCTAAAAAGGTAGTTCCCAC
TGAATCAAAGGCCATGGAGTCAAAGATTCAAATAGAGGACCTAACAGAACTC
GCCGTAAAGACTGGCGAACAGTTCATACAGAGTCTCTTACGACTCAATGACA
AGAAGAAAATCTTCGTCAACATGGTGGAGCACGACACACTTGTCTACTCCAA
AAATATCAAAGATACAGTCTCAGAAGACCAAAGGGCAATTGAGACTTTTCAA
CAAAGGGTAATATCCGGAAACCTCCTCGGATTCCATTGCCCAGCTATCTGTCA
CTTTATTGTGAAGATAGTGGAAAAGGAAGGTGGCTCCTACAAATGCCATCATT
GCGATAAAGGAAAGGCCATCGTTGAAGATGCCTCTGCCGACAGTGGTCCCAA
AGATGGACCCCCACCCACGAGGAGCATCGTGGAAAAAGAAGACGTTCCAAC
CACGTCTTCAAAGCAAGTGGATTGATGTGATATCTCCACTGACGTAAGGGAT
GACGCACAATCCCACTATCCTTCGCAAGACCCTTCCTCTATATAAGGAAGTTC
ATTTCATTTGGAGAGAACACGGGGGACTCTAGAGGATCCCCGGGTACCGAGC
TCGAATTTCCCCGATCGTTCAAACATTTGGCAATAAAGTTTCTTAAGATTGAA
TCCTGTTGCCGGTCTTGCGATGATTATCATATAATTTCTGTTGAATTACGTTAA
GCATGTAATAATTAACATGTAATGCATGACGTTATTTATGAGATGGGTTTTTATG
ATTAGAGTCCCGCAATTATACATTTAATACGCGATAGAAAACAAAATATAGCG
CGCAAACTAGGATAAATTATCGCGCGCGGTGTCATCTATGTTACTAGATCGGG
AATTCACTGGCCGTCGTTTTACAACGTCGTGACTGGGAAAACCCTGGCGTTA
CCCAACTTAATCGCCTTGCAGCACATCCCCCTTTCGCCAGCTGGCGTAATAGC
GAAGAGGCCCGCACCGATCGCCCTTCCCAACAGTTGCGCAGCCTGAATGGC
GCCCGCTCCTTTCGCTTTCTTCCCTTCCTTTCTCGCCACGTTCGCCGGCTTTCC
CCGTCAAGCTCTAAATCGGGGGCTCCCTTTAGGGTTCCGATTTAGTGCTTTAC
GGCACCTCGACCCCAAAAAACTTGATTTGGGTGATGGTTCACGTAGTGGGCC
ATCGCCCTGATAGACGGTTTTTCGCCCTTTGACGTTGGAGTCCACGTTCTTTA

ATAGTGGACTCTTGTTCCAAACTGGAACAACACTCAACCCTATCTCGGGCTAT
TCTTTTGATTTATAAGGGATTTTGCCGATTTCGGAACCACCATCAAACAGGAT
TTTCGCCTGCTGGGGCAAACCAGCGTGGACCGCTTGCTGCAACTCTCTCAGG
GCCAGGCGGTGAAGGGCAATCAGCTGTTGCCCGTCTCACTGGTGAAAAGAA
AAACCACCCCAGTACATTAAAAACGTCCGCAATGTGTTATTAAGTTGATCATG
GCGAGGAAATTCTCAAGAGTCTTGAGGAAGGAGATGATGATGACAAGTTCCT
TGCACTTTTGAGGTCAACCATTCAGTGCTTGACAAGACCAGAGCTTTACTTT
GTCGATGTTCTTCGTTCAGCAATCAACAAAACTGGAACTGATGAAGGAGCAC
TCACTAGAATTGTGACCACAAGAGCTGAGATTGACTTGAAGGTCATTGGAGA
GGAGTACCAGCGCAGGAACAGCATTCCTTTGGAGAAAGCTATTACCAAAGAC
ACTCGTGGAGATTACGAGAAGATGCTCGTCGCACTTCTCGGTGAAGATGATG
CTTAAtcaatcaatcctccacagagaaacataagctgctctacagcttctgttatctcttatctccctctctctctttgatgagt
ttcaaatcgtttgattttgtttctacaaaaaccttgtttgtttctgttgtgtgttttgagttcctaaataatgcaaaagagagagacagag
agaaccagtgtggtctcttaagttatatatatatgaagagcattggcctaaaacacagactaacaagtagttctggttttgacaaaa
gttgttgtcactacaaaaagggagaccaacaacaaaaaagttaagggcattgttttctctaaagccctatccgatcttgaaacac
aaaataacaacaacaacatttttttagttactaatcaaagTCACTTCTTCAAGATGGTCTTGGAGAAAA
TCTTCTTGCAGTAAGGGCTCGAGTGTAGTTTCCCGTACCTGTAAACCTTCGCC
ACCAATTT

Supplementary Figure 4: Gene map of *ANNAT1* SALK_095886C. UTRs in red, exons in orange, introns in yellow, stop/start codons in blue, T-DNA insertion in grey, kanamycin resistance (KanR) in green, LP primers in pink, RP primers in cyan, LBb1.3 primer in purple.

tcctcaaaacgaaaaatctcgacagaaataggctaattgcgtcatattacagtttcgtcttcgggggcatttatgtcaaacaccat
ccccagctacataattacacctcctaagtaaataactccgccttgaggaaaaaaaactaaaacggctctaaattgaaaacaaaa
gaagagagagagagagagagacgaagaaacagagagattctctcgaaaATGGCCACCATTAGAGTACC
AAACGAAGTTCCTTCTCCAGCTCAGGATTCTGAAACTCTCAAACAAGCTATT
CGCGgtacgttacatccatagccgcaagcatttgttgtgtgattcgatgcattaagacataaatctctgaatgaaagttttctcat
tcttgtagGATGGGGAACAGATGAGAAGGCGATTATACGAGTTTTAGGGCAAAGA
GACCAGAGCCAGAGAAGGAAGATTAGAGAAAGTTTTAGAGAGATTTATGGC
AAAGATCTTATCGATGTTCTATCCTCCGAACTGTCTGGTGATTTCATGgtaattatttc
tctaacatttctcaatcacgacttgagatttttttctaaaaagatgtgatttgattgaattgcagAAAGCTGTGGTTTCG
TGGACGTATGATCCAGCAGAGAGAGACGCAAGGCTTGTGAACAAGCCTGTG
GTTGGCATGCACATACAAATGGACGAACGGATAAACCTTTTCACGCCCTTTTA
AATATCCGATTATTCTAATAAACGCTCTTTTCTCTTAGGTTTACCCGCCAATATA
TCCTGTCAAACACTGATAGTTTAAACTGAAGGCGGGAAACGACAATCTGATC
ATGAGCGGAGAATTAAGGGAGTCACGTTATGACCCCCGCCGATGACGCGGGA
CAAGCCGTTTTACGTTTGGAACTGACAGAACCGCAACGTTGAAGGAGCCAC
TCAGCCGCGGGTTTCTGGAGTTTAATGAGCTAAGCACATACGTCAGAAACCA
TTATTGCGCGTTCAAAAGTCGCCTAAGGTCACTATCAGCTAGCAAATATTTCT
TGTCAAAAATGCTCCACTGACGTTCCATAAATTCCCCTCGGTATCCAATTAGA
GTCTCATATTCACTCTCAATCCAAATAATCTGCACCGGATCTGGATCGTTTCGC
ATGATTGAACAAGATGGATTGCACGCAGGTTCTCCGGCCGCTTGGGTGGAGA
GGCTATTCGGCTATGACTGGGCACAACAGACAATCGGCTGCTCTGATGCCGC
CGTGTTCCGGCTGTCAGCGCAGGGGCGCCCGGTTCTTTTTGTCAAGACCGAC
CTGTCCGGTGCCCTGAATGAACTGCAGGACGAGGCAGCGCGGCTATCGTGGC
TGGCCACGACGGGCGTTCCTTGCGCAGCTGTGCTCGACGTTGTCACTGAAGC
GGGAAGGGACTGGCTGCTATTGGGCGAAGTGCCGGGGCAGGATCTCCTGTC
ATCTCACCTTGCTCCTGCCGAGAAAGTATCCATCATGGCTGATGCAATGCGGC
GGCTGCATACGCTTGATCCGGCTACCTGCCCATTCGACCACCAAGCGAAACA
TCGCATCGAGCGAGCACGTACTCGGATGGAAGCCGGTCTTGTCGATCAGGAT
GATCTGGACGAAGAGCATCAGGGGCTCGCGCCAGCCGAACTGTTCGCCAGG
CTCAAGGCGCGCATGCCCGACGGCGATGATCTCGTCGTGACCCATGGCGATG
CCTGCTTGCCGAATATCATGGTGGAAAATGGCCGCTTTTCTGGATTCATCGAC
TGTGGCCGGCTGGGTGTGGCGGACCGCTATCAGGACATAGCGTTGGCTACCC
GTGATATTGCTGAAGAGCTTGGCGGCGAATGGGCTGACCGCTTCCTCGTGCT
TTACGGTATCGCCGCTCCCGATTCGCAGCGCATCGCCTTCTATCGCCTTCTTGA
CGAGTTCTTCTGAGCGGGACTCTGGGGTTCGAAATGACCGACCAAGCGACG
CCCAACCTGCCATCACGAGATTTCGATTCCACCGCCGCCTTCTATGAAAGGTT
GGGCTTCGGAATCGTTTTCCGGGACGCCGGCTGGATGATCCTCCAGCGCGGG
GATCTCATGCTGGAGTTCTTCGCCCACGGGATCTCTGCGGAACAGGCGGTCG
AAGGTGCCGATATCATTACGACAGCAACGGCCGACAAGCACAACGCCACGAT
CCTGAGCGACAATATGATCGGGCCCGGCGTCCACATCAACGGCGTCGGCGGC
GACTGCCCAGGCAAGACCGAGATGCACCGCGATATCTTGCTGCGTTCGGATA
TTTTCGTGGAGTTCCCGCCACAGACCCGGATGATCCCCGATCGTTCAAACATT
TGGCAATAAAGTTTCTTAAGATTGAATCCTGTTGCCGGTCTTGCGATGATTATC
ATATAATTTCTGTTGAATTACGTTAAGCATGTAATAATTAACATGTAATGCATGA
CGTTATTTATGAGATGGGTTTTTATGATTAGAGTCCCGCAATTATACATTTAATA
CGCGATAGAAAACAAAATATAGCGCGCAAACTAGGATAAATTATCGCGCGCG
GTGTCATCTATGTTACTAGATCGGGCCTCCTGTCAATGCTGGCGGCGGCTCTG
GTGGTGGTTCTGGTGGCGGCTCTGAGGGTGGTGGCTCTGAGGGTGGCGGTT
CTGAGGGTGGCGGCTCTGAGGGAGGCGGTTCCGGTGGTGGCTCTGGTTCCG
GTGATTTTGATTATGAAAAGATGGCAAACGCTAATAAGGGGGCTATGACCGA

AAATGCCGATGAAAACGCGCTACAGTCTGACGCTAAAGGCAAACTTGATTCT
GTCGCTACTGATTACGGTGCTGCTATCGATGGTTTCATTGGTGACGTTTCCGG
CCTTGCTAATGGTAATGGTGCTACTGGTGATTTTGCTGGCTCTAATTCCCAAAT
GGCTCAAGTCGGTGACGGTGATAATTCACCTTTAATGAATAATTTCCGTCAAT
ATTTACCTTCCCTCCCTCAATCGGTTGAATGTCGCCCTTTTGTCTTTGGCCCAA
TACGCAAACCGCCTCTCCCCGCGCGTTGGCCGATTCATTAATGCAGCTGGCA
CGACAGGTTTCCCGACTGGAAAGCGGGCAGTGAGCGCAACGCAATTAATGT
GAGTTAGCTCACTCATTAGGCACCCCAGGCTTTACACTTTATGCTTCCGGCTC
GTATGTTGTGTGGAATTGTGAGCGGATAACAATTTCACACAGGAAACAGCTAT
GACCATGATTACGCCAAGCTTGCATGCCTGCAGGTCCCCAGATTAGCCTTTTC
AATTTCAGAAAGAATGCTAACCCACAGATGGTTAGAGAGGCTTACGCAGCAG
GTCTCATCAAGACGATCTACCCGAGCAATAATCTCCAGGAAATCAAATACCTT
CCCAAGAAGGTTAAAGATGCAGTCAAAAGATTCAGGACTAACTGCATCAAG
AACACAGAGAAAGATATATTTCTCAAGATCAGAAGTACTATTCCAGTATGGAC
GATTCAAGGCTTGCTTCACAAACCAAGGCAAGTAATAGAGATTGGAGTCTCT
AAAAAGGTAGTTCCCACTGAATCAAAGGCCATGGAGTCAAAGATTCAAATAG
AGGACCTAACAGAACTCGCCGTAAAGACTGGCGAACAGTTCATACAGAGTC
TCTTACGACTCAATGACAAGAAGAAAATCTTCGTCAACATGGTGGAGCACGA
CACACTTGTCTACTCCAAAAATATCAAAGATACAGTCTCAGAAGACCAAAGG
GCAATTGAGACTTTTCAACAAAGGGTAATATCCGGAAACCTCCTCGGATTCC
ATTGCCCAGCTATCTGTCACTTTATTGTGAAGATAGTGGAAAAGGAAGGTGG
CTCCTACAAATGCCATCATTGCGATAAAGGAAAGGCCATCGTTGAAGATGCCT
CTGCCGACAGTGGTCCCAAAGATGGACCCCCACCCACGAGGAGCATCGTGG
AAAAAGAAGACGTTCCAACCACGTCTTCAAAGCAAGTGGATTGATGTGATAT
CTCCACTGACGTAAGGGATGACGCACAATCCCACTATCCTTCGCAAGACCCT
TCCTCTATATAAGGAAGTTCATTTCATTTGGAGAGAACACGGGGGACTCTAGA
GGATCCCCGGGTACCGAGCTCGAATTTCCCCGATCGTTCAAACATTTGGCAAT
AAAGTTTCTTAAGATTGAATCCTGTTGCCGGTCTTGCGATGATTATCATATAAT
TTCTGTTGAATTACGTTAAGCATGTAATAATTAACATGTAATGCATGACGTTAT
TTATGAGATGGGTTTTTATGATTAGAGTCCCGCAATTATACATTTAATACGCGA
TAGAAAACAAAATATAGCGCGCAAACTAGGATAAATTATCGCGCGCGGTGTC
ATCTATGTTACTAGATCGGGAATTCACTGGCCGTCGTTTTACAACGTCGTGAC
TGGGAAAACCCTGGCGTTACCCAACTTAATCGCCTTGCAGCACATCCCCCTTT
CGCCAGCTGGCGTAATAGCGAAGAGGCCCGCACCGATCGCCCTTCCCAACAG
TTGCGCAGCCTGAATGGCGCCCGCTCCTTTCGCTTTCTTCCCTTCCTTTCTCG
CCACGTTCGCCGGCTTTCCCCGTCAAGCTCTAAATCGGGGGCTCCCTTTAGG
GTTCCGATTTAGTGCTTTACGGCACCTCGACCCCAAAAAACTTGATTTGGGTG
ATGGTTCACGTAGTGGGCCATCGCCCTGATAGACGGTTTTTCGCCCTTTGACG
TTGGAGTCCACGTTCTTTAATAGTGGACTCTTGTTCCAAACTGGAACAACAC
TCAACCCTATCTCGGGCTATTCTTTTGATTTATAAGGGATTTTGCCGATTTCGG
AACCACCATCAAACAGGATTTTCGCCTGCTGGGGCAAACCAGCGTGGACCG
CTTGCTGCAACTCTCTCAGGGCCAGGCGGTGAAGGGCAATCAGCTGTTGCCC
GTCTCACTGGTGAAAAGAAAAACCACCCCAGTACATTAAAAACGTCCGCAAT
GTGTTATTAAGTTGATTTTGAACAAGGAGAAGAAGAAGAAAAGCTTAGAGA
ATTTGAAGGTTATAGTAGAGATCTCTTGCACGACTTCCCCAAACCATTTGATT
GCTGTGAGGAAAGCTTATTGTTCACTCTTTGACTCTTCTCTTGAAGAACACAT
TGCTTCTTCTCTGCCTTTTCCTCTTGCAAAGgtcagtcctttcttcaagattagataagacatttttttg
gttttgtttgccttatgagaagctcaaaatgttgattgtatgaaattgcagTTACTGGTGACATTGGCAAGTAC
ATTCAGATATGACAAAGATAGGACTGATGCAGAAGTAGCTACTATTGAGGCG
GCTATGCTACGTGAAGCCATAGAGAAGAAACAATTAGATCATGACCATGTCCT

GTACATATTAGGAACGCGTAGTATCTATCAGCTCAGAGAAACTTTTGTTGCTT
ACAAGAAGAATTATGGGGTCACAATTGATAAGgttcagattctcatggtttggtttggtgactttggt
ctcatgtgtttggttttcttttcttggattataacatgttgtgttgtatggacagGATGTTGATGGATGTCCAGGA
GATGCTGATCTGAGAAGTCTATTGAAGGTGGCAATCTTTTGTATTGATACTCCT
GAGAAACACTTTGCAAAGgtactacactaaacatttgagcaagactagagtcaaaaagtattttgaaggtgtttt
gtttgttccttaagtttttgtgttttaatttggcagGTGGTAAGAGATTCGATTGAGGGTTTTGGAACA
GATGAGGATTCGTTGACGAGGGCGATTGTGACGCGTGCAGAGATCGATTTGA
TGAAAGTAAGAGGAGAGTATTTCAACATGTATAATACAAGCATGGACAATGCT
ATTACTGGTGATATTTCTGGAGACTACAAGGACTTCATTATCACCTTACTTGGA
TCCAAAATCTGAtcgttctttcgtttctttgtcagttgttatattcttggctttgcttgtgacttgtataatcaatcaatacattg
tattccaactccagtttgaattgtttaaaaaataatcaaatttctcttgattcttgcatttttgaatcaaagcaaatctatgtttaattttgtt
ttcaaaattcg

Supplementary Figure 5: Gene map of *ANNAT3* SALK_082344C. UTRs in red, exons in orange, introns in yellow, stop/start codons in blue, T-DNA insertion in grey, kanamycin resistance (KanR) in green, LP primer in pink, RP primer in cyan, LBb1.3 primer in purple.

ctaaaacacccttctcttctcccataaaccacaacattacccttaatcatcatataaaacgtcttgtccctcttccatagatttccaca
gaaaccaaaccaagagccggaaatcaaaaacagtaataaaagatcaactgcaagaaaATGGCTCTTCCTCTCG
AGCTCGAAAGCCTCACTGAAGCCATCTCAGCTGgtaattgtaatatttaattcttgattttattatggt
tcttggaagatacaaagaatgatttggatttgagattgaaaatctaaaaaatgtatgtttgttgtttatagGGATGGGAATG
GGAGTTGATGAGAATGCATTGATAAGCACACTGGGGAAATCGCAAAAGGAA
CATAGAAAATTGTTTAGGAAAGCAAGCAAAAGTTTCTTTGTTGAAGATGAGG
AAAGAGCTTTTGAGAAATGTCATGATCACTTCGTCAGACACCTCAAGCTTGA
GTTCTCCCGCTTCAATgtcagttcttttcttccattaatcttctttccatttttaacattttctaaatgtttttaccaaataaa
aaatctttattttggggtcaaacctaataataaatggaaccattcttgtttttacctaataaaagtataaacccaaccatatgttacaat
ttaatacaaaaaactaaaacaattctaaaattgcttaatttggttaatgtaattaatacagaaactatataacaaaaataattattaca
gctggtttatttttttctttatgaattagtatttataaaggatctcaaacatttctttaaaaataaaccaataatttactgctcaaaaaatca
cagaagatgatacgatggaaatgatgaagtttttcattcataactaattggtcaatgagtagataaaattcacattctatttcaaaaa
tagttgacaatgagtgaaaaagtcacattctagtattgaaacgtatctccacttcagatatggaattttaagaacaatttggtgtgtg
atgtgtagACTGCGGTGGTGATGTGGGCAATGCATCCATGGGAGAGAGATGCAAG
GTTGGTGAAGAAAGCTTTGAAGAAAGGAGAAGAAGCTTACAACCTCATCGT
TGAGGTCTCATGCACACGCTCTGCTGAGGATCTCCTCGGTGCACGTAAAGCT
TACCACTCTCTCTTCGACCAATCAATGGAAGAAGACATTGCCTCTCACGTCCA
CGGTCCTCAGCGCAAGgtcaatatttttatatactctagtgtgttggtctctttcaaacttcttttatctcactcattgtct
ctgttttttgtgcagTTGCTTGTGGGGCTCGTGAGTGCTTATAGATACGAAGGAAATAA
GGTGAAGGATGATTCTGCCAAATCCGATGCTAAGATTCTAGCCGAAGCAGTG
GCTTCTTCAGGCGAAGAAGCCGTGGAGAAGGATGAGGTTGTTAGGATTTTGA
CCACAAGAAGCAAACTTCATCTCCAACATCTCTACAAACACTTTAACGAAAT
CAAAGGCTCTGATCTTCTTGGGgtaacataaatataacaacaactcacttcttgtatatactaatgttttgatatt
ctctaatgaaaatcttgtggtttaatttggtcattagGGTGTATCTAAGTCTTCTCTTCTCAATGAAGC
ATTGATTTGTTTGCTCAAACCGGCTCTGTATTTCAGCAAGgtatatatgaaccatattcttca
ttgcggttgttttataacgccaatttctgcgtttgtgtttatgttttgtcgtgatttggttttagATTTTGGATGCGTCTCT
GAACAAAGACGCAGACAAGACTACCAAGAAATGGTTGACAAGAGTGTTCGT
TACAAGAGCAGATCATAGTGATGAGATGAATGAGATCAAAGAAGAGTACAAT
AACCCCTGTGGTTGGCATGCACATACAAATGGACGAACGGATAAACCTTTTC
ACGCCCTTTTAAATATCCGATTATTCTAATAAACGCTCTTTTCTCTTAGGTTTAC
CCGCCAATATATCCTGTCAAACACTGATAGTTTAAACTGAAGGCGGGAAACG
ACAATCTGATCATGAGCGGAGAATTAAGGGAGTCACGTTATGACCCCCGCCG
ATGACGCGGGACAAGCCGTTTTACGTTTGGAACTGACAGAACCGCAACGTT
GAAGGAGCCACTCAGCCGCGGGTTTCTGGAGTTTAATGAGCTAAGCACATAC
GTCAGAAACCATTATTGCGCGTTCAAAAGTCGCCTAAGGTCACTATCAGCTA
GCAAATATTTCTTGTCAAAAATGCTCCACTGACGTTCCATAAATTCCCCTCGG
TATCCAATTAGAGTCTCATATTCACTCTCAATCCAAATAATCTGCACCGGATCT
GGATCGTTTCGCATGATTGAACAAGATGGATTGCACGCAGGTTCTCCGGCCG
CTTGGGTGGAGAGGCTATTCGGCTATGACTGGGCACAACAGACAATCGGCTG
CTCTGATGCCGCCGTGTTCCGGCTGTCAGCGCAGGGGCGCCCGGTTCTTTTT
GTCAAGACCGACCTGTCCGGTGCCCTGAATGAACTGCAGGACGAGGCAGCG
CGGCTATCGTGGCTGGCCACGACGGGCGTTCCTTGCGCAGCTGTGCTCGACG
TTGTCACTGAAGCGGGAAGGGACTGGCTGCTATTGGGCGAAGTGCCGGGGC
AGGATCTCCTGTCATCTCACCTTGCTCCTGCCGAGAAAGTATCCATCATGGCT
GATGCAATGCGGCGGCTGCATACGCTTGATCCGGCTACCTGCCCATTCGACCA
CCAAGCGAAACATCGCATCGAGCGAGCACGTACTCGGATGGAAGCCGGTCTT
GTCGATCAGGATGATCTGGACGAAGAGCATCAGGGGCTCGCGCCAGCCGAA
CTGTTCGCCAGGCTCAAGGCGCGCATGCCCGACGGCGATGATCTCGTCGTGA
CCCATGGCGATGCCTGCTTGCCGAATATCATGGTGGAAAATGGCCGCTTTTCT
GGATTCATCGACTGTGGCCGGCTGGGTGTGGCGGACCGCTATCAGGACATAG

CGTTGGCTACCCGTGATATTGCTGAAGAGCTTGGCGGCGAATGGGCTGACCG
CTTCCTCGTGCTTTACGGTATCGCCGCTCCCGATTCGCAGCGCATCGCCTTCT
ATCGCCTTCTTGACGAGTTCTTCTGAGCGGGACTCTGGGGTTCGAAATGACC
GACCAAGCGACGCCCAACCTGCCATCACGAGATTTCGATTCCACCGCCGCCT
TCTATGAAAGGTTGGGCTTCGGAATCGTTTTCCGGGACGCCGGCTGGATGAT
CCTCCAGCGCGGGGATCTCATGCTGGAGTTCTTCGCCCACGGGATCTCTGCG
GAACAGGCGGTCGAAGGTGCCGATATCATTACGACAGCAACGGCCGACAAG
CACAACGCCACGATCCTGAGCGACAATATGATCGGGCCCGGCGTCCACATCA
ACGGCGTCGGCGGCGACTGCCCAGGCAAGACCGAGATGCACCGCGATATCTT
GCTGCGTTCGGATATTTTCGTGGAGTTCCCGCCACAGACCCGGATGATCCCCG
ATCGTTCAAACATTTGGCAATAAAGTTTCTTAAGATTGAATCCTGTTGCCGGT
CTTGCGATGATTATCATATAATTTCTGTTGAATTACGTTAAGCATGTAATAATTA
ACATGTAATGCATGACGTTATTTATGAGATGGGTTTTTATGATTAGAGTCCCGC
AATTATACATTTAATACGCGATAGAAAACAAAATATAGCGCGCAAACTAGGAT
AAATTATCGCGCGCGGTGTCATCTATGTTACTAGATCGGGCCTCCTGTCAATG
CTGGCGGCGGCTCTGGTGGTGGTTCTGGTGGCGGCTCTGAGGGTGGTGGCTC
TGAGGGTGGCGGTTCTGAGGGTGGCGGCTCTGAGGGAGGCGGTTCCGGTGG
TGGCTCTGGTTCCGGTGATTTTGATTATGAAAAGATGGCAAACGCTAATAAGG
GGGCTATGACCGAAAATGCCGATGAAAACGCGCTACAGTCTGACGCTAAAGG
CAAACTTGATTCTGTCGCTACTGATTACGGTGCTGCTATCGATGGTTTCATTGG
TGACGTTTCCGGCCTTGCTAATGGTAATGGTGCTACTGGTGATTTTGCTGGCT
CTAATTCCCAAATGGCTCAAGTCGGTGACGGTGATAATTCACCTTTAATGAAT
AATTTCCGTCAATATTTACCTTCCCTCCCTCAATCGGTTGAATGTCGCCCTTTT
GTCTTTGGCCCAATACGCAAACCGCCTCTCCCCGCGCGTTGGCCGATTCATTA
ATGCAGCTGGCACGACAGGTTTCCCGACTGGAAAGCGGGCAGTGAGCGCAA
CGCAATTAATGTGAGTTAGCTCACTCATTAGGCACCCCAGGCTTTACACTTTA
TGCTTCCGGCTCGTATGTTGTGTGGAATTGTGAGCGGATAACAATTTCACACA
GGAAACAGCTATGACCATGATTACGCCAAGCTTGCATGCCTGCAGGTCCCCA
GATTAGCCTTTTCAATTTCAGAAAGAATGCTAACCCACAGATGGTTAGAGAG
GCTTACGCAGCAGGTCTCATCAAGACGATCTACCCGAGCAATAATCTCCAGG
AAATCAAATACCTTCCCAAGAAGGTTAAAGATGCAGTCAAAAGATTCAGGAC
TAACTGCATCAAGAACACAGAGAAAGATATATTTCTCAAGATCAGAAGTACT
ATTCCAGTATGGACGATTCAAGGCTTGCTTCACAAACCAAGGCAAGTAATAG
AGATTGGAGTCTCTAAAAAGGTAGTTCCCACTGAATCAAAGGCCATGGAGTC
AAAGATTCAAATAGAGGACCTAACAGAACTCGCCGTAAAGACTGGCGAACA
GTTCATACAGAGTCTCTTACGACTCAATGACAAGAAGAAAATCTTCGTCAAC
ATGGTGGAGCACGACACACTTGTCTACTCCAAAAATATCAAAGATACAGTCT
CAGAAGACCAAAGGGCAATTGAGACTTTTCAACAAAGGGTAATATCCGGAA
ACCTCCTCGGATTCCATTGCCCAGCTATCTGTCACTTTATTGTGAAGATAGTGG
AAAAGGAAGGTGGCTCCTACAAATGCCATCATTGCGATAAAGGAAAGGCCAT
CGTTGAAGATGCCTCTGCCGACAGTGGTCCCAAAGATGGACCCCCACCCACG
AGGAGCATCGTGGAAAAAGAAGACGTTCCAACCACGTCTTCAAAGCAAGTG
GATTGATGTGATATCTCCACTGACGTAAGGGATGACGCACAATCCCACTATCC
TTCGCAAGACCCTTCCTCTATATAAGGAAGTTCATTTCATTTGGAGAGAACAC
GGGGGACTCTAGAGGATCCCCGGGTACCGAGCTCGAATTTCCCCGATCGTTC
AAACATTTGGCAATAAAGTTTCTTAAGATTGAATCCTGTTGCCGGTCTTGCGA
TGATTATCATATAATTTCTGTTGAATTACGTTAAGCATGTAATAATTAACATGTA
ATGCATGACGTTATTTATGAGATGGGTTTTTATGATTAGAGTCCCGCAATTATA
CATTTAATACGCGATAGAAAACAAAATATAGCGCGCAAACTAGGATAAATTAT
CGCGCGCGGTGTCATCTATGTTACTAGATCGGGAATTCACTGGCCGTCGTTTT

ACAACGTCGTGACTGGGAAAACCCTGGCGTTACCCAACTTAATCGCCTTGCA
GCACATCCCCCTTTCGCCAGCTGGCGTAATAGCGAAGAGGCCCGCACCGATC
GCCCTTCCCAACAGTTGCGCAGCCTGAATGGCGCCCGCTCCTTTCGCTTTCTT
CCCTTCCTTTCTCGCCACGTTCGCCGGCTTTCCCCGTCAAGCTCTAAATCGGG
GGCTCCCTTTAGGGTTCCGATTTAGTGCTTTACGGCACCTCGACCCCAAAAA
ACTTGATTTGGGTGATGGTTCACGTAGTGGGCCATCGCCCTGATAGACGGTTT
TTCGCCCTTTGACGTTGGAGTCCACGTTCTTTAATAGTGGACTCTTGTTCCAA
ACTGGAACAACACTCAACCCTATCTCGGGCTATTCTTTTGATTTATAAGGGATT
TTGCCGATTTCGGAACCACCATCAAACAGGATTTTCGCCTGCTGGGGCAAA
CCAGCGTGGACCGCTTGCTGCAACTCTCTCAGGGCCAGGCGGTGAAGGGCA
ATCAGCTGTTGCCCGTCTCACTGGTGAAAAGAAAAACCACCCCAGTACATTA
AAAACGTCCGCAATGTGTTATTAAGTTGTTTATGGTGAGACTTTGGCTCAAAG
AATCCAAGAGAAGATAAAAGGGAACTACAGAGATTTCTTGCTCACACTTCTC
TCCAAATCCGATTGAtttcgtgttgagaaacctattaccaatacttttggttattgaagatttatgatttccctttttatggt
tttatgtttctaattcctaaatttgcgttttctctaccgtttggtaataaagacatgaaaatttgatgaactcggtgaatcgagagtaag
agttttgcgattgtgacaatgagtgattaatacaaggattaagctccaataaaaaaatgttgcataaatcagaaatgaaacttgtaa
ctcttctttttctttatgtgaaacttgtaactctatttgaaagattctatgtgaccactaaaccgaattacggattccaaccgaatttcac
ct

Supplementary Figure 6: Gene map of *ANNAT4* SALK_019725C. UTRs in red, exons in orange, introns in yellow, stop/start codons in blue, T-DNA insertion in grey, kanamycin resistance (KanR) in green, LP primer in pink, RP primer in cyan, LBb1.3 primer in purple.